(NASA-CR-4132) CONTROL AUGMENTED STRUCTURAL SYNTHESIS (California Univ.) 193 pCSCL 01C

N88-20290

Unclas
H1/05 0124865

NASA Contractor Report 4132

Control Augmented Structural Synthesis

Robert V. Lust and Lucien A. Schmit
University of California, Los Angeles
Los Angeles, California

Prepared for
Langley Research Center
under Grant NSG-1490

National Aeronautics
and Space Administration

Scientific and Technical
Information Division

1988

TABLE OF CONTENTS

LIST OF TABLES vi

LIST OF FIGURES ix

LIST OF SYMBOLS xi

ACKNOWLEDGMENT xvii

ABSTRACT xviii

CHAPTER I. Introduction 1

1.1 Introduction 1

1.2 Background 2

1.3 Scope of the Work 9

CHAPTER II. The Control Augmented Structural Synthesis Problem 12

2.1 Introduction 12

2.2 Problem Formulation 12

CHAPTER III. Structural Analysis 20

3.1 Introduction 20

3.2 Static Analysis 21

3.3 Dynamic Response Analysis 24

3.4 Eigenvalue Analysis 32

CHAPTER IV. Approximate Problem Generation 34

4.1 Introduction 34

4.2 Objective Function Evaluation 34

4.3 Constraint Evaluation 36

4.4 Temporary Constraint Deletion 40

4.5 Objective Function and Constraint Approximations 41

4.6 Move Limits 45
CHAPTER V. Optimization 47
5.1 Introduction 47
5.2 Design Optimization 47
CHAPTER VI. Numerical Results 55
6.1 Introduction 55
6.2 Problem 1 - Cantilevered Beam, Mass Minimization 55
6.2.1 Case A - Uniform Structural Design 56
6.2.2 Case B - Non-Uniform Structural Design 57
6.3 Problem 2 - Cantilevered Beam Response Minimization 59
6.3.1 Case A - Uniform Structural Design 59
6.3.2 Case B - Non-Uniform Structural Design 60
6.4 Problem 3 - Cantilevered Beam, Control Force Minimization 61
6.4.1 Case A - Uniform Structural Design 62
6.4.2 Case B - Non-uniform Structural Design 63
6.5 Problem 4 - Cantilevered Beam, Multiple Loading Conditions 63
6.6 Problem 5 - Cantilevered Beam, Lumped Mass Design Elements 65
6.7 Problem 6 - Cantilevered Beam, Independent Actuator Gains 67
6.8 Problem 7 - Planar Truss, Control Force Minimization 69
6.9 Problem 8 - Antenna, Response Minimization 72
6.10 Problem 9 - Grillage 74
CHAPTER VII. Conclusions and Recommendations 77
7.1 Conclusions 77
7.2 Recommendations for Future Work 80
REFERENCES 82

APPENDIX A Stiffness Matrices, Mass Matrices and Load Vectors for Structural Elements 90

APPENDIX B Position and Velocity Feedback Gain Matrices for Member Controller Element 100

APPENDIX C Alternate Steady State Response Solution Scheme 102

APPENDIX D Derivatives of Structural Response Quantities with Respect to Reciprocal Element Properties 105

TABLES 117

FIGURES 151

LIST OF TABLES

Page

Table 1 Iteration History Data for Problem 1, Case A Cantilevered Beam, Mass Minimization....117

Table 2 Final Designs for Problem 1, Case A Cantilevered Beam, Mass Minimization....118

Table 3 Final Design Response Ratios for Problem 1, Case A Cantilevered Beam, Mass Minimization....119

Table 4 Iteration History Data for Problem 1, Case B Cantilevered Beam, Mass Minimization....120

Table 5 Final Designs for Problem 1, Case B Cantilevered Beam, Mass Minimization....121

Table 6 Final Design Response Ratios for Problem 1, Case B Cantilevered Beam, Mass Minimization....122

Table 7 Iteration History Data for Problem 2, Case A Cantilevered Beam, Response Minimization....123

Table 8 Final Designs for Problem 2, Case A Cantilevered Beam, Response Minimization....124

Table 9 Final Design Response Ratios for Problem 2, Case A Cantilevered Beam, Response Minimization....125

Table 10 Iteration History Data for Problem 2, Case B Cantilevered Beam, Response Minimization....126

Table 11 Final Designs for Problem 2, Case B Cantilevered Beam, Response Minimization....127

Table 12 Final Design Response Ratios for Problem 2, Case B Cantilevered Beam, Response Minimization....128

Table 13 Iteration History Data for Problem 3, Case A Cantilevered Beam, Control Force Minimization....129

Table 14 Final Designs for Problem 3, Case A Cantilevered Beam, Control Force Minimization....130

Table 15 Final Design Response Ratios for Problem 3, Case A Cantilevered Beam, Control Force Minimization....131

Table 16 Iteration History Data for Problem 3, Case B
Cantilevered Beam, Control Force Minimization.....132

Table 17 Final Designs for Problem 3, Case B
Cantilevered Beam, Control Force Minimization.....133

Table 18 Final Design Response Ratios for Problem 3, Case B
Cantilevered Beam, Control Force Minimization.....134

Table 19 Iteration History Data for Problem 4
Cantilevered Beam, Multiple Loading Conditions.....135

Table 20 Final Designs for Problem 4
Cantilevered Beam, Multiple Loading Conditions.....136

Table 21 Final Design Response Ratios for Problem 4
Cantilevered Beam, Multiple Loading Conditions.....137

Table 22 Iteration History Data for Problem 5
Cantilevered Beam, Lumped Mass Design Elements 138

Table 23 Final Designs for Problem 5
Cantilevered Beam, Lumped Mass Design Elements 139

Table 24 Final Design Response Ratios for Problem 5
Cantilevered Beam, Lumped Mass Design Elements 140

Table 25 Iteration History Data for Problem 6
Cantilevered Beam, Independent Actuator Gains 141

Table 26 Final Designs for Problem 6
Cantilevered Beam, Independent Actuator Gains 142

Table 27 Final Design Response Ratios for Problem 6
Cantilevered Beam, Independent Actuator Gains 143

Table 28 Iteration History Data for Problem 7
Planar Truss, Control Force Minimization.....144

Table 29 Final Designs for Problem 7
Planar Truss, Control Force Minimization.....145

Table 30 Iteration History Data for Problem 8
Antenna, Response Minimization 146

Table 31 Final Structural Designs for Problem 8
Antenna, Response Minimization 147

Table 32 Final Design Actuator Forces for Problem 8
Antenna, Response Minimization 148

Table 33 Iteration History Data for Problem 9

Grillage 149

Table 34 Actuator Forces for Problem 9 Grillage 150

LIST OF FIGURES

Page

Fig. 1 Design Methodology Flow Diagram 151

Fig. 2 Structural Element Orientation 152

Fig. 3 Cantilevered Beam, Problems 1-6 153

Fig. 4 Iteration Histories for Problem 1, Case A
Cantilevered Beam, Mass Minimization 154

Fig. 5 Iteration Histories for Problem 1, Case B
Cantilevered Beam, Mass Minimization 155

Fig. 6 Iteration Histories for Problem 2, Case A
Cantilevered Beam, Response Minimization 156

Fig. 7 Iteration Histories for Problem 2, Case B
Cantilevered Beam, Response Minimization 157

Fig. 8 Iteration Histories for Problem 3, Case A
Cantilevered Beam, Control Force Minimization 158

Fig. 9 Iteration Histories for Problem 3, Case B
Cantilevered Beam, Control Force Minimization 159

Fig. 10 Iteration Histories for Problem 4
Cantilevered Beam, Multiple Loading Conditions 160

Fig. 11 Final Design Thickness Distributions for Problem 4
Cantilevered Beam, Multiple Loading Conditions 161

Fig. 12 Iteration Histories for Problem 5
Cantilevered Beam, Lumped Mass Design Elements 162

Fig. 13 Final Design Thickness Distributions for Problem 5
Cantilevered Beam, Lumped Mass Design Elements 163

Fig. 14 Iteration Histories for Problem 6
Cantilevered Beam, Independent Actuator Gains 164

Fig. 15 Planar Truss, Problem 7 165

Fig. 16 Iteration Histories for Problem 7
Planar Truss, Control Force Minimization 166

Fig. 17 Antenna, Problem 8 167

Fig. 18 Beam Cross Section 168
Fig. 19 Iteration Histories for Problem 8
Antenna, Response Minimization 169
Fig. 20 Grillage, Problem 9 170
Fig. 21 Iteration Histories for Problem 9, Grillage 171
Fig. A1 Space Frame Element 172
Fig. A2 Space Truss Element 173
Fig. A3 Axial Control Element 174

LIST OF SYMBOLS

B	Number of design variables.
$[b_a]$	Boolean matrix defining the location of the actuators.
$[b_p]$	Boolean matrix defining the location of the position sensors.
$[b_v]$	Boolean matrix defining the location of the velocity sensors.
[C]	System level (global) viscous damping matrix.
$[C_A]$	Augmented system level (global) damping matrix.
c_{bq}	Partial derivative of the q-th retained constraint with respect to the b-th design variable.
$[C]^e$	Element viscous damping matrix.
c_1, c_2	Objective function weighting coefficients.
d_m	Move limit parameter.
E^n	Euclidean n-space.
$f(\bar{Y})$	A general function of $\bar{Y}$.
$\tilde{f}_I(\bar{Y})$	Explicit first order approximation of $f(\bar{Y})$ in terms of the reciprocal variables $1/Y_b$.
$\tilde{f}_L(\bar{Y})$	Explicit linear approximation of $f(\bar{Y})$ in terms of Y_b.
$\tilde{f}_M(\bar{Y})$	Explicit mixed variable (hybrid) approximation of $f(\bar{Y})$.
$\bar{F}$	Vector of element end forces (static).
$F_A(\bar{X})$, $F_A(\bar{Y})$	Dynamic actuator force.
{F}	Vector of static element end forces.
{FEF}	Vector of static fixed end forces due to distributed applied loads.
g_q	The q-th retained constraint.

$\tilde{g}_q(\bar{Y})$	Explicit approximation of the q-th retained constraint.
$\bar{G}(\bar{Y})$	Vector of implicit behavior constraint functions.
$[G_p]$	System level (global) position gain matrix.
$[G_v]$	System level (global) velocity gain matrix.
h_p	Position gain.
$\tilde{h}_q(\bar{Y})$	Explicit approximation of the q-th retained constraint in dual formulation.
h_v	Velocity gain.
$[H_p]$	Control element position gain matrix.
$[H_v]$	Control element velocity gain matrix.
i	The imaginary unit.
I	Number of analysis elements.
I_C	The set of actuator forces included in J_C.
I_f	The set of static element forces associated with the function f.
$J(\bar{Y})$, J^U	Performance index, upper bound.
$\tilde{J}(\bar{Y})$	Explicit approximation of $J(\bar{Y})$.
J_b	Set of reciprocal element properties associated with the b-th design variable.
$\tilde{J}_C(\bar{X}), J_C(\bar{Y}), J_C^U$	Part of performance index associated with the actuator forces, upper bound.
$J_C(\bar{Y})$	Explicit approximation of $J_C(\bar{Y})$.
J_f	Set of dynamic actuator forces associated with the function f.
$J_R(\bar{X}), J_R(\bar{Y}), J_R^U$	Part of performance index associated with the dynamic response.
$\tilde{J}_R(\bar{Y})$	Explicit approximation of $J_R(\bar{Y})$.

K_d	Number of independent dynamic loading conditions.
K_s	Number of independent static loading conditions.
[K]	System level (global) stiffness matrix.
$[K_A]$	System level (global) augmented stiffness matrix.
$[K]_i$	i-th element level stiffness matrix.
$l(\bar{\lambda})$	Dual function.
$L(\bar{Y},\bar{\lambda}),L_b(Y_b,\bar{\lambda})$	Lagrangian function, portion of the Lagrangian corresponding to the b-th design variable.
$M(\bar{X}),M(\bar{Y}),M^U$	Structural mass, upper bound.
$\tilde{M}(\bar{Y})$	Explicit approximation of the structural mass.
M_f	Set of natural frequencies associated with the function f.
[M]	System level (global) mass matrix.
$[M]_i$	i-th element level mass matrix.
N	Number of displacement degrees of freedom.
N_f	Set of dynamic displacements associated with the function f.
N_R	Set of dynamic displacements associated with J_R.
$\{N(t)\}$	Vector of active control forces.
{P}	Vector of applied static loads.
{P(t)}	Vector of applied dynamic loads.
Q_{ik}	Weighting coefficients associated with the dynamic displacements.
$\hat{Q}$	Set of retained constraints (dual formulation).
Q_R	Set of retained behavior constaints.
R_{ik}	Weighting coefficients associated with the actuator forces.
R_c	Response ratio cutoff parameter.

$R_q(\bar{X}),R_q(\bar{X},\bar{Y})$	Response ratio for the q-th constraint.
$[R_\alpha],[R_\beta],[R_\theta]$	Coordinate system rotation matrices.
t	Time.
[T]	Local to global coordinate transformation matrix.
u	Nodal displacement.
$\bar{u}(\bar{X})$	Vector of nodal displacements.
$\{u\}_k$	Vector of nodal displacements for the k-th loading condition, in the global coordinate system.
$\{\dot{u}\}_k$	Vector of nodal velocities for the k-th loading condition, in the global coordinate system.
$\{\ddot{u}\}_k$	Vector of nodal accelerations for the k-th loading condition, in the global coordinate system.
$\{\bar{u}\}_k$	Vector of complex nodal displacements for the k-th loading condition, in the global coordinate system.
$\{u\}_{ik}$	Vector of nodal displacements corresponding to the i-th element for the k-th loading condition.
$\bar{X}$	Vector of reciprocal element properties.
$Y_b,\bar{Y},\bar{Y}^U,\bar{Y}^L$	b-th design variable, vector of design variables, vectors of upper and lower bounds.
$\tilde{\bar{Y}}^U,\tilde{\bar{Y}}^L$	Vectors of upper and lower bounds on the design variables during a design step.
$\bar{Y}^*$	Vector of optimal values of the design variables.

Greek

γ	Structural damping coefficient.
$\lambda_q,\bar{\lambda}$	Dual variable associated with the q-th retained constraint, vector of dual variables.
ν	Actuator force phase angle.
ξ	Actuator force phase angle.

ρ	Material density.
σ	Element stress (static).
ϕ	Dynamic displacement phase angle.
$\{\phi\}$	Structural eigenvector.
$[\phi]$	Matrix of structural eigenvectors.
ψ	Dynamic displacement phase angle.
ω	Undamped natural frequency.
Ω_k	Forcing function frequency for the k-th dynamic loading condition.

Subscripts

a : F_{a_k}	Denotes an allowable value.
b : Y_b	Index for design variables.
i : $[K_i]$	Index for analysis elements.
I : $\{u_I\}_k$	Denotes the imaginary part of a complex quantity.
k : $\{u\}_k$	Index for independent loading conditions.
m : ω_m	Index for natural frequencies.
n : $u_n(\overline{X})$	Index for dynamic displacements.
q : g_q	Index for constraints.
R : $\{u_R\}_k$	Denotes the real part of a complex quantity.
0 : Y_0	Denotes a quantity evaluated at the beginning of a design step.

Superscripts

e : $[K]_i^e$	Denotes a quantity described in the element (local) coordinate system.
g : $[K]_i^g$	Denotes a quantity described in the global (system) coordinate system.

$L : \overline{Y}^L$	Denotes a lower bound quantity.
$T : [T]_i^T$	Transpose.
$U : \overline{Y}^U$	Denotes an upper bound quantity.
$* : \overline{Y}^*$	Denotes an optimal quantity.

Special Symbols

$- : \overline{X}$	Vector quantity.
$: \{\overline{u}\}_k$	Complex quantity.
$\sim : g_q(\overline{Y})$	Explicit approximation of the associated quantity or quantity is associated with the approximate problem.
$\hat{} : \hat{Q}$	Distinguishing mark.
$\partial : \frac{\partial f}{\partial Y_b}$	Partial differential operator.
$d : \frac{df}{dX_j}$	Differential operator.
$\| \| : \|u_{jk}\|$	Denotes the magnitude of the associated quantity.
$[\ ] : [\mathrm{K}]$	Matrix quantity.
$\{\ \} : \{Y\}$	Vector quantity.

ACKNOWLEDGMENT

This report presents some results of a continuing research program entitled "Fundamental Studies of Methods for Structural Synthesis" sponsored by NASA Research Grant No. NSG-1490. The work reported herein was carried out in the School of Engineering and Applied Science at UCLA during the period from January 1985 to December 1986.

The authors want to take this opportunity to express their appreciation to Deborah Haines for her patience and careful attention to detail during the preparation of this manuscript.

ABSTRACT

A methodology for control augmented structural synthesis is proposed for a class of structures which can be modeled as an assemblage of frame and/or truss elements. It is assumed that both the plant (structure) and the active control system dynamics can be adequately represented with a linear model. The structural sizing variables, active control system feedback gains and non-structural lumped masses are treated simultaneously as independent design variables. Design constraints are imposed on static and dynamic displacements, static stresses, actuator forces and natural frequencies to ensure acceptable system behavior. Multiple static and dynamic loading conditions are considered. Side constraints imposed on the design variables protect against the generation of unrealizable designs. While the proposed approach is fundamentally more general, here the methodology is developed and demonstrated for the case where: (1) the dynamic loading is harmonic and thus the steady state response is of primary interest; (2) direct output feedback is used for the control system model; and (3) the actuators and sensors are collocated.

The synthesis methodology is implemented in a research computer program and is used to solve several example problems. These problems were chosen so that in addition to demonstrating the basic features of the design methodology, the results could be critically evaluated through insights into the physical behavior of the system.

CHAPTER I

Introduction

1.1 Introduction

The design of efficient structural systems is of fundamental interest to both structural and control system engineers. Systematic methodologies for both structural and active control system synthesis (e.g. structural optimization and linear optimal control theory) are well known and are receiving increased application in the design environment. However, these design techniques, for the most part, have been applied independently within the overall design process. Specifically, a conventional design methodology has evolved in which the structure is designed subject to prescribed strength and stiffness requirements (while ignoring the existence of the active control system) with the active control system being subsequently designed under the assumption that the structure is prescribed. The success of this approach has been largely due to the fact that the active control systems have been used primarily to control gross structural motions (e.g. attitude control of orbiting space structures) while local structural vibrations were suppressed via the structural design.

Recently, increased interest in the design of highly flexible orbiting space structures, as well as light weight fuel efficient aerospace and ground transportation vehicles, has motivated a reconsideration of the conventional structure/control system design approach. There is

now a growing awareness that the design of the next generation of structural systems will require that the structural and control system design functions be integrated in some manner. Therefore, the primary objective of this work is to set forth and demonstrate a control augmented structural synthesis methodology for the simultaneous design of a structure and its associated active control system.

1.2 Background

Since the early 1970's there has been considerable interest in the design of efficient control augmented structural systems (Refs. 1-3). This interest has been particularly intense within the aerospace community as a result of challenging problems associated with the design of large flexible orbiting space structures (Ref. 4). It is now generally recognized that the inherently low stiffness and damping characteristics of this new generation of structures will require the use of active control systems, not only for maneuvering and attitude control, but also for vibration suppression and shape control. Consequently, the application of active control technology to the problem of vibration control in flexible structures has recently received much attention in the literature (Ref. 5).

Various methods for the design of active control systems for flexible structures are discussed in Refs. 6-14. The three most common approaches have come to be known as direct output feedback (DOFB), modern modal control (MMC) and independent modal space control (IMSC). Direct output feedback (Refs. 15-18) is, conceptually, the simplest of the feedback control techniques. This method utilizes

control inputs which are explicit linear functions of the system response. The actuator commands are obtained by electronically multiplying the sensor outputs by the feedback gains. These gains are usually determined via a class of techniques known as pole placement or pole allocation in which the output feedback gains are chosen so that a selected set of the closed loop eigenvalues (poles) of the system take on prescribed values (Ref. 19); although the use of linear optimal control techniques is possible (Ref. 20). Also, two constrained optimization techniques have recently been suggested in Refs. 21 and 22 where the damping characteristics of the system are enhanced while minimizing the feedback gains.

As an alternative to calculating the control forces directly from the system outputs, the modern modal control methods are based on the concept of state variable feedback. In this approach the actuator commands are determined via multiplication of the system states and the state feedback gains. While this approach is conceptually similar to DOFB, additional complexity arises from the fact that, in general, the states are not directly measurable. Therefore, MMC requires that the state variables be reconstructed from the sensor output measurements through the construction of an auxiliary dynamical system known as an observer (Ref. 19). Fortunately, the controller and observer design problems are separable. Therefore, the state feedback gains can be determined independently, under the assumption that the states are observable. As was the case with the DOFB approach, the state feedback gains can be determined via both pole placement and linear optimal control techniques. However, the application of linear

optimal control techniques is most prevalent in the literature (e.g. Refs. 23-26).

The last of the three common active control design techniques is known as independent modal space control (Refs. 27-29). This method utilizes both internal and external decoupling mechanisms such that the control is applied to each mode of the structure independently. The decoupling process consists of, first, decoupling the uncontrolled system equations of motion via the normal mode method (Ref. 30) and then introducing the controls directly into the modal equations of motion. These modal control forces are assumed to be functions only of the coordinates associated with a single modal equation and are given by the product of the modal coordinates and the modal feedback gains. As before, the feedback gains can be calculated by both pole placement and linear optimal control techniques. Moreover, since the modal controls are independent of each other the computation of the gains for each mode can be performed independently, thereby significantly reducing the computation effort associated with the design process. However, since the controls are designed in the modal space, the IMSC method requires a final additional step for implementation. In this step the real actuator forces must be determined from the modal control forces. This is accomplished, in effect, through the construction of a modal observer which reconstructs the modal coordinates from the sensor output measurements. A relatively simple observer can be constructed if the numbers of actuators and sensors is equal to the number of modes to be controlled (Ref. 31). Unfortunately, this requirement can represent a rather serious burden in terms of hardware

costs for large systems. Recently, however, an alternative modal observer formulation (based on a pseudo-inverse) which requires fewer actuators and sensors was proposed (Ref. 32).

The active control system design techniques described above all operate under the assumption that the structure (plant) has been previously designed and, therefore, its stiffness, mass and damping characteristics are known. The actual design of the structure is traditionally the responsibility of the structural engineer. The development of systematic methodologies for structural synthesis has received much attention over the past 25 years and techniques applicable to a significant class of structural design problems are well developed. A history of its development and the current state-of-the-art of structural synthesis are given in Refs. 33-38.

Primarily, three approaches to systematic structural design have been explored. Two of these approaches, one based on mathematical programming methods (Ref. 39) and the other on optimality criteria (e.g. Refs. 40-41) have received the most attention. The optimality criteria methods are based on a statement of the necessary conditions that must be satisfied at the optimum design. This optimality criterion is formulated via a priori assumptions as to the number and types of failure modes characterizing the optimum design (e.g. fully stressed design). These methods are generally computationally efficient and yield good results, if the failure modes have been correctly identified, but suffer somewhat in that they are not easily applied to a general class of structural design problems.

In the mathematical programming based techniques, the structural design problem is formulated as a nonlinear programming problem (NLP) in terms of a design objective and performance requirements (behavior constraints). The NLP is then solved for the optimal values of the design variables. This approach is quite general and can easily accommodate different design objectives and the simultaneous consideration of a variety of possible failure modes. Its generality of application and its recent interpretation as a generalized optimality criteria method (Refs. 42-43) have established this approach as the predominate structural synthesis tool.

Another structural design technique has received some limited attention. This approach, based on optimal control theory, has, for the most part, been applied to the design of distributed parameter systems (e.g. Ref. 44, Chapter 6). It has been demonstrated, primarily, on small component level design problems. The application of optimal control techniques to the design of large structures modelled as lumped parameter systems has seen only limited investigation (e.g. Ref. 45).

In the past, the structural (passive) and active control system design techniques described herein have been applied independently within the overall design process. Recent concerns over the design of large flexible space structures have generated interest in interdisciplinary approaches to the design problem (Refs. 46-47). This interest has been heightened as a result of both numerical and experimental demonstrations of the synergic nature of active and passive control techniques (Refs. 48-50). Consequently, in the past few years several

simultaneous design methodologies have been proposed.

One class of methods utilizes linear optimal control theory to unify the structure/control design process. In this approach, the optimal controls are expressed as a function of the structural design variables and a design problem is then formulated in terms of the structural variables alone. In Ref. 51, this design problem consists of the minimization of a quadratic performance index subject to a constant structural mass constraint. Reference 52 constructs a composite objective function (structural mass plus quadratic performance index) which is minimized subject to constraints on the open loop eigenvalues via an optimality criterion method. In both cases the optimality conditions for linear optimal control are used to reduce the dimensionality of the design space.

An alternative approach, which treats both the structural and control variables as design quantities, is given in Ref. 53. In this case the structural and active control system design problems are performed sequentially within an iteration loop and are coupled through the constraints of the structural synthesis problem. The control system is designed first with the structural variables held constant. Then the structural mass is minimized subject to inequality constraints on the closed loop eigenvalues, with the control variables held constant. The process is repeated until convergence is attained.

Neither of the approaches discussed above actually integrates the structural and active control system design problems into a single synthesis problem statement in terms of an independent set of structural

and control design variables. Several other recent works, however, have begun to address this task. In Ref. 54, the integrated design problem is posed as the minimization of a composite objective function (structural mass plus quadratic performance index). The minimization process is carried out via numerical solution of the necessary conditions for the existence of an extremal control-structural parameter pair. In Ref. 55, a minimum modification strategy is developed which uses either direct output feedback control or steady state regulator control in conjunction with two distinct objective functions, namely, eigenvalue placement and minimum control gain Euclidian norm. The design variables considered include structural parameters, actuator locations, sensor locations and control gains. In Ref. 56 an eigenspace optimization approach is presented which also includes structural parameters, sensor/actuator locations, and control feedback gains in the design variable set. Two basic ideas underlie the approach taken in Ref. 56: (1) regions of the design space where the eigenvalue solution exhibits "extremely high sensitivity are generally undesirable," and (2) "rather than attempting to prescribe an exact point location for every eigenvalue, it is more reasonable to move all of the eigenvalues into an acceptable region of the complex plane." In Ref. 57, a truss structure, modeled as an equivalent continuum, is designed together with its active control system. The design problem is posed as the minimization of a composite objective function (structural mass plus steady state response) subject to inequality constraints on the closed loop eigenvalues and the structural design parameters. The analysis is formulated in the frequency domain and the optimization is carried out

using a nonlinear least squares algorithm.

1.3 Scope of the Work

Previous approaches to integration of the structural and active control system design functions into a unified synthesis methodology (with independent structural and control design variables) are deficient in several aspects. Probably the most serious difficulty with these methods is their failure to impose design constraints directly on the structural response quantities (e.g. dynamic displacements) and the actuator forces. Instead, the design of a system having acceptable response characteristics and control effort requirements is attempted through: 1) the imposition of constraints on the closed loop eigenvalues and/or 2) the selection of appropriate weighting matrices to be used in the formulation of a quadratic performance index. In either case, considerable experience and insight are required to select the parameters which will yield an acceptable design. This is especially true in the selection of the weighting matrices, where it is not uncommon to iterate several times in order to achieve the desired system response (e.g. Ref. 58).

Another shortcoming of many existing structure-control synthesis methodologies is that they are not easily extended to include of constraints associated with static loading conditions (e.g. static displacement and stress constraints). While it is true that many structural design problems may be dominated by constraints associated with dynamic loading alone, it is nevertheless important, for a significant class of structures, to address the possibility that both static and

dynamic failure modes as well as multiple load conditions will drive the design.

Other important considerations in the simultaneous design of structure-control systems, which have not been treated and will not specifically be addressed in this work, include: 1) plant modeling errors, 2) output sensing errors and 3) time delays in the control system dynamics.

In this work, a general methodology for control augmented structural synthesis is proposed for a class of structures which can be modeled as an assemblage of frame and/or truss elements. Structural sizing variables, active control feedback gains and lumped non-structural masses are treated simultaneously as independent design variables. Lower bound side constraints on the feedback gains are used to indirectly guard against dynamic instability (Ref. 18). Design constraints are imposed on dynamic displacements, actuator forces, undamped natural frequencies, static displacements, and static stresses. Multiple static and dynamic load conditions can be taken into account. Furthermore, the option to expand the design space by allowing independent feedback gain design variables, for each of several dynamic load conditions, is included. It is assumed that both the plant (structure) and the active control system dynamics can be adequately approximated with a linear model. While the proposed approach is fundamentally more general, here the methodology is developed and demonstrated for the case where: (1) the dynamic loadings are harmonic and therefore the steady state responses are of primary interest;

(2) direct output feedback is used for the control system model; and

(3) the actuators and sensors are collocated.

CHAPTER II

The Control Augmented Structural Synthesis Problem

2.1 Introduction

During the past decade optimization via general nonlinear mathematical programming methods has become widely accepted as a viable methodology for structural design. Here, mathematical programming methods have been coupled with finite element based structural analysis techniques, through the application of approximation concepts (Refs. 59-61), to yield a powerful design tool. Due to its generality, this approach is well suited for application to the design of control augmented structures. In this chapter the control augmented structural synthesis problem is formulated as a general nonlinear inequality constrained mathematical programming problem having a composite objective function. This problem is then replaced by three alternative nonlinear programming problems, each of which has a single distinct design objective.

2.2 Problem Formulation

An important class of control augmented structural synthesis problems may be stated as follows: seek a design $\bar{Y}^*$ which minimizes some measure of the system's performance subject to the condition that all appropriate measures of the system's behavior and all design variables remain within prescribed bounds. Mathematically, this statement can be written in the form of a nonlinear mathematical

programming problem as

$$\begin{aligned} \min_{\bar{D}} \quad & c_1 M(\bar{Y}) + c_2 J(\bar{Y}) \\ s.t. \quad & \bar{G}(\bar{Y}) \le \bar{0} \\ & \bar{Y}^L \le \bar{Y} \le \bar{Y}^U \end{aligned} \tag{2-1}$$

where the objective function is a weighted sum of the mass M and a performance index J, $\bar{Y}$ is a vector of design variables, $\bar{G}$ is a vector of behavior constraints (e.g. static and dynamic displacements, frequencies, static stresses, actuator forces), and $\bar{Y}^U$ and $\bar{Y}^L$ are upper and lower bounds on the design variables. In this work it is assumed that the structural topology, configuration, materials and loading conditions are prescribed and that the number and locations of the control system actuators and sensors are also specified. The design variables include the structural sizing variables. the control system feedback gains and lumped non-structural masses. For frame-truss structures the element sizing variables are, typically, cross sectional dimensions (CSD's) and/or the element reciprocal section properties (Ref. 61). Here the element CSD's have been chosen as the sizing variables.

Either of two options may be selected with respect to control system feedback gain design variables when multiple dynamic load conditions are involved: (1) the number of feedback gain design variables is equal to 2 per actuator (position gain and rate gain); (2) the number of feedback gain design variables is equal to 2 x K_d per actuator, where K_d equals the number of distinct dynamic load conditions. It should be understood that the foregoing options describe the number

of independent feedback gains prior to any linking of the control system design variables.

The synthesis problem statement represented by Eq. (2-1) is not completely defined until the weighting factors (c_1 and c_2) in the objective function are selected. While there is no conceptual difficulty with solving the problem, given specific values for the weighting coefficients, the a priori selection of appropriate values for c_1 and c_2 can be quite difficult. In fact, it is often necessary to solve such a problem several times with different values of the weighting coefficients before the desired design objective is obtained. An alternative approach to the problem is to consider the following two special cases: 1) the case where $c_1 = 1$ and $c_2 = 0$, and 2) the case where $c_1 = 0$ and $c_2 = 1$.

In the first case, the design problem objective function is simply the mass. A constraint can be added to the problem statement to limit the maximum allowable value of J, since it is not now represented in the objective function. The resulting problem statement is as follows:

$$\begin{aligned} &\min_{\overline{Y}} \; M(\overline{Y}) \\ &s.t. \;\; \overline{G}(\overline{Y}) \le \overline{0} \\ &\qquad J(\overline{Y}) \le J^U \\ &\qquad \overline{Y}^L \le \overline{Y} \le \overline{Y}^U \end{aligned} \tag{2-2}$$

where J^U is the upper bound on the performance index.

In the second case, the objective function includes only the performance index. Placing an upper bound constraint on the mass yields the following problem statement:

$$\begin{aligned} &\min_{\bar{Y}} \; J(\bar{Y}) \\ &s.t. \;\; \bar{G}(\bar{Y}) \le \bar{0} \\ &\qquad M(\bar{Y}) \le M^U \\ &\qquad \bar{Y}^L \le \bar{Y} \le \bar{Y}^U \end{aligned} \tag{2-3}$$

where M^U is the upper bound on the mass.

To complete the control augmented structural synthesis problem statements given by Eqs. (2-2) and (2-3) the form of the performance index must be considered. Typically, in the design of active control systems, a quadratic measure of the system response and control effort is used. In this work, since the loading under consideration is harmonic and the response of interest is steady state, the following linear form can be used:

$$J(\bar{Y}) = J_R(\bar{Y}) + J_C(\bar{Y}) = \sum_k \sum_j Q_{jk}|u_{jk}(\bar{Y})| + \sum_k \sum_i R_{ik}|F_{Aik}(\bar{Y})| \tag{2-4}$$

where J_R and J_C are the portions of the performance index associated with the system response and control effort, respectively. In Eq. 2.4 $|u_{jk}(\bar{Y})|$ represents the magnitude of the j-th displacement degree of freedom in the k-th dynamic load condition, $|F_{A_{ik}}(\bar{Y})|$ represents the magnitude of the i-th actuator force in the k-th dynamic load condition, and the Q_{jk}, R_{ik} denote the corresponding weighting factors.

The direct substitution of Eq. (2-4) into Eqs. (2-2) and (2-3) will yield a complete statement of the control augmented synthesis prob-

lem. However, the form of the performance index (Eq. (2-4)) leads to computational difficulties similar to those discussed relative to the use of a composite objective function formulation (i.e. structural mass plus performance index). Specifically, the design problem solution is dependent on the relative values assigned to thc two sets of weighting factors Q_{jk} and R_{ik}.

For the problem represented by Eq. (2-2) this difficulty can be alleviated by replacing the single performance index constraint with two constraints, giving

$$\begin{aligned} &\min_{\overline{Y}} \; M(\overline{Y}) \\ &s.t.\; \overline{G}(\overline{Y}) \le \overline{0} \\ &\quad J_R(\overline{Y}) \le J_R^U \\ &\quad J_C(\overline{Y}) \le J_C^U \\ &\quad \overline{Y}^L \le \overline{Y} \le \overline{Y}^U \end{aligned} \tag{2-5}$$

where J_R^U and J_C^U are upper bounds on a measure of system response and control effort, respectively. It should be noted that for many practical design problems the existence of nodal displacement constraints in the set of behavior constraints ($\overline{G}(\overline{Y})$) will adequately constrain the system response and, in those cases, the constraint on J_R can be removed from the problem statement.

For the design problem given by Eq. (2-3) the substitution of Eq. (2-4) leads to a composite form of the objective function. Again, it is useful to consider two special cases. First, letting the $R_{ik} = 0$ Eqs. (2-3) and (2-4) combine to yield

$$
\begin{aligned}
&\min_{\bar{Y}} \; J_R(\bar{Y}) \\
&s.t.\ \bar{G}(\bar{Y}) \le \bar{0} \\
&\quad M(\bar{Y}) \le M^U \\
&\quad J_C(\bar{Y}) \le J_C^U \\
&\quad \bar{Y}^L \le \bar{Y} \le \bar{Y}^U
\end{aligned}
\tag{2-6}
$$

where the upper bound constraint on J_C is added to compensate for the removal of the control effort measure from the objective function. Similarly, letting the $Q_{jk} = 0$ gives

$$
\begin{aligned}
&\min_{\bar{Y}} \; J_C(\bar{Y}) \\
&s.t.\ \bar{G}(\bar{Y}) \le \bar{0} \\
&\quad M(\bar{Y}) \le M^U \\
&\quad J_R(\bar{Y}) \le J_R^U \\
&\quad \bar{Y}^L \le \bar{Y} \le \bar{Y}^U
\end{aligned}
\tag{2-7}
$$

where the upper bound constraint on J_R is added to compensate for the removal of the response measure from the objective function (although it may be ignored for certain problems as described previously).

The three control augmented structural synthesis problems stated in Eqs. (2-5), (2-6) and (2-7) are applicable to the design of a significant class of structures and their associated active control systems. These problem formulations can be applied to achieve any one of the following three design objectives: 1) minimization of mass (Eq. (2-5)), 2) minimization of the structural response associated with selected degrees of freedom (Eq. (2-6)) and 3) minimization of total control effort (Eq. (2-7)). The solution to these problems can be

attempted via the direct application of various nonlinear programming algorithms. However, since both the objective functions and the constraints are, in general, complicated, implicit, nonlinear functions of the design variables this direct approach is computationally impractical even for small systems. A more tractable approach to the solution is to replace these implicit nonlinear problems with explicit approximate problems of reduced dimensionality. These problem statements are as follows:

$$\begin{aligned} &\min_{\bar{Y}} \ \tilde{M}(\bar{Y}) \\ &s.t. \ \tilde{g}_q(\bar{Y}) \le 0; \quad q \in Q_R \\ &\quad \tilde{J}_R(\bar{Y}) \le J_R^U \\ &\quad \tilde{J}_C(\bar{Y}) \le J_C^U \\ &\quad \tilde{Y}^L \le \bar{Y} \le \tilde{Y}^U \end{aligned} \tag{2-8}$$

$$\begin{aligned} &\min_{\bar{Y}} \ \tilde{J}_R(\bar{Y}) \\ &s.t. \ \tilde{g}_q(\bar{Y}) \le 0; \quad q \in Q_R \\ &\quad \tilde{M}(\bar{Y}) \le M^U \\ &\quad \tilde{J}_C(\bar{Y}) \le J_C^U \\ &\quad \tilde{Y}^L \le \bar{Y} \le \tilde{Y}^U \end{aligned} \tag{2-9}$$

and

$$\begin{aligned} &\min_{\bar{Y}} \ \tilde{J}_C(\bar{Y}) \\ &s.t. \ \tilde{g}_q(\bar{Y}) \le 0; \quad q \in Q_R \\ &\quad \tilde{M}(\bar{Y}) \le M^U \\ &\quad \tilde{J}_R(\bar{Y}) \le J_R^U \\ &\quad \tilde{Y}^L \le \bar{Y} \le \tilde{Y}^U \end{aligned} \tag{2-10}$$

where $\tilde{M}$, $\tilde{J}_R$ and $\tilde{J}_C$ are explicit approximations of the mass, response

measure and control effort measure, $\tilde{g}_q$ are explicit approximations of a subset Q_R of the original behavior constraints and $\bar{Y}$ is now the vector of linked design variables. The vectors $\tilde{\bar{Y}}^U$ and $\tilde{\bar{Y}}^L$ are the stepwise upper and lower bounds on the design variables and they are chosen to protect the quality of the approximations.

The solution to the original problems (Eqs. (2-5) - (2-7)) is obtained via the iterative construction and solution of a sequence of approximate problems having the form of Eqs. (2-8) - (2-10). The generation and solution of each approximate problem consists of the following three phases: 1) analysis, 2) approximate problem generation and 3) optimization. These three solution phases are applied iteratively (see Fig. 1) until convergence is attained. Each of these phases is described in detail in the following chapters.

CHAPTER III

Structural Analysis

3.1 Introduction

The structural analysis is an essential phase in the solution of the control augmented structural synthesis problem. The solution of the analysis problem yields the primary response quantities (e.g. frequencies, nodal displacements and element forces) required for the evaluation of the design constraints. While there are several techniques available for solving this problem, the method chosen here is the well known finite element displacement method (e.g. Ref. 62). This method is particularly attractive within the context the control augmented structural synthesis because 1) a variety of structures and loading conditions can be treated in a unified manner, 2) the method is relatively efficient and easy to implement, 3) the method is well suited for subsequent response quantity sensitivity calculations and 4) the method lends itself to the integration of the structural and control system models.

While the finite element method is applicable to a more general class of problems, those considered here are control augmented frame-truss structures subject to multiple static and harmonic dynamic loading conditions (including discrete nodal loads and loads uniformly distributed along the element) with homogeneous displacement boundary conditions. The underlying analysis equations are described in detail

in the following sections.

3.2 Static Analysis

The equations governing the response of a linear structural system subject to multiple static loading conditions are of the form

$$[K]\{u\}_k = \{P\}_k \; ; \quad k = 1,2,...K_s \tag{3-1}$$

where [K] is the structural stiffness matrix, $\{u\}_k$ and $\{P\}_k$ are the vectors of unknown displacements and known applied nodal loads (corresponding to the k-th loading condition), and K_s is the total number of static loading conditions. Eqs. (3-1) represent a set of linear simultaneous equations which can be generated from the element level stiffness matrices $[K]_i^e$ and load vectors $\{P\}_{ik}^e$ using an assembly technique known as the direct stiffness method (Ref. 62). The stiffness matrices and work equivalent load vectors (for uniformly distributed loading) for the space frame and truss elements are given in Appendix A.

Prior to the actual assembly of the system stiffness matrix and load vectors the element level quantities $[K]_i^e$ and $\{P\}_{ik}^e$ must be expressed in terms of a common system level or global coordinate system. This is accomplished by using the following transformation equations

$$[K]_i^g = [T]_i^T [K]_i^e [T]_i$$

$$\{P\}_{ik}^g = [T]_i^T \{P\}_{ik}^e \tag{3-2}$$

where $[K]_i^g$ and $\{P\}_{ik}^g$ are the element level stiffness matrix and load

vector, in global coordinates, for the i-th structural element. The orthogonal transformation matrix $[T]_i$ has the general form

$$[T]_i = \begin{bmatrix} [t_i] & & & \\ & [t_i] & & \\ & & [t_i] & \\ & & & [t_i] \end{bmatrix} \tag{3-3}$$

where (dropping the subscript i for convenience)

$$[t] = [R_\alpha][R_\theta][R_\beta] \tag{3-4}$$

and

$$[R_\alpha] = \begin{bmatrix} 1 & 0 & 0 \\ 0 & \cos\alpha & \sin\alpha \\ 0 & -\sin\alpha & \cos\alpha \end{bmatrix}$$

$$[R_\theta] = \begin{bmatrix} \cos\theta & \sin\theta & 1 \\ -\sin\theta & \cos\theta & 0 \\ 0 & 0 & 0 \end{bmatrix} \tag{3-5}$$

$$[R_\beta] = \begin{bmatrix} \cos\beta & 0 & \sin\beta \\ 0 & 1 & 0 \\ -\sin\beta & 0 & \cos\beta \end{bmatrix}$$

The angles α, θ and β, between the local and global coordinate systems, are shown in Fig. 2. It should be noted that the matrix [t] for the space truss element reduces to the form

$$[t] = [R_\theta][R_\beta] \tag{3-6}$$

by virtue of the fact that α may be arbitrarily set to zero making $[R_\alpha]$ an identity matrix.

Once Eqs. (3-1) have been assembled the homogeneous displacement boundary conditions may be applied. Conceptually this is done by eliminating those equations associated with the boundary degrees of freedom (in actual implementation these equations are never assembled). With the appropriate boundary conditions imposed Eqs. (3-1) represent a positive definite system of equations which can be solved for the unknown displacement vectors $\{u\}_k$. The solution method used here is based on a modified Cholesky decomposition technique which replaces [K] by a factorization of the form

$$[K] = [L][D][L]^T \tag{3-7}$$

where [L] is a lower triangular matrix and [D] is a nonsingular diagonal matrix. Once [K] has been decomposed the solution vectors $\{u\}_k$ are obtained through the usual series of forward and backward substitutions. It is important to recognize that significant computational and computer storage savings can be realized by taking advantage of the banded structure of Eqs. (3-1). Therefore, in this study, the solution method described above is implemented for a compact "skyline" storage arrangement of [K] as described in Ref. 63.

Having calculated the nodal displacement vector $\{u\}_k$; $k = 1,2,...K_s$, the end forces for the i-th structural element are given by

$$\{F\}^e_{ik} = [K]^e_i \{u\}^e_{ik} + \{FEF\}^e_{ik} \tag{3-8}$$

where $\{F\}^e_{ik}$, $\{u\}^e_{ik}$ and $\{FEF\}^e_{ik}$ are the forces, displacements and fixed end forces (corresponding to the uniformly distributed loading) associated with the i-th element for the k-th loading condition, written in the local coordinate system. The local displacements $\{u\}^e_{ik}$ are calculated from the global displacement vector $\{u\}_{ik}$ via the transformation

$$\{u\}^e_{ik} = [T]_i \{u\}_{ik} \tag{3-9}$$

where it is understood that $\{u\}_{ik}$ is the subset of the global displacement vector $\{u\}_k$ associated with the i-th element. The fixed end forces $\{FEF\}^e_{ik}$ for the uniformly distributed loading are given by

$$\{FEF\}^e_{ik} = - \{P\}^e_{ik} \tag{3-10}$$

where $\{P\}^e_{ik}$ is the work equivalent loading vector as defined in Eqs. (A-13) and (A-23) for the frame and truss elements, respectively.

3.3 Dynamic Response Analysis

The discretized equations of motion for a linear structural system subject to multiple dynamic loading conditions are given by the following second order differential equation:

$$[M]\{\ddot{u}\}_k + [C]\{\dot{u}\}_k + [K]\{u\}_k = \{P(t)\}_k; \quad k = \quad 1,2...K_d \tag{3-11}$$

where [M] is the system mass matrix, [C] is the viscous damping matrix, [K] is the structural stiffness matrix, and $\{\ddot{u}\}_k$, $\{\dot{u}\}_k$ and $\{u\}_k$ are the nodal accelerations, velocities and displacements corresponding to the k-th dynamic loading vector $\{P(t)\}_k$. Note that the system mass matrix [M] consists of two parts, that is

$$[M] = [M_S] + [M_L] \tag{3-12}$$

where $[M_S]$ denotes the structural mass matrix and $[M_L]$ represents the mass matrix associated with nonstructural lumped masses. Equation (3-11) can be generated via the assembly of the element level matrices $[M_i]^e$, $[C_i]^e$ and $[K_i]^e$, along with the load vectors $\{P_i\}_k^e$, in the same way that Eqs. (3-1) are formed. The stiffness and consistent mass matrices for the space frame and truss elements are given in Appendix A. The element level damping matrix ($[C_i]^e$) for a viscous damper can be generated from the truss element stiffness matrix by replacing $(EA/L)_i$ by the viscous damping coefficient c_i.

Equation (3-11) can be augmented to include the effects of the active control system by introducing the discretized control system actuator forces $\{N(t)\}_k$, giving

$$[M]\{\ddot{u}\}_k + [C]\{\dot{u}\}_k + [K]\{u\}_k = \{N(t)\}_k + \{P(t)\}_k \ ; \quad k=1,2...K_d \tag{3-13}$$

As was discussed in Chapter I, the actuator forces can be described in terms of either output, state or modal feedback gains. In this investigation, direct output feedback (Refs. 15-18) is used for the following reasons: 1) it leads to a control system which is relatively easy to implement, 2) a stable control system design based on an uncertain plant model will not result in an unstable system when applied to the real structure (i.e. the controller is robust, Refs. 6, 15, 18), 3) both the controllability and observability of the system are independent

of the feedback gains (Ref. 19) and 4) the robustness properties of the controller are preserved in the face of certain unmodeled sensor/actuator dynamics (Ref. 64).

The actuator forces can be written in terms of the system level position and velocity feedback gain matrices $[G_p]_k$ and $[G_v]_k$ as

$$\{N(t)\}_k = - [G_v]_k\{\dot{u}\}_k - [G_p]_k\{u\}_k \tag{3-14}$$

For the general case, the feedback gain matrices can be obtained from the equations (Refs. 15, 18)

$$[G_v]_k = [b_a][H_v]_k[b_v] \tag{3-15}$$

and

$$[G_p]_k = [b_a][H_p]_k[b_p] \tag{3-16}$$

where the jxm matrix $[b_a]$ relates the actuator outputs to the components of $\{N(t)\}_k$. The mxn matrices $[H_v]_k$ and $[H_p]_k$ contain the velocity and position feedback gains for the k-th dynamic load condition, and the nxj matrices $[b_v]$ and $[b_p]$ relate the components of $\{\dot{u}\}_k$ and $\{u\}_k$ to the velocity and position measurements. The dimensional quantities j, m, and n represent the number of degrees of freedom in the structural model, the number of actuators and the number of sensors, respectively. From the form of Eqs. (3-15) and (3-16) it is clear that the construction of system level feedback gain matrices depends on the location and orientation of the actuators and sensors and on how the sensor measurements are fed back to the actuators.

As an alternative to the general representation of the feedback gain matrices given by Eqs. (3-15) and (3-16), it is also possible to generate $[G_v]_k$ and $[G_p]_k$ via the concept of a control element. In this approach, the system level feedback gain matrices are assembled from element level gain matrices associated with control elements having pre-defined numbers of actuator and sensors and known actuator/sensor feedback schemes. One such element, which is similar in concept to a member damper (Ref. 6), is the member controller. This element (see Appendix B) can be thought of as a single force actuator connected between two points on the structure with a position and velocity sensor at each end of the actuator. These elements can be introduced into the system model as required and then assembled into the system feedback gain matrices in the same way that the structural elements are assembled. In this work the control system representation implemented is based exclusively on the use of axial force controller elements.

Given that the actuator forces have the form of Eq. (3-14), the closed loop equations of motion (Eq. (3-13)) can be written as follows:

$$[M]\{\ddot{u}\}_k + [C_A]_k\{\dot{u}\}_k + [K_A]_k\{u\}_k = \{P(t)\}_k; \qquad k=1,2...K_d \tag{3-17}$$

where the control augmented damping and stiffness matrices are given by

$$[C_A]_k = [C] + [G_v]_k \tag{3-18}$$

and

$$[K_A]_k = [K] + [G_p]_k \tag{3-19}$$

For the case where the external dynamic loading is harmonic, that is

$$\{P(t)\}_k = \{P\}_k\,(cos\Omega_k t + i\ \sin\Omega_k t) = \{P\}_k e^{i\Omega_k t} \tag{3-20}$$

the steady state solution of Eq. (3-17) has the form

$$\{u\}_k = \{u_R\}_k + i\{u_I\}_k = (\{c_R\}_k + i\{c_I\}_k)e^{i\Omega_k t} \tag{3-21}$$

Substituting Eqs. (3-20) and (3-21) into Eq. (3-17) gives

$$(-\Omega_k^2[M] + i\Omega_k[C_A]_k + [K_A]_k)(\{c_R\}_k + i\{c_I\}_k)e^{i\Omega_k t} = \{P\}_k e^{i\Omega_k t} \tag{3-22}$$

Equation (3-22) can be modified to include structural damping as follows

$$(\Omega_k^2[M] + i\Omega_k[C_A]_k + [K_A]_k + i\gamma[K])(\{c_R\}_k + i\{c_I\}_k)e^{i\Omega_k t} = \{P\}_k e^{i\Omega_k t} \tag{3-23}$$

where γ denotes the structural damping coefficient.

Eliminating $e^{i\Omega_k t}$ from both sides and equating the real and imaginary parts of Eq. (3-23) leads to the following matrix equations:

$$\begin{matrix} [K_A]_k - \Omega_k^2[M] & -\Omega_k[C_A]_k - \gamma[K] & \{c_R\}_k & \{P\}_k \\ & & = & \\ \Omega_k[C_A]_k + \gamma[K] & [K_A]_k - \Omega_k^2[M] & \{c_I\}_k & \{0\} \end{matrix}$$

$$k=1,2,\ldots K_d \tag{3-24}$$

For the general case, Eq. (3-24) represents a 2n x 2n set of indefinite,

non-symmetric linear simultaneous algebraic equations in the unknowns $\{c_R\}_k$ and $\{c_I\}_k$, where n is the order of the system model. These equations can be solved directly using any one of a number of well known linear equation solvers, although numerical ill-conditioning may occur near resonance if the system is not sufficiently damped. An alternative to the direct solution of Eq. (3-24), which requires the solution of two n x n sets of linear algebraic equations, is described in Appendix C. It should also be noted that the efficiency of the solution process can be enhanced for the case where $[K_A]_k$ and $[C_A]_k$ are symmetric by rewriting Eq. (3-24) in the following symmetric form:

$$\begin{bmatrix} \Omega_k[C_A]_k+\gamma[K] & [K_A]_k-\Omega_k^2[M] \\ [K_A]_k-\Omega_k^2[M] & -\Omega_k[C_A]_k-\gamma[K] \end{bmatrix} \begin{Bmatrix} \{c_R\}_k \\ \{c_I\}_k \end{Bmatrix} = \begin{Bmatrix} \{0\} \\ \{P\}_k \end{Bmatrix}; \quad k = 1,2,...K_d \tag{3-25}$$

This will be the case when the active control system is modeled with the member controller elements described previously.

Once Eq. (3-25) has been solved the steady state solution is obtained by substituting $\{c_R\}_k$ and $\{c_I\}_k$ into Eq. (3-21). Substituting the following well known identity

$$e^{i\Omega_k t} = \cos\Omega_k t + i \sin\Omega_k t \tag{3-26}$$

into Eq. (3-21) yields the steady state response in the alternate form

$$\{u\}_k = \{u_R\}_k + i\{u_I\}_k \tag{3-27}$$

where

$$\{u_R\}_k = \{c_R\}_k \cos\Omega_k t - \{c_I\}_k \sin\Omega_k t \tag{3-28}$$

and

$$\{u_I\}_k = \{c_R\}_k \sin\Omega_k t + \{c_I\}_k \cos\Omega_k t \tag{3-29}$$

The sine and cosine components of the dynamic displacements can be combined for the j-th degree of freedom as follows:

$$u_{R_{jk}} = |u_{jk}|\sin(\Omega_k t + \Psi_{jk}) \tag{3-30}$$

$$u_{I_{jk}} = |u_{jk}|\sin(\Omega_k t + \phi_{jk}) \tag{3-31}$$

where

$$|u_{jk}| = (c_{R_{jk}}^2 + c_{I_{jk}}^2)^{1/2} \tag{3-32}$$

$$\tan\Psi_{jk} = -c_{R_{jk}}/c_{I_{jk}} \tag{3-33}$$

$$\tan\phi_{jk} = c_{I_{jk}}/c_{R_{jk}} \tag{3-34}$$

Having calculated the steady state dynamic displacements using Eqs. (3-27), (3-28) and (3-29) it is now possible to recover the corresponding actuator forces. The velocity vector is obtained by differentiating Eqs. (3-27), (3-28) and (3-29) with respect to t yielding

$$\{\dot{u}\}_k = \{\dot{u}_R\}_k + i\{\dot{u}_I\}_k \tag{3-35}$$

$$\{\dot{u}_R\}_k = -\Omega_k\{c_R\}_k \sin\Omega_k t - \Omega_k\{c_I\}_k \cos\Omega_k t = -\Omega_k\{u_I\}_k \tag{3-36}$$

and

$$\{\dot{u}_I\}_k = \Omega_k\{c_R\}_k \cos\Omega_k t - \Omega_k\{c_I\}_k \sin\Omega_k t = \Omega_k\{u_R\}_k \tag{3-37}$$

For the general case, the steady state dynamic actuator forces are

obtained by substituting Eqs. (3-27) - (3-29) and Eqs. (3-35) - (3-37) into the actuator force equation

$$\{F_A\}_k = -[H_v]_k[b_v]\{\dot{u}\}_k - [H_p]_k[b_p]\{u\}_k \tag{3-38}$$

For the member controller, the element level steady state actuator forces are obtained for the ith actuator by substituting Eqs. (3-27) - (3-29) and Eqs. (3-35) - (3-37) into Eq. B-4 giving

$$\{F_A\}^e_{ik} = \{F_{AR}\}^e_{ik} + i\{F_{AI}\}^e_{ik} \tag{3-39}$$

$$\{F_{AR}\}^e_{ik} = -\{F_2\}^e_{ik}\,\sin\Omega_k t + \{F_1\}^e_{ik}\,\cos\Omega_k t \tag{3-40}$$

and

$$\{F_{AI}\}^e_{ik} = +\{F_1\}^e_{ik}\,\sin\Omega_k t + \{F_2\}^e_{ik}\,\cos\Omega_k t \tag{3-41}$$

where

$$\{F_1\}^e_{ik} = \Omega_k[H_v]^e_{ik}\{c_I\}^e_{ik} - [H_p]^e_{ik}\{c_R\}^e_{ik} \tag{3-42}$$

and

$$\{F_2\}^e_{ik} = -\Omega_k[H_v]^e_{ik}\{c_R\}^e_{ik} - [H_p]^e_{ik}\{c_I\}^e_{ik} \tag{3-43}$$

In Eqs. (3-42) and (3-43) $[H_p]^e_{ik}$ and $[H_v]^e_{ik}$ represent the position and velocity feedback gain matrices for the i-th control element in the k-th dynamic load condition. The vectors $\{c_R\}^e_{ik}$ and $\{c_I\}^e_{ik}$ are calculated from $\{c_R\}_k$ and $\{c_I\}_k$ via the transformations

$$\{c_R\}^e_{ik} = [T]_i\{c_R\}_{ik} \tag{3-44}$$

and

$$\{c_I\}^e_{ik} = [T]_i\{c_I\}_{ik} \tag{3-45}$$

where it is understood that the vectors $\{c_R\}_{ik}$ and $\{c_I\}_{ik}$ are subsets of the vectors $\{c_R\}_k$ and $\{c_I\}_k$ associated with the i-th control element.

Like the dynamic displacements [see Eqs. (3-30) - (3-34)] the sine and cosine terms of the actuator forces can be combined for each force component giving

$$F^e_{AI_{ik}} = |F^e_{A_{ik}}|\sin(\Omega_k t + \xi_{ik}) \tag{3-46}$$

and

$$F^e_{AR_{ik}} = |F^e_{A_{ik}}|\sin(\Omega_k t + \nu_{ik}) \tag{3-47}$$

where

$$|F^e_{A_{ik}}| = [(F^e_{1_{ik}})^2 + (F^e_{2_{ik}})^2]^{1/2} \tag{3-48}$$

$$\tan \xi_{ik} = F^e_{2_{ik}}/F^e_{1_{ik}} \tag{3-49}$$

$$\tan \nu_{ik} = - F^e_{1_{ik}}/F^e_{2_{ik}} \tag{3-50}$$

3.4 Eigenvalue Analysis

The discretized equations of motion governing the undamped vibration of a linear structural system are given by

$$[M]\{\ddot{u}\} + [K]\{u\} = \{0\} \tag{3-51}$$

where [M] is the system mass matrix (see Eq. 3-12), [K] is the structural stiffness matrix and where $\{\ddot{u}\}$ and $\{u\}$ are vectors of nodal accelerations and displacements, respectively. It is well known (e.g. Ref. 30) that the solution to Eq. (3-51) has the form

$$\{u(t)\} = \{\phi\}e^{i\omega t} \tag{3-52}$$

where $\{\phi\}$ and ω represent the spatial distribution and frequency of the motion. Substituting Eq. (3-52) into Eq. (3-51) and simplifying yields the structural dynamic eigenvalue problem given by the following equation:

$$[K]\{\phi\} = \omega^2 [M]\{\phi\} \tag{3-53}$$

Alternatively, Eq. (3-53) may be written to include all of the modeled frequencies and mode shapes as follows:

$$[K][\phi] = [M][\phi][\omega^2] \tag{3-54}$$

where $[\omega^2]$ is the diagonal matrix of natural frequencies and where $[\phi]$ contains the corresponding mode shapes. Various methods can be employed to solve Eq. (3-54). In this work a subspace iteration technique is used to solve for a subset of the natural frequencies and mode shapes (Refs. 65-66) of the undamped structural system.

CHAPTER IV

Approximate Problem Generation

4.1 Introduction

The key to a tractable control augmented structural synthesis formulation lies in the replacement of the original implicit nonlinear design problem with a sequence of explicit approximate problems of reduced dimensionality. The generation of these approximate problems is accomplished through the application of a variety of techniques commonly referred to as approximation concepts (Refs. 59-61). Primarily, these techniques serve to 1) reduce the numbers of design variables and constraints in the design problem and 2) reduce the required number of detailed (exact) constraint and objective function evaluations. There are various methods available for this purpose. Those implemented here include design variable linking, temporary constraint deletion and explicit first order constraint approximations. These techniques form the foundation of the approximate problem generation procedure which consists of the following steps: 1) objective function evaluation, 2) constraint evaluation, 3) temporary constraint deletion and 4) objective function and constraint approximation. This procedure is described in detail in the following sections.

4.2 Objective Function Evaluation

As was discussed in Chapter II three distinct choices of objective function are available. They are 1) system mass, 2) dynamic response at selected degrees of freedom and 3) control effort. Each of

these objective functions can be written as a function of the intermediate variables $\bar{X}$ which are chosen to be the reciprocal element properties (REP's) (i.e. 1/A for truss elements; $1/A$, $1/J$, $1/I_y$ and $1/I_z$ for frame elements; $1/h_{pk}$ and $1/h_{vk}$ for control elements; and $1/m$ for non-structural mass elements). In the first case the objective function is given by

$$M(\bar{X}) = \sum_i \rho_i A_i L_i + \sum_l m_l \tag{4-1}$$

where ρ_i, A_i and L_i are the mass density, area and length of the i-th structural element and m_l denotes the l-th lumped mass.

For the second case the objective function can be written as

$$J_R(\bar{X}) = \sum_k \sum_j Q_{jk} \, |u_{jk}(\bar{X})| \tag{4-2}$$

where $|u_{jk}(\bar{X})|$ is the magnitude of the j-th dynamic displacement in the k-th dynamic load condition and Q_{jk} is its associated weighting coefficient. The weighting coefficients are chosen such that Q_{jk} is equal to zero for displacement quantities which are not to be included in the objective function. Otherwise,

$$Q_{jk} = u_{a_{jk}}^{-1} \tag{4-3}$$

where $u_{a_{jk}}^{-1}$ is the allowable value associated with the dynamic displacement constraint imposed on $u_{jk}(\bar{X})$. Consequently, Eq. (4-2) can be rewritten as

$$J_R(\bar{X}) = \sum_{j,k \in N_R} \frac{|u_{jk}(\bar{X})|}{u_{a_{jk}}} \tag{4-4}$$

where N_R is the set of dynamic displacements included in J_R by the nonzero Q_{jk}.

In the third case the objective function is given by

$$J_C(\bar{X}) = \sum_{k=1}^{K_d} \sum_{i \in I_C} R_{ik} \, |F_{A_{ik}}(\bar{X})| \tag{4-5}$$

where $|F_{A_{ik}}(\bar{X})|$ is the magnitude of the i-th actuator force in the k-th dynamic load condition, R_{ik} is its associated scaling factor, I_C denotes the set of actuator forces included in J_C, and K_d equals the number of independent dynamic loading conditions. The R_{ik} coefficients are given by

$$R_{ik} = F_{a_{ik}}^{-1} \tag{4-6}$$

where $F_{a_{ik}}$ is the allowable value of the i-th actuator force. Using Eq. (4-6) the control effort objective function can be written as

$$J_C(\bar{X}) = \sum_{k=1}^{K_d} \sum_{i \in I_C} \frac{|F_{A_{ik}}(\bar{X})|}{F_{a_{ik}}} \tag{4-7}$$

4.3 Constraint Evaluation

The definitions of acceptable behavior are central to the control augmented structural synthesis problem statement. These definitions are included in the mathematical problem statement in the form of behavior constraints. Five basic types of behavior constraints are included here: 1) constraints on overall static structural stiffness (in the

form of nodal displacement/rotation constraints), 2) constraints on local element static strength (i.e. stress constraints) 3) constraints on steady state dynamic nodal displacements and rotations, 4) constraints on dynamic steady state actuator forces and 5) constraints on undamped natural frequencies.

The following options to impose additional constraints are included: 1) upper limits on response index J_R and control effort index J_C when mass minimization is the objective (see Eqs. 2-5); 2) upper limits on system mass M and control effort index J_C when response index minimization is the objective (see Eqs. 2-6); and 3) upper limits on system mass M and response index J_R when control effort index minimization is the objective (see Eqs. 2-7).

All of the constraints described above can be written as follows;

$$g_q = R_q - 1 \leq 0 \tag{4-8}$$

where the response ratio R_q is the ratio of some measure of the system behavior to its associated allowable value. This ratio is constructed such that it approaches unity as the behavior constraint becomes critical.

For each type of constraint the response ratio can be written in terms of the primary structural response quantities, the element REP's ($\overline{X}$), the design variables ($\overline{Y}$) and the allowable values. For the static displacement constraints R_q is given by

$$R_q(\bar{X}) = \frac{u_q(\bar{X})}{u_{a_q}} \tag{4-9}$$

where $u_q(\bar{X})$ is a single displacement quantity associated with the q-th displacement constraint and u_{a_q} is its associated allowable value. Similarly, for the static stress constraints R_q is written as

$$R_q(\bar{X},\bar{Y}) = \frac{\sigma_q(\bar{F}(\bar{u}(\bar{X}),\bar{X}),\bar{X},\bar{Y})}{\sigma_{a_q}} \tag{4-10}$$

where σ_q is a measure of the elemental stress state (which is dependent on the element cross section type) associated with the q-th strength constraint and σ_{a_q} is the allowable value.

In the case of the dynamic displacement and actuator force constraints, writing the response ratios directly in terms of the system response quantities would lead to a time dependent constraint formulation (see Eqs. (3-30) and (3-31)). However, since the steady state dynamic response is harmonic in nature, this time dependent constraint formulation can be replaced by a constraint on the magnitude of the response (see Eq. (3-32)). This is equivalent to constraining the response over the entire time interval of interest under the assumption that the interval is greater than or equal to the natural period of the response. Taking this approach the response ratios for a constraint on a single dynamic displacement quantity is given by

$$R_q(\bar{X}) = \frac{|u_q(\bar{X})|}{u_{a_q}} \tag{4-11}$$

where $|u_q(\bar{X})|$ is the magnitude of the displacement quantity (see Eq.

(3-32)) associated with the q-th dynamic displacement constraint and u_{a_q} is its allowable value. Similarly, the response ratio for a constraint on a combination of dynamic displacements is

$$R_q(\bar{X}) = \frac{J_R(\bar{X})}{J_R^U} \tag{4-12}$$

where $J_R(\bar{X})$ is given by Eq. (4-2) (with the weighting coefficients Q_{jk} chosen so that only the displacements of interest are included in the constraint) and where J_R^U is the upper bound allowable value.

Making the same assumption with respect to the time period of interest, the response ratio for a constraint on a single actuator force is written as

$$R_q(\bar{X}) = \frac{|F_{A_q}(\bar{u}(\bar{X}),\bar{X})|}{F_{a_q}} \tag{4-13}$$

where $|F_{A_q}(\bar{u}(\bar{X}),\bar{X})|$ is the magnitude of the actuator force (see Eq. (3-48) associated with the q-th constraint and F_{a_q} is its allowable value. Likewise, the response ratio for the control effort constraint is given by

$$R_q(\bar{X}) = \frac{J_C(\bar{X})}{J_C^U} \tag{4-14}$$

where $J_C(\bar{X})$ is given by Eq. (4-5) and J_C^U is the allowable upper bound value.

For the frequency constraints the response ratio is given by either

$$R_q(\bar{X}) = \frac{2\omega_{q_a}^2 - \omega_q^2(\bar{X})}{\omega_{q_a}^2} \tag{4-15}$$

when ω_{q_a} is the lower bound allowable value for the frequency, or by

$$R_q(\bar{X}) = \frac{\omega_q^2(\bar{X})}{\omega_{q_a}^2} \tag{4-16}$$

when ω_{q_a} is the upper bound allowable. In both instances $\omega_q(\bar{X})$ is the natural frequency associated with the q-th constraint.

Finally, the response ratio for the system mass constraint is

$$R_q(\bar{X}) = \frac{M(\bar{X})}{M^U} \tag{4-17}$$

where $M(\bar{X})$ is given by Eq. (4-1) and M^U is its allowable upper bound value.

4.4 Temporary Constraint Deletion

Proper design of a structural system usually requires the consideration of a substantial number of possible failure modes since, in general, the critical failure modes are not known at the outset of the design process. As a result, the synthesis problem statement may contain a large number of inequality constraints. In order to reduce the number of constraints, and the associated computational burden, it is possible to temporarily ignore certain constraints which are not expected to currently participate in the design. In effect, this process reduces the number of constraints by approximating the critical constraint set.

The criteria by which particular constraints are judged to be participating (active) or non-participating (passive) forms the basis of the constraint deletion technique. Various criteria are conceivable, however a relatively simple but effective strategy consists of deleting all constraints with response ratios (R_q) less than a specified constraint truncation parameter CTP. The value of CTP may, in general, be chosen separately for each constraint type and may change during the design process. In this work, a single value for CTP is used for all behavior constraints. The value of CTP is either set equal to a user prescribed value or it is calculated automatically such that: 1) constraints with $R_q \geq .7$ are always retained, 2) constraints with $R_q < .3$ are always deleted and 3) constraints with $.3 \leq R_q < .7$ are retained or deleted depending on the value of the response ratio cutoff parameter R_c. This criteria can be written as

$$CTP = \min\left\{ \max\{R_c, .3\}, .7 \right\} \tag{4-18}$$

where R_c is the maximum response ratio rounded down to the nearest tenth (e.g. if $\max_{q \in Q} R_q = .65$ then $R_c = .6$). When CTP is prescribed by the user its value is held constant during the entire design process. Otherwise, the value of CTP is updated for each approximate problem.

4.5 Objective Function and Constraint Approximations

A key element in the efficient solution of the structural synthesis problem lies in the construction of accurate explicit objective and constraint function approximations. This is particularly true in the case of the behavior constraint functions because, in general, exact evaluation

of these constraints requires that the structural analysis problem be solved. Various methods are available for the construction of these approximations, with the most commonly used techniques requiring only the first derivatives of the functions to be approximated (Refs. 60 and 67).

The most commonly used approximation consists of expanding the function in a linear first order Taylor series of the form

$$f(\bar{Y}) \cong \tilde{f}_L(\bar{Y}) = f(\bar{Y}_0) + \sum_{b=1}^{B} \frac{\partial f(\bar{Y}_0)}{\partial Y_b} (Y_b - Y_{0_b}) \tag{4-19}$$

where the expansion variables $\bar{Y}$ are chosen so that the resulting approximation is of the highest possible quality. In many cases, however, no single set of expansion variables may be chosen such that all function approximations are sufficiently robust . In this case it has been suggested (Ref. 68) that a hybrid or mixed variable approximation might be a useful alternative. This approximation can be constructed by the comparison of Eq. (4-19) with a first order Taylor series expansion of the form

$$f(\bar{Y}) \cong \tilde{f}_I(\bar{Y}) = f(\bar{Y}_0) + \sum_{b=1}^{B} \frac{\partial f(\bar{Y}_0)}{\partial (1/Y_b)} \left[\frac{1}{Y_b} - \frac{1}{Y_{0_b}} \right] \tag{4-20}$$

or, equivalently,

$$f(\bar{Y}) \cong \tilde{f}_I(\bar{Y}) = f(\bar{Y}_0) + \sum_{b=1}^{B} \frac{\partial f(\bar{Y}_0)}{\partial Y_b} \left[- Y_{0_b}^2 \left[\frac{1}{Y_b} - \frac{1}{Y_{0_b}} \right] \right] \tag{4-21}$$

Subtracting Eq. (4-19) from Eq. (4-21) gives

$$\tilde{f}_I(\bar{Y}) - \tilde{f}_L(\bar{Y}) = - \sum_{b=1}^{B} \frac{\partial f(\bar{Y}_0)}{\partial Y_b} \left[\frac{(Y_b - Y_{0_b})^2}{Y_b} \right] \tag{4-22}$$

For the case where $f(\bar{Y})$ represents an objective function to be minimized or a constraint function of the form $f(\bar{Y}) \leq 0$ Eq. (4-22) indicates that $\tilde{f}_I$ is more conservative than $\tilde{f}_L$ when

$$\frac{1}{Y_b} \frac{\partial f(\bar{Y}_0)}{\partial Y_b} < 0 \tag{4-23}$$

or, if Y_b represents some physical variable known to be positive in sign, when

$$\frac{\partial f(\bar{Y}_0)}{\partial Y_b} < 0 \tag{4-24}$$

Consequently, comparison of $\tilde{f}_I$ and $\tilde{f}_L$ on a term by term basis leads to the following first order mixed variable approximation:

$$f(\bar{Y}) \cong \tilde{f}_M(\bar{Y}) = f(\bar{Y}_0) + \sum_{b=1}^{B} \frac{\partial f(\bar{Y}_0)}{\partial Y_b} B_b \tag{4-25}$$

where

$$B_b = \begin{cases} (Y_b - Y_{0_b}) & \text{if} \quad \dfrac{\partial f(\bar{Y}_0)}{\partial Y_b} > 0 \\ \\ - Y_{0_b}^2 \quad (1/Y_b) - (1/Y_{0_b}) & \text{if} \quad \dfrac{\partial f(\bar{Y}_0)}{\partial Y_b} < 0 \end{cases} \tag{4-26}$$

This mixed variable approximation ($\tilde{f}_M(\bar{Y})$) is more conservative than either the pure linear approximation ($\tilde{f}_L(\bar{Y})$, see Eq. (4-19)) or the pure inverse approximation ($\tilde{f}_I(\bar{Y})$, see Eq. (4-20) or (4-21)). Numerical

experience has shown this approximation to be quite robust, yielding good results for a significant class of structural synthesis problems (e.g. Refs. 61 and 69). In this work, the mixed variable approximation defined by Eqs. (4-25) and (4-26) will be used for both the objective function and constraint approximations.

Clearly, from Eq. (4-25), construction of the objective function and constraint approximations requires the calculation of the partial derivatives of the function which is to be approximated. For the general case these derivatives can be written as

$$\frac{\partial f(\bar{Y}_o)}{\partial Y_b} = \left[\frac{\partial f}{\partial Y_b} + \sum_{j \in J_b} \frac{df}{dX_j} \frac{\partial X_j}{\partial Y_b} \right]_{\bar{X}_o, \bar{Y}_o} \tag{4-27}$$

where J_b is the set of REP's associated with the b-th design variable. The derivative of f with respect to X_j is given by either

$$\frac{df}{\partial X_j} = \frac{\partial f}{\partial X_j} + \sum_{n \in N_f} \frac{\partial f}{\partial u_n} \frac{\partial u_n}{\partial X_j} + \sum_{i \in I_f} \frac{\partial f}{\partial F_i} \frac{\partial F_i}{\partial X_j} \tag{4-28}$$

for the case where f is a function of the static response quantities,

$$\frac{df}{\partial X_j} = \frac{\partial f}{\partial X_j} + \sum_{n \in N_f} \frac{\partial f}{\partial |u_n|} \frac{\partial |u_n|}{\partial X_j} + \sum_{i \in J_f} \frac{\partial f}{\partial |F_{A_i}|} \frac{\partial |F_{A_i}|}{\partial X_j} \tag{4-29}$$

when f is a function of the dynamic response quantities or

$$\frac{df}{dX_j} = \sum_{m \in M_f} \frac{\partial f}{\partial \omega_m^2} \frac{\partial \omega_m^2}{\partial X_j} \tag{4-30}$$

when f is a function of the natural frequencies; where N_f, I_f, J_f and M_f are the sets of displacement degrees of freedom, element end forces,

actuator forces and frequencies associated with the function f.

The displacement derivatives required in Eqs. (4-28) and (4-29) can be computed in several ways (Ref. 70). In this work the partial inverse form of the pseudo-load method (Ref. 60) is employed. The eigenvalue derivatives needed in Eq. (4-30) are obtained via implicit differentiation of Eq. (3-53). Detailed formulations for the displacement, force and eigenvalue sensitivities, as implemented here, are given in Appendix D.

4.6 Move Limits

While the objective function and constraint approximations described previously are constructed to be of high quality, these approximations do not, in general, accurately represent the true functions over the entire design space. To ensure that the approximations are accurate enough during the solution of each approximate design problem a move limit strategy is employed. Specifically, side constraints are placed on the design variables to temporarily restrict the design space to a region over which the approximating functions are believed to be robust. These stepwise upper and lower bounds are calculated using the designer supplied move limit parameter d_m as follows:

$$\tilde{Y}_b^L = \max[Y_b^L, Y_b - d_m Y_b] \tag{4-31}$$

$$\tilde{Y}_b^U = \min[Y_b^U, Y_b + d_m Y_b] \tag{4-32}$$

where Y_b is the value of the b-th design variable at the beginning of

each approximate problem step and where Y_b^U and Y_b^L are the original side constraints on Y_b (see Eq. (2-1)).

CHAPTER V

Optimization

5.1 Introduction

By using the approximate problem generation techniques described in Chapter IV it is possible to replace each of the implicit nonlinear mathematical programming problems given by Eqs. (2-5), (2-6) and (2-7) with a sequence of explicit approximate problems, each having the form

$$\min_{\bar{Y}} \ \tilde{J}(\bar{Y})$$

$$s.t.\ \tilde{h}_q(\bar{Y}) \le 0 \ ; \ q \in \hat{Q}$$

$$\tilde{\bar{Y}}^L \le \bar{Y} \le \tilde{\bar{Y}}^U \tag{5-1}$$

where $\tilde{J}$ and $\tilde{h}_q$ are hybrid approximations (see Eqs. (4-25) and (4-26)) of the objective function and constraints and where $\tilde{\bar{Y}}^U$ and $\tilde{\bar{Y}}^L$ are the stepwise upper and lower bounds on the design variables. Each of these approximate problems is an explicit, separable, convex inequality constrained mathematical programming problem. The solution of these problems is discussed in the following section.

5.2 Design Optimization

The solution to the approximate design problem posed in Eq. (5-1) can be obtained either by solving the problem directly (i.e., solving the primal problem) or by constructing and solving the associated dual problem. The primal problem can be solved via any one of a

number of well known nonlinear inequality constrained minimization (Ref. 71-72) techniques. In this work, a modified feasible directions method (Ref. 73), as implemented in the CONMIN program (Ref. 74), is used.

The dual of Eq. (5-1) is given by

$$\max_{\bar{\lambda} \geq \bar{0}} l(\bar{\lambda}) \tag{5-2}$$

The dual function $l(\bar{\lambda})$ is defined as

$$l(\bar{\lambda}) = \min_{\bar{Y} \in \bar{Y}_F} L(\bar{Y},\bar{\lambda}) \tag{5-3}$$

where the Lagrangian function is given by

$$L(\bar{Y},\bar{\lambda}) = J(\bar{Y}) + \sum_{q \in \hat{Q}} \lambda_q \tilde{h}_q \tag{5-4}$$

and where $\bar{Y}_F$ is defined by

$$\bar{Y}_F = \{\bar{Y} \mid \tilde{\bar{Y}}^L \leq \bar{Y} \leq \tilde{\bar{Y}}^U\} \tag{5-5}$$

Solving Eq. (5-2) for the optimal dual variables $\bar{\lambda}^*$ will yield the optimal values for the primal variables $\bar{Y}^*$ if the dual maximization problem has a unique solution (saddle point).

It is well known that if the primal problem (Eq. (5-1)) is convex program (i.e., $\tilde{J}(\bar{Y})$ and $\tilde{h}_q(\bar{Y})$; $q \in \hat{Q}$ are convex functions and $\bar{Y}$ is contained in a convex subset of E^n) and has at least one strictly feasible solution (i.e., there exists some $\bar{Y}$ *s.t.* $\tilde{h}_q(\bar{Y}) < 0$, $q \in \hat{Q}$), then the dual problem has a unique saddle point $(\bar{Y}^*, \bar{\lambda}^*)$. If this saddle point can be found then $\bar{Y}^*$ solves the primal problem (Ref. 75). Since the hybrid approximations used in constructing Eq. (5-1) are convex (Ref. 69), it

follows (under the assumption that a strictly feasible design exists) that the solution to the approximate design problem can be obtained by maximizing the dual function.

While the dual method described above is clearly applicable to the solution of Eq. (5-1), the efficiency of such a solution scheme is an important consideration. In general, maximization of the dual function is complicated considerably by the imbedded Lagrangian minimization problem represented by Eq. (5-3). However, if $L(\overline{Y},\overline{\lambda})$ is additively separable then the solvability of Eq. (5-2) is enhanced by the fact that the Lagrangian minimization can be performed as a sequence of smaller minimization problems (Ref. 75). Furthermore, when this separability is complete the minimization of $L(\overline{Y},\overline{\lambda})$ simply consists of solving a sequence of single variable minimization problems (Refs. 76-77). Since the hybrid approximations used to construct the primal design problem are additively separable into functions of a single variable, an efficient explicit mixed variable dual method can be devised (Ref. 69).

Introducing the hybrid expressions for $\tilde{J}$ and $\tilde{h}_q$; $q\in\hat{Q}$ (see Eqs. (4-25) and (4-26)) Eq. (5-1) can be rewritten as

$$\min_{\bar{Y}} \sum_{m_b>0} m_b Y_b - \sum_{m_b<0} \frac{m_b}{Y_b} Y_{0_b}^2 + \hat{J}$$

$$s.t. \sum_{c_{bq}>0} c_{bq} Y_b - \sum_{c_{bq}<0} \frac{c_{bq}}{Y_b} Y_{0_b}^2 + \hat{h}_q \le 0 \quad ; \quad q = 1,2,...\hat{Q}$$

$$\tilde{Y}_b^L \le Y_b \le \tilde{Y}_b^U \quad ; \quad b = 1,2,...B \tag{5-6}$$

where

$$m_b = \frac{\partial J}{\partial Y_b} \tag{5-7}$$

$$c_{bq} = \frac{\partial h_q}{\partial Y_b} \tag{5-8}$$

$$\hat{J} = J(\bar{Y}_0) - \sum_{m_b>0} m_b Y_{0_b} + \sum_{m_b<0} m_b Y_{0_b} \tag{5-9}$$

$$\hat{h}_q = h_q(\bar{Y}_0) - \sum_{c_{bq}>0} c_{bq} Y_{0_b} + \sum_{c_{bq}<0} c_{bq} Y_{0_b} \tag{5-10}$$

The dual problem (Eq. (5-2)) may now be written as

$$\max_{\bar{\lambda} \ge 0} \min_{\bar{Y} \in \bar{Y}_F} L(\bar{Y},\bar{\lambda}) \tag{5-11}$$

where

$$L(\bar{Y},\bar{\lambda}) = \sum_{m_b>0} m_b Y_b - \sum_{m_b<0} \frac{m_b}{Y_b} Y_{0_b}^2 + \hat{J} +$$

$$\sum_{q \in Q} \lambda_q \left[\sum_{c_{bq}>0} c_{bq} Y_b - \sum_{c_{bq}<0} \frac{c_{bq}}{Y_b} Y_{0_b}^2 + \hat{h}_q \right] \tag{5-12}$$

Interchanging the order of the double summation in the fourth and fifth

terms, Eq. (5-12) can be rewritten as

$$L(\bar{Y},\bar{\lambda}) = \sum_{m_b>0} m_b Y_b - \sum_{m_b<0} \frac{m_b}{Y_b} Y_{0_b}^2 +$$

$$\sum_{c_{bq}>0} \left[\sum_{q\in Q} \lambda_q c_{bq} \right] Y_b -$$

$$\sum_{c_{bq}<0} \left[\sum_{q\in Q} \lambda_q c_{bq} \right] \frac{Y_{0_b}^2}{Y_b} + \sum_{q\in Q} \lambda_q \hat{h}_q + \hat{J} \qquad (5\text{-}13)$$

Letting

$$n_b = - m_b Y_{0_b}^2 \quad ; \quad m_b<0$$

$$C_b = \sum_{q\in Q} \lambda_q c_{bq} \quad ; \quad c_{bq}>0$$

$$D_b = - \sum_{q\in Q} \lambda_q c_{bq} Y_{0_b}^2 \quad ; \quad c_{bq}<0 \qquad (5\text{-}14)$$

and substituting into Eq. (5-13) yields

$$L(\bar{Y},\bar{\lambda}) = \sum_{m_b>0} m_b Y_b + \sum_{m_b<0} \frac{n_b}{Y_b} + \sum_{c_{bq}>0} C_b Y_b +$$

$$\sum_{c_{bq}<0} \frac{D_b}{Y_b} + \sum_{q\in Q} \lambda_q \hat{h}_q + \hat{J} \qquad (5\text{-}15)$$

Recognizing that the last two terms of Eq. (5-15) are constant with respect to $\bar{Y}$ and that the remaining terms are additively separable, the minimization of $L(\bar{Y},\bar{\lambda})$ can be performed via B single variable minimizations, i.e.:

$$\min_{\overline{Y}\in\overline{Y}_F} L(\overline{Y},\overline{\lambda}) = \sum_{b=1}^{B} \left[\min_{Y_b^L \le Y_b \le Y_b^U} L_b(Y_b,\overline{\lambda}) \right] \tag{5-16}$$

where

$$L_b(Y_b,\overline{\lambda}) = \begin{cases} m_b Y_b + C_b Y_b + \dfrac{D_b}{Y_b} & ; \quad m_b>0 \\ C_b Y_b + \dfrac{D_b}{Y_b} & ; \quad m_b=0 \\ \dfrac{n_b}{Y_b} + C_b Y_b + \dfrac{D_b}{Y_b} & ; \quad m_b<0 \end{cases} \tag{5-17}$$

The solution to the b-th single variable minimization, (temporarily ignoring the side constraints on Y_b), is given by

$$Y_b^2 = \begin{cases} \dfrac{D_b}{m_b + C_b} & ; \quad m_b>0 \\ \dfrac{D_b}{C_b} & ; \quad m_b=0 \\ \dfrac{D_b + n_b}{C_b} & ; \quad m_b<0 \end{cases} \tag{5-18}$$

Taking the side constraints into consideration, the solution to the b-th single variable minimization becomes (for C_b, $D_b > 0$)

$$Y_b = \begin{cases} \alpha_b \ \text{ if } \ (\widetilde{Y}_b^L)^2 \le \alpha_b^2 \le (\widetilde{Y}_b^U)^2 \\ \widetilde{Y}_b^L \ \text{ if } \ \alpha_b^2 \le (\widetilde{Y}_b^L)^2 \qquad ; \text{ for } \ m_b>0 \\ \widetilde{Y}_b^U \ \text{ if } \ \alpha_b^2 \ge (\widetilde{Y}_b^U)^2 \end{cases}$$

$$Y_b = \begin{cases} \gamma_b \text{ if } (\tilde{Y}_b^L)^2 \le \gamma_b^2 \le (\tilde{Y}_b^U)^2 \\ \tilde{Y}_b^L \text{ if } \gamma_b^2 \le (\tilde{Y}_b^L)^2 \quad ; \text{ for } m_b=0 \\ \tilde{Y}_b^U \text{ if } \gamma_b^2 \ge (\tilde{Y}_b^U)^2 \end{cases}$$

$$Y_b = \begin{cases} \beta_b \text{ if } (\tilde{Y}_b^L)^2 \le \beta_b^2 \le (\tilde{Y}_b^U)^2 \\ \tilde{Y}_b^L \text{ if } \beta_b^2 \le (\tilde{Y}_b^L)^2 \quad ; \text{ for } m_b<0 \\ \tilde{Y}_b^U \text{ if } \beta_b^2 \ge (\tilde{Y}_b^U)^2 \end{cases} \tag{5-19}$$

where

$$\alpha_b^2 = \frac{D_b}{m_b + C_b}$$

$$\beta_b^2 = \frac{D_b + n_b}{C_b}$$

$$\gamma_b^2 = \frac{D_b}{C_b} \tag{5-20}$$

Note also the following special cases:

$$Y_b = \tilde{Y}_b^L \text{ if } m_b \le 0 \text{ and } D_b = 0$$

$$Y_b = \tilde{Y}_b^U \text{ if } m_b \le 0 \text{ and } C_b = 0$$

$$\tilde{Y}_b^L \le Y_b \le \tilde{Y}_b^U \text{ if } m_b = C_b = D_b = 0 \tag{5-21}$$

Finally, using Eqs. (5-19) - (5-21), the dual problem may be written as an explicit problem in terms of $\bar{\lambda}$, that is

$$\max_{\bar{\lambda} \ge \bar{0}} l(\bar{Y}(\bar{\lambda}),\bar{\lambda}) \tag{5-22}$$

The dual problem given by Eq. (5-22) represents the quasi-unconstrained maximization of a concave function and, as such, is

solvable by various mathematical programming methods. Gradient based techniques are particularly attractive in this case since the first derivative of the dual function is immediately available from the primal constraint values (Ref. 75), i.e.:

$$\frac{\partial l(\bar{\lambda})}{\partial \lambda_q} = \tilde{h}_q \quad ; \quad q \in \hat{Q} \tag{5-23}$$

However, if $l(\bar{\lambda})$ does not possess continuous first derivatives these methods may exhibit slow or nonconvergent behavior. The dual function can be shown to be continuously first order differentiable under the following conditions: 1) $\bar{Y}$ is contained in a closed and bounded subset (S) of E^n, 2) $\tilde{J}$ and $\tilde{h}_q$; $q \in \hat{Q}$ are continuous on S and 3) $L(\bar{Y},\bar{\lambda})$ is minimized over S at a unique point $\bar{Y}(\bar{\lambda})$ for all $\bar{\lambda} \geq \bar{0}$. From Eqs. (5-18)-(5-21) it can be seen that these conditions are satisfied except for the case when m_b, C_b and D_b are all equal to zero. For the approximate design problems given by Eqs. (2-9) and (2-10) (i.e., the response minimization and control force minimization problems) it can be argued that the coefficients m_b will always be nonzero. Therefore, in these two cases a gradient based mathematical programming method can be used to solve the dual problem. In this work the dual problem is solved in the full dual variable space using the feasible directions method discussed previously. The dimensionality of the dual space is equal to the number of retained constraints. Therefore, solving the dual is generally more efficient than solving the primal if the number of retained constraints is less than the number of primal design variables.

CHAPTER VI

Numerical Results

6.1 Introduction

The control augmented structural synthesis methodology described in the preceding chapters has been implemented in a research computer program which is operational on the IBM 3090 computer at UCLA. This program has been used to generate numerical results for various example problems. These problems were selected so that, in addition to demonstrating the basic features of the design methodology, the results could be critically evaluated through insights into the physical behavior of the system.

6.2 Problem I - Cantilevered Beam, Mass Minimization

The first example problem is that of finding the minimum mass design of the cantilevered beam shown in Fig. 3. The beam is modeled with ten beam type finite elements (see Appendix A) each 1.0 m in length. The motion of the beam is constrained such that only vertical displacements and in-plane rotations are allowed. A concentrated mass (200 kg) is located at the midspan node and a vertical harmonic load ($P_1(t)$ = 4000 Nt sin (3.9 Hz)t) is applied at the tip. Two percent structural damping (γ = .02) is assumed. The design variables for this problem are the web and flange thickness (t_h,t_b) of the beam elements and the position and velocity feedback gains (h_p,h_v) of the control elements.

6.2.1 Case A - Uniform Structural Design

Two cases were studied for this problem. In the first case (Case A) the web and flange thickness variables are linked along the entire length of the beam. The initial values of these variables was taken to be 5.0 cm with side constraints imposed so that .5 cm $\leq t_h, t_b \leq$ 10.0 cm.

Three runs were made for Case A. In each run the magnitude of the vertical dynamic tip displacement is constrained to be less than 10.0 cm and the first undamped natural frequency must be greater than 4.0 Hz. Stepwise move limits of 30% (d_m = .3) were imposed on the design variables. In the first run (uncontrolled) there are no active control devices in the system. For the second run actuator #1 is added to the system and in final run actuators 1 and 2 are included. The initial values of the feedback gains are h_p = 20.0 Nt/cm and h_v = 5.0 Nt-sec/cm. Lower bound side constraints on the feedback gains ($h_p \geq$ .05 Nt/cm, $h_v \geq$ .05 Nt-sec/cm) ensure that the final designs will be dynamically stable (Ref. 18). The magnitude of each actuator force is constrained to be less than 20% of the external loading (800 Nt) and the total control force must be less than 35% of the loading (1400 Nt).

The iteration history data, final designs and final design response ratios for all three runs of Case A are given in Tables 1-3. The iteration history plots are shown in Fig. 4. In all three runs the tip displacement constraint is critical for the final design. The outboard actuator constraint is also critical for both of the controlled runs and the total control force constraint is critical in the final run. It is

interesting to note that when two actuators are included in the system the outboard actuator is favored in the final design. This is not unexpected since, for this problem, the undamped natural frequencies are all greater than the forcing function frequency and, therefore, the dynamic response is dominated by first mode behavior.

For all three runs the structural designs are changed from an initial uniform thickness distribution to the intuitively satisfying final designs in which the web thickness (t_h) takes on its minimum gage value. Also, the actuator position gains (h_p) consistently dominate the velocity gains (h_v) for the final designs. This is primarily due to the fact that the undamped natural frequencies are well above the forcing function frequency resulting in the stiffness augmentation being relatively more effective (as compared to the damping augmentation) in reducing the steady state response.

Examination of the objective function values for the final designs shows a large improvement over the initial infeasible designs for all runs. Also, moderate (13-20%) improvements in the final design mass are obtained as a result of the addition of active control.

6.2.2 Case B - Non-uniform Structural Design

The problem definition for Case B is identical to that of Case A except that the thickness design variables are allowed to vary along the length of the structure. The beam element thickness is linked pairwise along the length of the beam resulting in ten independent structural design variables.

Again, three runs were made; uncontrolled, controlled with one actuator and controlled with two actuators. Stepwise move limits of 30% were imposed on the design variables during the solution process. The iteration history data, final designs and final design response ratios are given in Tables 4-6. The iteration history plots are shown in Fig. 5. As in Case A, the tip displacement constraint is critical in the final design for all three runs. The outboard actuator constraint is also critical in both of the controlled runs. The total control force constraint is critical in the final run with the outboard actuator being favored over the inboard actuator.

From Table 5 one can observe that, as in Case A, the web thicknesses are at minimum gage in all final designs. However in this case the flange thicknesses taper along the length of the structure from a maximum value at the root to minimum gage at the tip. This tapered design is to be expected when the response is dominated by first mode behavior. Also note that the velocity gains are, once again, dominated by the position gains.

Examination of the objective function values for the final designs shows a large improvement over the initial infeasible designs for all runs. Small (6-9%) improvements in the final design mass are obtained as the actuators are added to the system. Finally, it should be noted that the final design objective function value for the uncontrolled run in this case is less than the two actuator run for Case A. This observation underscores the importance of utilizing any available structural design freedom as a means of achieving overall design goals.

6.3 Problem 2 - Cantilevered Beam, Response Minimization

In the second example the design goal is to minimize the dynamic tip displacement of the cantilevered beam shown in Fig. 3. The loading condition, design variables, initial design, behavior constraints, and side constraints are the same as those for Problem 1. In addition an upper bound constraint of 1000 kg is imposed on the structural mass.

6.3.1 Case A - Uniform Structural Design

Again, two cases were studied for this problem. In the first case the web and flange thicknesses are linked along the entire length of the beam. Three runs were made for Case A with stepwise move limits of 40% imposed on the design variables. The iteration history data, final designs and final design response ratios are given in Tables 7-9. The iteration history plots are shown in Fig. 6. The structural mass constraint is critical for all final designs and the outboard actuator constraint is critical for both controlled runs. For the final run the total control force constraint is also critical, with the outboard actuator being favored over the inboard actuator due to its greater effectiveness in controlling the tip response.

It is interesting to observe that the final structural designs are virtually identical for all three runs. This is intuitively satisfying since it is expected that the limited amount of structural material would exhibit a unique optimal distribution. As in Problem 1, the contributions to the actuator forces due to velocity feedback are small compared to

that due to the position feedback. Again this is due to the relative ineffectiveness of damping augmentation away from a resonance condition.

Finally, examination of the final design objective function values show a large improvement over the initial infeasible designs for all runs. Also, significant improvements (18-29%) in the final design tip displacement values are realized with the addition of active control.

6.3.2 Case B - Non-uniform Structural Design

Case B, for this problem, is identical to Case A except that the thickness design variables are allowed to vary along the length of the beam. The element thicknesses are linked pairwise along the length of the beam resulting in ten independent structural design variables. Three runs were made with stepwise move limits of 40% imposed on the design variables. In this case each approximate problem was solved in its dual form since the number of primal design variables is significantly greater than the average number of retained constraints.

The iteration history data, final designs and final design response ratios for all three runs are given in Tables 10-12. The iteration history plots are shown in Fig. 7. As in Case A, the structural mass constraint is critical in all three runs and the outboard actuator force constraint is critical for both controlled runs. The total control force constraint is also critical in the final run.

All three final designs have virtually identical material distributions with the flange thicknesses at minimum gage and the web thicknesses tapering from a maximum value at the root to minimum gage at the tip. Again, the actuator forces are dominated by the contribution due to the position gains.

The final design objective function values for all three runs are greatly improved over the initial infeasible designs. Also, the final design objective function value is significantly reduced (20-30%) with the addition of the active control devices. Finally, it should be noted that, as in Problem 1, the final objective function value for the uncontrolled run of Case B is less than the two actuator run of Case A.

6.4 Problem 3 - Cantilevered Beam, Control Force Minimization

In this example the design goal is to minimize the total control force for the control augmented cantilevered beam shown in Fig. 3. The loading condition, design variables, side constraints and frequency constraint are the same as in Problem 1. The magnitudes of the actuator forces are constrained to be less than 4000 Nt and the structural mass must be less than 400 kg.

Two cases were considered for this problem. Three runs were made for each case. In the first run only actuator #1 is included in the system. Only actuator #2 is included in the second while in the final run both actuators are included.

6.4.1 Case A - Uniform Structural Design

In Case A the web and flange thicknesses are linked along the length of the structure. The initial designs are given by $t_h = t_b = 2.5$ cm, $h_p = 20.0$ Nt/cm and $h_v = 5.0$ Nt-sec/cm. The magnitude of the tip displacement is constrained to be less than 5.0 cm and 40% move limits are imposed on the design variables.

The iteration history data, final designs and final design response ratios are given in Tables 13-15. The iteration history plots are shown in Fig. 8. The structural mass and tip displacement constraints are critical for all three final designs. The actuator force constraint is nearly critical in Run 2, indicating that the feasible region in this case is relatively small.

Comparison of the final design objective function values underscores the importance of proper selection of the actuator location. Clearly, when the actuator is placed at the inboard position (Run 2) rather than at the tip (Run 1), the required control force is significantly greater (38.1%). This is due to the fact that the first structural mode is more readily controlled at the outboard position. In the final run, where both actuators are included, the inboard actuator tends to "vanish" in favor of the outboard actuator yielding a final objective function value that is within 1.2% of that of Run 1.

Finally, it should be noted that the final structural designs are nearly identical for all three runs. Again, as in Problem 2, this is an indication of an essentially unique material distribution given a limited

amount of material for the problem.

6.4.2 Case B - Non-uniform Structural Design

In Case B the web and flange thicknesses are linked pairwise along the length of the beam. The initial designs for Runs 1 and 3 are given by t_b = 2.0 cm, t_h = .75 cm, h_p = 50.0 Nt/cm and h_v = 5.0 Nt-sec/cm. For the second run the initial design was t_b = 2.0 cm, t_h = .75 cm, h_p = 100.0 Nt/cm and h_v = 7.5 Nt-sec/cm. The magnitude of the tip displacement is constrained to be less than 4.0 cm and 40% move limits are imposed on the design variables.

The iteration history data, final designs and final design response ratios are given in Tables 16-18. The iteration history plots are shown in Fig. 9. The structural mass and tip displacement constraints are critical for all three final designs. As in Case A positioning the actuator at the outboard location results in significantly reduced control effort (49.9%). Also, in the final run the inboard actuator tends to "vanish", although in this case the objective function value is approximately 6.9% greater than that of Run 1. However, a subsequent run with tighter convergence criterion resulted in a difference of less than 1.7%

6.5 Problem 4 - Cantilevered Beam, Multiple Loading Conditions

This problem is the same as Problem 1, Case B except that three independent loading conditions are considered. The three loading conditions are given by $P_1(t)$ = 4000 Nt sin (3.9 Hz)t $P_2(t)$ = 4000 Nt sin (5.0 Hz)t and P_3 = 4000 Nt, M_3 = 2.0 x 10^5 Nt-cm, respectively.

Note that the third loading condition is a static loading condition (see Fig. 3). In addition to the constraints imposed in Problem 1, the static tip rotation is constrained to be less than .00796 rad and the lowest undamped natural frequency must lie between 4.0 Hz and 4.9 Hz.

Three runs were made for this problem using stepwise move limits of 30%. The iteration history data, final designs and final design response ratios are given in Tables 19-21. The iteration history plots are shown in Fig. 10. The dynamic tip displacement constraints (under both loading conditions) and upper bound frequency constraints are either critical or near critical for all three final designs. In addition, the outboard actuator force constraint (under loading condition #1) is critical in the second run and, in the final run, the static rotation constraint and both actuator force constraints (under loading condition #1) are critical.

For this problem several interesting observations can be made from the final design data. First, for the uncontrolled run the final structural material distribution exhibits characteristics typical of a vibration absorber. Specifically, while the flange thickness distribution initially tapers from the root towards the tip it increases again for the outboard elements (see Fig. 11). Also, the web thickness is significantly greater than its lower bound value near the tip. Both of these conditions combine to simulate a sprung non-structural mass near the tip of the beam. This behavior is also seen, to a lesser degree, in the final design for Run 2. The existence of the vibration absorber characteristics in these designs results from the upper bound on the

undamped natural frequency which prohibits the purely tapered designs achieved in Problem 1.

It is also interesting to note that the contribution to the actuator forces due to velocity feedback is more significant for this problem than it was for Problem 1. This is due to the fact that the first natural frequencies for the final structural designs are near the 5.0 Hz forcing function frequency of load condition 2. As a result the effectiveness of the damping augmentation in controlling the steady state response is increased.

The addition of the inboard actuator in the third run resulted in satisfaction of the dynamic displacement constraints without resorting to the vibration absorber type of design. In this case the structural stiffness was allowed to decrease enough to cause the static tip rotation constraint to become critical.

Finally, examination of the final design objective function values shows a significant decrease (16-49%) in the structural mass with the introduction of active control.

6.6 Problem 5 - Cantilevered Beam, Lumped Mass Design Elements

The problem statement for this example is the same as that for Problem 4 except that two lumped non-structural mass design variables are included in addition to the structural and control variables considered previously. One lumped mass is located at each end of element #10. The design goal is to minimize the total system mass

(structural plus non-structural mass) subject to the same constraints imposed in Problem 4.

Three runs were made; uncontrolled, controlled with one actuator and controlled with two actuators. The initial values for the lumped masses are given by m = 5.0 kg, lower bound side constraints imposed such that $m \geq .1$ kg. Stepwise move limits of 30% were imposed on the design variables.

The iteration history data, final designs and final design response ratios are given in Tables 22-24. The iteration history plots are shown in Fig. 12. The dynamic tip displacement constraints (under both loading conditions) and upper bound frequency constraints are either critical or near critical for all three final designs. The outboard actuator force constraint (under loading condition #1) is also critical in the second run. The static rotation constraint and the force in actuator 1 (under loading conditions 1 and 2) are critical in the final run.

It is interesting to note that for Runs 1 and 2 the inclusion of the lumped mass design variables resulted in overall mass reductions as compared to Runs 1 and 2 for Problem 4. Specifically, in Run 1 the addition of 9.37 kg of non-structural mass resulted in a reduction of 4.28 kg in total system mass. In Run 2 the system mass was reduced by 9.10 kg when 6.73 kg of non-structural mass was added. This should not be too surprising given the nature of the final designs. Apparently, a more efficient vibration absorber design was realizable with the addition of the lumped masses since the absorber stiffness and mass are not completely coupled as before. The changes in the

structural material distribution can be seen by comparing Fig. 13 with Fig. 11.

In the final run the addition of the lumped mass design variables resulted in a final design objective function value which is slightly greater than that obtained without the lumped masses. In this case the final design is driven by the static tip rotation constraint and does not exhibit the characteristics of a vibration absorber. Therefore, the lumped masses would not be expected to improve the design. A subsequent run with tighter convergence tolerance gave a final system mass value which was very close to that obtained in Problem 4, Run 3.

6.7 Problem 6 - Cantilevered Beam, Independent Actuator Gains

Problem 6 is the same as Problem 4 except that in this case the actuator gain design variables are determined independently for each dynamic loading condition. It is assumed here that the service environment under which the system must operate is either known or can be detected and that the system experiences either dynamic loading condition #1 or #2, but not both simultaneously. The structural frequency and static displacement constraints are imposed regardless of the dynamic loading. In this way the structure is designed for all operating conditions simultaneously while the system as a whole is optimally adaptable to the service environment by switching between appropriate sets of optimal actuator gains.

Two runs were made for this problem. In the first run only the outboard actuator is included in the system. Both actuators are included in the second run. Stepwise move limits of 30% are imposed on the design variables for both cases. The iteration history data, final designs and final design response ratios are given in Tables 25-27. The iteration history plots are shown in Fig. 14. The dynamic tip displacement constraint (under loading condition #1) and the upper bound frequency constraint are critical for both runs. The outboard actuator force constraint (under loading condition #1) is critical in Run 1 while the static tip rotation constraint and both actuator force constraints (under loading condition #1) are critical in the final run.

Several interesting observations can be made here. First, the actuator gains corresponding to loading condition #2 do not change from the initial design values. This is due to the fact that the tip displacement constraint for loading condition #2 is so far from its upper bound value that it is never retained in the approximate design problem. The absence of this constraint as a design driver suggests that active control devices are not required when the system is subjected only to loading condition #2. By removing the actuator from the system for this loading condition and obtaining the same final structural design the foregoing conjecture was verified. It was also observed that the dynamic tip displacement was reduced indicating that the addition of active control actually adversely affects the tip displacement for loading condition #2. This can be attributed to the fact that the initial actuator gains used in this example increase the effective stiffness of the system, moving the design closer to resonance.

The previous observations are consistent with the fact that the final design mass for Run 1 is 16% less than that obtained when one set of actuator gains are used for both dynamic loading conditions. By allowing the actuator gains for the first loading condition to change independently of those for the second loading condition the stiffness augmentation is increased thereby pushing the closed loop frequencies away from the forcing function frequency of loading condition #1 without adversely affecting the response associated with the second loading condition.

Finally, it should be noted that allowing independent actuator gains does not appreciably change the final design objective function value for the second run. This is not unexpected since the structural design tends to be driven by the static tip rotation constraint. However, even though the final structural design is not much different than that obtained in Problem 4, Run 3 the control system design and active constraint set differs significantly.

6.8 Problem 7 - Planar Truss, Control Force Minimization

The design goal in this example is to minimize the total control force for the control augmented planar truss structure shown in Fig. 15. This structure has previously been used to study the interaction of active and passive control techniques in Ref. 48. The system consists of an assemblage of ten truss elements (see Appendix A) and four active control elements. The motion of the structure is constrained so that only horizontal and vertical displacements are allowed. The truss members are made of aluminum with $E = 10.0 \times 10^6$ psi and $\rho = .1$

lb/in^3, and the actuators act in the y-direction only. In addition, a single concentrated non-structural mass (1.29 lb-sec/in) is placed at each of nodes 1-4 to represent the mass of the actuators and sensors. Two percent structural damping is assumed.

Two loading conditions are considered for this problem. Loading condition #1 consists of a two dynamics loads acting in the vertical direction at nodes 3 and 4. The form of each load is given by $P_1(t)$ = 500 lb sin (3.0 Hz)t. The second loading condition consists of a static load P_2 = 500 lb acting in the negative y direction at node numbers 1-4.

Three cases are considered for this problem. In the first case (Case I) the structural design is fixed with the area of each truss given by A = .1 in. The design variables are the position and velocity gains for the four actuators. The initial values of the gains are given by h_p = 10.0 lb/in and h_v = 10.0 lb-sec/in. Side constraints limit the gains so that $h_p \geq .05$ lb/in and $h_v \geq .05$ lb-sec/in. The magnitudes of the vertical dynamic displacements are constrained to be less than .5 in and the force output of each actuator is limited to 200.0 lb.

In the second case (Case II) both the truss areas and actuator gains are allowed to vary. The initial structural design is uniform with A = 1.0 in and upper and lower bound side constraints of 1.0 in and .01 in are imposed. The initial values and lower bounds for the position and velocity gains are the same as in Case I. In addition to the dynamic displacement and actuator force constraints described previously the following constraints are imposed for this case: 1) the

structural mass must be less than or equal to that of the original structure (4.88 lb), 2) the first mode frequency must be greater than the forcing function frequency (3.0 Hz) but less than the first mode frequency of the original structure (3.44 Hz) and 3) the axial stress in any truss member must not exceed 20.0 ksi. Case III is identical to Case II except that the allowable stress is increased to 22.0 ksi.

The iteration history data and final designs for all three cases are given in Tables 28 and 29. The iteration history plots are shown in Fig. 16. The dynamic displacement constraints at nodes 2 and 4 are critical in the final designs for all three cases. The upper bound frequency and structural mass constraints are critical in Cases II and III. In Case II the stress constraints for truss members 1,3,4,6,7, and 8 are critical while members 1,3,7 and 8 are stress critical in Case III.

The important observation here concerns how the structural material distribution effects the control force required to meet the dynamic displacement constraints imposed on the problem. It should be noted that the structural mass and first mode undamped natural frequency are the same in all three cases. However, as Table 29 shows, the material distributions are significantly different. In Case II allowing the structural design to change resulted in a 61.5% reduction in total control force over Case I, even with the addition of the stress constraints. An additional 13.4% reduction was obtained by relaxing the stress constraint by 10%. Clearly, changes in the structural design (in terms of both material distribution and selection) can significantly effect active control system requirements.

6.9 Problem 8 - Antenna, Response Minimization

In Problem 8 the antenna structure shown in Fig. 17 is to be designed so that the magnitudes of the vertical dynamic displacements are minimized. The structure consists of an assemblage of eight aluminum beams ($E = 7.3 \times 10^6$ Nt/cm, $\mu = .325$, $\rho = 2.77 \times 10^{-3}$ kg/cm) each having a rectangular cross section (see Fig. 18). Two percent structural damping is assumed. Actuators, located at the corner nodes (2,4,5 and 7), act in the vertical direction. The structure is subjected to two independent dynamic loading conditions. In each loading condition a single harmonic force is applied to member #4 at a distance of 10.0 cm from the centerline of the structure causing excitation of both symmetric and anti-symmetric modes. The forces are given by $P(t) = 100$ Nt $\sin(\omega)t$, where $\omega = 5.0$ Hz for the first loading condition and $\omega = 10.0$ Hz for the second loading condition. In addition to the dynamic loads the structure is also subjected to a uniformly distributed static loading of 1.5 Nt/cm along the length of each beam member, acting in the negative y direction.

Two cases were considered for this problem. In the first case (uncontrolled) the actuators are removed from the system and the thicknesses, widths and heights of the structural members are designed to minimize the sum of the magnitudes of the vertical dynamic displacements at nodes 2,4,5 and 7 (summed over the two dynamic loading conditions). Linking is employed to force the final design to be symmetric with respect to the x-y plane leaving 15 independent design variables. The initial design is uniform ($t = .5$ cm, $b = h = 20.0$ cm)

with side constraints imposed so that .1 cm $\leq t \leq$ 1.0 cm and 10.0 cm $\leq b,h \leq$ 25.0 cm. Move limits of 10% were imposed during the design process. In addition to the side constraints the following behavior constraints are also included: 1) the fourth mode frequency must be greater than or equal to 8.0 Hz, 2) the fifth mode frequency must be greater than or equal to 9.25 Hz, 3) the Von-Mises static stress (as evaluated at the points shown in Fig. 18) at both ends of each beam member must not be greater than 2.0 x 10^4 Nt/cm^2 and 4) the total structural mass must be less than or equal to 700.0 kg.

The second case (controlled) is identical to the first except that control elements at the corner nodes are included. In this case the beam cross sectional dimensions (CSD's) and the actuator position and velocity gains are varied. As in Problem 6, the gains are determined independently for each loading condition, so that there are a total of 31 design variables for the problem (15 CSD's plus 16 gains). The initial structural design, side constraints and move limits are the same as those used for the controlled case. The initial actuator gains are given by h_p = 100.0 Nt/cm and h_v = 10.0 Nt-sec/cm with side constraints imposed so that $h_p \geq$ .05 Nt/cm and $h_v \geq$ .05 Nt-sec/cm. In addition to the constraints imposed previously, each actuator force output is limited to a maximum of 15.0 Nt in this case.

The iteration history data and final structural designs for both cases are given in Tables 30 and 31. The iteration history plots are shown in Fig. 19. In both cases the critical constraints include 1) the lower bound frequency constraints on the fourth and fifth modes, 2)

the static stress constraint for member #1 (at the fixed end) and 3) the structural mass constraint. The objective function value is significantly improved over that of the initial infeasible design as a result of both the addition and redistribution of structural material. The addition of active control resulted in a further reduction of 40.9% as compared to the uncontrolled case.

The complexity of the structure and the modes participating in the response does not allow for a simple interpretation of the final designs in this case. However, it is interesting to note that even though the structural design is forced to be symmetric via linking, the final actuator forces are not (see Table 32). This is to be expected since, as mentioned previously, the point of application of the external dynamic force causes both the symmetric and anti-symmetric modes to be excited, leading to a non-symmetric response.

6.10 Problem 9 - Grillage

The final example problem involves the design of the 8 by 11 planar grillage shown in Fig. 20. The grillage, similar to the one described in Ref. 78, consists of a lattice of 19 aluminum frame members (ρ = .1 lb/in, E = 10.5 x 10^6 psi, ν = .3) placed on one foot centers and cantilevered from two fixed supports by 20 inch long flexible beams. Each solid rectangular member is 2.0 in wide and has an initial thickness of .25 in. The members are oriented so that the width dimension lies in the plane of the structure. The grillage is augmented with 24 active control elements, uniformly distributed over the grillage, acting in the z direction. The mass of each actuator (1.296 x 10^{-3} lb-

sec^2/in) is modeled as fixed non-structural mass. The grillage is subjected to a dynamic loading (P(t) = 16.9 lb sin(2.0 Hz)t) applied at node 6 in the z direction. Two percent structural damping is assumed.

Two runs were made for this problem. In the first run (control force minimization) the design goal is to minimize the total control force subject to upper bound constraints of 1.0 in on the magnitudes of the out-of-plane dynamic displacements at the four corners of the grillage. The design variables are the control element position and velocity feedback gains which are initially set to h_p = .1 lb/in and h_v = .25 lb-sec/in for all actuators. Lower bounds are imposed on the gains so that $h_p \geq$ .001 lb/in and $h_v \geq$ .001 lb-sec/in. The design variables associated with each actuator are linked with those of the actuator located at its symmetric (relative to the y-z plane) grid point (see Fig. 20) resulting in 24 independent design variables. Actuator force constraints are also employed to limit each actuator output to a maximum of 2.0 lb. Note that the structural design is fixed (w = 2.0 in, t = .25 in) for this run.

In the second run (weight minimization) the design goal is to minimize the structural weight of the grillage. In this case both the actuator gains and the structural member thicknesses are included as design variables. The initial values and lower bounds for the gains are the same as in Run 1. The member thicknesses are initially .25 in. with side constraints imposed so that .1 in $\leq$ t $\leq$ .5 in. In addition to the dynamic displacement and actuator force constraints, an upper bound constraint is imposed on the total control force for this run.

The upper bound value was chosen to be equal to the final design value of the total control force for Run 1 (3.61 lb).

Iteration history data as well as initial and final design actuator forces for these runs are given in Tables 33 and 34. The iteration history plots are shown in Fig. 21. A significant reduction (60%) in the total force was realized in Run 1 by redistributing the actuator forces to more efficiently control the second and third structural modes.

For the second run, all of the structural members achieve the lower bound thickness value (.1 in) except for members 2,8,11 and 17. The final thickness values for these members are t_2 = .2993 in, t_8 = .2284 in, and $t_{11} = t_{17}$ = .3959 in. It should be noted that, although symmetry of the actuator gains was enforced through design variable linking, the expected structural symmetry in the final structural design was obtained without without linking. Also, the thickness of the main load carrying members (11 and 17) has increased by 58%. Finally, a 58.9% reduction in the structural weight was obtained with no increase in the total control force over that of Run 1.

CHAPTER VII

Conclusions and Recommendations

7.1 Conclusions

A synthesis methodology for the design of control augmented structures modeled as assemblages of frame and/or truss elements has been presented. The control system is modeled with specialized active control elements designed to represent collocated actuator-sensor pairs employing a direct output feedback scheme. It is assumed that the behavior of both the structure and the active control system is linear. Multiple static and steady state dynamic loading conditions are considered simultaneously.

The design problem is posed as a general nonlinear programming problem in which the structural sizing variables, non-structural lumped masses and control system feedback gains are treated simultaneously as design variables. The objective function can be chosen to be either total system mass, total active control force or a measure of the system dynamic response. Constraints on static displacements and stresses, natural frequencies, dynamic displacements, actuator forces, total control force, and total system mass are considered. Side constraints on the design variables are included to prevent the generation of unrealizable structural designs and to maintain dynamic stability.

The general design problem is solved through the iterative construction and solution of a sequence of explicit approximate problems.

Each approximate problem is generated through the application of a variety of approximation concepts and then solved using a feasible directions algorithm.

The methodology summarized above has been implemented in a research computer program and has been used to solve a number of illustrative example problems. These problems serve to demonstrate the viability of the proposed design technique. Near optimal designs can typically be obtained within 10-15 design iterations. It is expected that improvements in both the constraint and objective function approximations would lead to even faster convergence.

In addition to validating the proposed design methodology, the numerical examples presented in this work serve to underscore the importance of integrating the structural and control system design processes. Clearly, the extent to which the structural and/or control system design can be improved by an integrated design process is problem dependent. However, it is demonstrated here that the best designs are consistently obtained when the structure and control system are designed simultaneously. It has been shown that both structural mass and system response can be effectively reduced through the addition of active control devices (see Problems 1,2,4,5,6 and 8). It was also observed that even more significant reductions in active control force can be realized through optimal structural modifications (see Problems 3,7 and 9).

7.2 Recommendations for Future Work

The synthesis methodology presented in this work can be used to design a significant class of control augmented structural systems. While this work represents an important step towards the practical integration of the structural and control system design processes, several areas of future investigation can be identified which will lead to increases in efficiency of the design process and/or broaden its applicability.

Within the context of the current capability several possibilities exist for improving solution efficiency. Since the majority of the expense for each design iteration lies in the solution of the governing equations, reducing the number of design iterations will lead to significant reductions in total solution time. The key to fewer design iterations is the construction of more robust approximate problems. One possible way to improve the accuracy of the approximate problem is to replace the current constraint and objective function approximations with a scheme whereby only the implicit quantities appearing in these functions are approximated, with the remaining explicit nonlinearity being retained in the approximate problem.

In addition to reducing the number of analyses required in the design process, efficiencies can be gained by reducing the expense of each individual analysis. Two possible techniques for reducing the analysis cost are 1) to devise a reduced order analysis method based on pre and post multiplication of the steady state response equations by a subset of the undamped normal modes of the structure and 2) to

implement the solution scheme outlined in Appendix C for either the full or reduced order system.

In order to extend the methodology to a broader class of problems it will be important to consider more general control system models. Non-collocated actuator-sensor pair nodels could be implemented directly into the current capability for the case where symmetric feedback was used. Non-symmetric feedback would destroy the symmetry of the equations governing the steady state response and thus would require the implementation of an appropriate equation solver. The consideration of other forms of feedback (other than direct output feedback) may require that an alternative method be used to solve for the dynamic response. However, it should be emphasized that any appropriate analysis method can be incorporated into the design methodology.

Other areas of investigation which will be important for the solution of practical problems include 1) investigating the feasibility of directly constraining dynamic stability via constraints on the real parts of the closed loop eigenvalues, 2) the implementation of dynamic stress constraints and 3) the consideration of loading conditions composed of forces having different forcing function frequencies.

REFERENCES

1. Yao, James T.P., "Concept of Structural Control," *Journal of the Structural Division*, ASCE, Vol. 98, No. ST7, July 1972, pp. 1567-1574.

2. Hedrick, J.K. and Wormley, D.N., "Active Suspension for Ground Transportation Vehicles -- A State-of-the-Art Review," *Mechanics of Transportation Systems*, AMD, Vol. 15, ASME, 1975, pp. 21-40.

3. Seltzer, Sherman M., "Dynamics and Control of Large Space Structures: An Overview," *The Journal of Astronautical Sciences*, Vol. XXVII, No. 2, April-June 1979, pp. 95-101.

4. Likins, Peter, "The New Generation of Dynamic Interaction Problems," *The Journal of Astronautical Sciences*, Vol. XXVII, No. 2, April-June 1979, pp. 103-113.

5. Nurre, G.S., Ryan, R.S., Scofield, H.N. and Sims, J.L., "Dynamics and Control of Large Space Structures," *Journal of Guidance, Control and Dynamics*, Vol. 7, No. 5, Sept.-Oct. 1984, pp. 514-526.

6. Soosar, K., et al., "Passive and Active Suppression of Vibration Response in Precision Structures -- State-of-the-Assessment, Technical Report R-1138, Vol. 2, The Charles Stark Draper Laboratories, Inc., Cambridge, Massachusetts, Feb. 1978.

7. Canavin, J.R., "Control Technology for Large Space Structures," *Proceedings of the AIAA Conference on Large Space Platforms: Future Needs and Capabilities*, Paper No. 78-1691, Sept. 1978.

8. Balas, Mark J., "Some Trends in Large Space Structure Control Theory: Fondest Hopes; Wildest Dreams," *Proceedings of the 1979 Joint Automatic Control Conference*, Denver, Colorado, June 17-21, 1979, pp. 42-55.

9. Meirovitch, L. and Öz, H., "An Assessment of Methods for the Control of Large Space Structures," *Proceedings of the 1979 Joint Automatic Control Conference*, Denver, Colorado June 17-21, 1979, pp. 24-41.

10. Croopnick, S.R., Lin, Y.H. and Strunce, R.R., "A Survey of

Automatic Control Techniques for Large Space Structures," *Proceedings of the 8th IFAC Symposium*, Oxford, England, July 2-6, 1979, pp. 275-284.

11. Gran, R. and Rossi, M., "A Survey of the Large Structures Controls Problem," *Proceedings of the 18th IEEE Conference on Decision and Control*, Ft. Lauderdale, Florida, Dec. 12-14, 1979, pp. 1002-1007.

12. Meirovitch, L., Baruh, H. and Öz, H., "A Comparison of Control Techniques for Large Flexible Systems," *Journal of Guidance, Control and Dynamics*, Vol. 6, No. 4, July-August 1983, pp. 302-310.

13. Floyd, M.A., Lindberg, R.E. and Lyons, M.G., "Comments on 'A Comparison of Control Techniques for Large Flexible Systems'," *Journal of Guidance, Control and Dynamics*, Vol. 7, No. 5, Sept.-Oct. 1984, pp. 634-637.

14. Meirovitch, L., Baruh, H. and Öz, H., "Reply by Authors to M.A. Floyd, R.E. Lindberg and M.G. Lyons," *Journal of Guidance, Control and Dynamics*, Vol. 7, No. 5, Sept.-Oct. 1984, pp. 634-637.

15. Canavin, J.R., "The Control of Spacecraft Vibrations Using Multivariable Output Feedback," *Proceedings of the AIAA/AAS Astrodynamics Conference*, Palo Alto, CA, August 7-9, 1978, Paper No. 78-1419.

16. Balas, Mark J., "Direct Output Feedback Control of Large Space Structures," *The Journal of the Astronautical Sciences*, Vol. XXVII, No. 2, April-June 1979, pp. 157-180.

17. Balas, Mark J., "Direct Velocity Feedback Control of Large Space Structures," *Journal of Guidance and Control*, Vol. 2, No. 3, May-June 1979, pp. 252-253.

18. Elliott, L.E., Mingori, D.L. and Iwens, R.P., "Performance of Robust Output Feedback Controller for Flexible Spacecraft," *Proceedings of the Second VPI & SU/AIAA Conference on Dynamics and Control of Large Flexible Spacecraft*, Blacksburg, VA., June 21-23, 1979, pp. 409-420.

19. Brogan, William L., *Modern Control Theory*, Second Edition,

Prentice-Hall, New Jersey, 1985, Chapter 16.

20. Joshi, S.M. and Groom, N.J., "Optimal Member Damper Controller Design for Large Space Structures," *Journal of Guidance and Control*, Vol. 3, No. 4, July-August 1980.

21. Lin, J.G., Lin, Y.H. and Preston, R.B., "Stability Augmentation for Large Space Structures by Modal Dashpots and Modal Springs," *Proceedings of the Third VPI & SU/AIAA Conference on Dynamics and Control of Large Flexible Spacecraft*, Blacksburg, VA., June 15-17, 1981, pp. 393-408.

22. DeCaro, S.M. and Inman, D.J., "Eigenvalue Placement and Stabilization by Constrained Optimization," *Proceedings of the Workshop on Identification and Control of Flexible Space Structures*, JPL Publication 85-29, April 1, 1985, pp. 37-46.

23. Yang, Jann-Nan, "Application of Optimal Control Theory to Civil Engineering Structures," *Journal of the Engineering Mechanics Division*, ASCE, Vol. 101 No. EM6, December 1975, pp. 819-838.

24. Balas, M.J., "Active Control of Flexible Systems," *Journal of Optimization Theory and Applications*, Vol. 25, No. 3, July 1978, pp. 415-436.

25. Alexandridis, A.A. and Weber, T.R., "Active Vibration Isolation of Truck Cabs," *Proceedings of the 1984 American Control Conference*, San Diego, CA., June 6-8, 1984, pp. 1199-1208.

26. Gibson, J.S., Mingori, D.L., Adamian, A. and Jabbari, F., "Approximation of Optimal Infinite Dimensional Compensators for Flexible Structures," presented at the "Workshop on Identification and Control of Flexible Space Structures," San Diego, CA., June 4-6, 1984.

27. Meirovitch, L. and Öz, H., "Modal Space Control of Distributed Gyroscopic Systems," *Journal of Guidance and Control*, Vol. 3, No. 2, March-April 1980, pp. 140-150.

28. Öz, H. and Meirovitch, L., "Optimal Modal-Space Control of Flexible Gyroscopic Systems," *Journal of Guidance and Control*, Vol. 3, No. 3, May-June 1980, pp. 218-226.

29. Meirovitch, L. and Öz, H., "Modal-Space Control of Large Flexible Spacecraft Possessing Ignorable Coordinates," *Journal of Guidance and Control*, Vol. 3, No. 6, Nov.-Dec. 1980. pp. 569-577.

30. Hurty, W.C. and Rubinstein, M.F., *Dynamics of Structures*, Prentice-Hall, New Jersey, 1964.

31. Meirovitch, L. and Silverberg, L.M., "Control of Structures Subject to Seismic Excitation," *Journal of Engineering Mechanics*, ASCE, Vol. 109, No. 2, April 1983, pp. 604-618.

32. Lindberg, R.E. and Longman, R.W., "On the Number and Placement of Actuators for Independent Modal Space Control," *Journal of Guidance, Control and Dynamics*, Vol. 7, No. 2, March-April 1984, pp. 215-221.

33. Schmit, L.A., "Structural Synthesis - Its Genesis and Development," *AIAA Journal*, Vol. 19, No. 10, October 1981, pp. 1249-1263.

34. Vanderplaats, G.N., "Structural Optimization - Past, Present and Future," *AIAA Journal*, Vol. 20, No. 7, July 1982, pp. 992-1000.

35. Venkayya, V.B., "Structural Optimization: A Review and Some Recommendations," *International Journal for Numerical Methods in Engineering*, Vol. 13, 1978, pp. 203-228.

36. Rangacharyulu, M.A.V. and Done, G.T.S., "A Survey of Structural Optimization Under Dynamic Constraints," *The Shock and Vibration Digest*, Vol. 11, No. 12, December 1979, pp. 15-25.

37. Rao, S.S., "Structural Optimization Under Shock and Vibration Environment," *The Shock and Vibration Digest*, Vol. 11, No. 2, February 1979, pp. 3-12.

38. Pierson, Bion L., "A Survey of Optimal Structural Design Under Dynamic Constraints," *International Journal for Numerical Methods in Engineering*, Vol. 4, 1972, pp. 491-499.

39. Schmit, L.A., "Structural Design by Systematic Synthesis," *Proceedings of the 2nd Conference on Electronic Computation*, ASCE, New York, 1960, pp. 105-132.

40. Gellatly, R. and Berke, L., "Optimal Structural Design," AFFDL-TR-70-165, April 1971.

41. Venkayya, V.B., "Design of Optimum Structures," *Computers and Structures*," Vol. 1, No. 1-2, August 1971, pp. 265-309.

42. Fleury, C. and Geradin, M., "Optimality Criteria and Mathematical Programming in Structural Weight Optimization," *Computers and Structures*, Vol. 8, No. 1, 1978, pp. 7-17.

43. Fleury, C., "A Unified Approach to Structural Weight Minimization," *Computer Methods in Applied Mechanics and Engineering*, Vol. 20, 1979, pp. 17-38.

44. Haug, E.J. and Arora, J.S., *Applied Optimal Design*, Wiley, New York, 1979.

45. Hanks, B.R. and Skelton, R.E., "Designing Structures for Reduced Response by Modern Control Theory," presented at the "24th AIAA/ASME/ASCE/AHS Structures, Structural Dynamics and Materials Conference," Lake Tahoe, Nevada, May 2-4, 1983, AIAA Paper No. 83-0815.

46. Trudell, R.W., Curley, R.C., and Rogers, L.C., "Passive Damping in Large Precision Space Structures," *Proceedings of the 21st AIAA/ASME/ASCE/AHS Structures, Structural Dynamics and Materials Conference*, Seattle, Washington, May 1980, pp. 124-136.

47. Garibotti, J.F., "Requirements and Issues for the Control of Flexible Space Structures," *Proceedings of the 25th AIAA/ASME/ASCE/AHS Structures, Structural Dynamics and Materials Conference*, Palm Springs, California, May 14-16, 1984, pp. 338-347.

48. Venkayya, V.B. and Tischler, V.A., "Frequency Control and the Effect on Dynamic Response of Flexible Structures, *Proceedings of the 25th AIAA/ASME/ASCE/AHS Structures, Structural Dynamics and Materials Conference*, Palm Springs, California, May 14-16, 1984, pp. 431-441.

49. Haftka, R.T., Martinovic, Z.N. and Hallauer, W.L., "Enhanced Vibration Controllability by Minor Structural Modifications," *AIAA Journal*, Vol. 23, No. 8, August 1985, pp. 1260-1266.

50. Haftka, R.T., Martinovic, Z.N., Hallauer, W.L. and Schamel, G., "Sensitivity of Optimized Control Systems to Minor Structural Modifications," *Proceedings of the 26th AIAA/ASME/ASCE/AHS Structures, Structural Dynamics and Materials Conference*, Orlando, Florida, April 15-17, 1985, pp. 642-650.

51. Messac, A. and Turner, J., "Dual Structural-Control Optimization of Large Space Structures," presented at the "NASA Symposium on Recent Experiences in Multidisciplinary Analysis and Optimization," April 1984.

52. Salama, M., Hamidi, M. and Demsetz, L., "Optimization of Controlled Structures," *Proceedings of the Workshop on Identification and Control of Flexible Space Structures*," San Diego, California, July 4-6, 1984, pp. 311-327.

53. Khot, N.S., Eastep, F.E. and Venkayya, V.B., "Optimal Structural Modifications to Enhance the Optimal Active Vibration Control of Large Flexible Structures," *Proceedings of the 26th AIAA/ASME/ASCE/AHS Structures, Structural Dynamics and Materials Conference*, Orlando, Florida, April 15-17, 1985, pp. 134-142.

54. Hale, A.L., Lisowski, R.J. and Dahl, W.E., "Optimal Simultaneous Structural and Control Design of Maneuvering Flexible Spacecraft," *Journal of Guidance, Control and Dynamics*, Vol. 8, No. 1, Jan.-Feb. 1985, pp. 86-93.

55. Junkins, J.L. and Bodden, D.S., "A Unified Approach to Structure and Control System Design Iterations," presented at the "Fourth International Conference on Applied Numerical Modeling," Tainan, Taiwan, December 27-29, 1984.

56. Bodden, D.S. and Junkins, J.L., "Eigenvalue Optimization Algorithms for Structure/Controller Design Iterations," *Journal of Guidance, Control and Dynamics*, Vol. 8, No. 6, Nov.-Dec. 1985, pp. 697-706.

57. Gustafson, C.L., Aswani, M., Doran, A.L. and Tseng, G.T., ISAAC (Integrated Structural Analysis and Control) Via Continuum Modeling and Distributed Frequency Domain Design Techniques," *Proceedings of the Workshop on Identification and Control of Flexible Space Structures*," JPL Publication 85-29,

April 1, 1985, pp. 287-310.

58. Abdel-Rohman, M. and Leipholz, H.H.E., "A General Approach to Active Structural Control," *Journal of the Engineering Mechanics Division*, ASCE, Vol. 105, No. EM6, Dec. 1979, pp. 1007-1023.

59. Schmit, L.A. and Farshi, B., "Some Approximation Concepts for Structural Synthesis," *AIAA Journal*, Vol. 12, No. 5, May 1974, pp. 692-699.

60. Schmit, L.A. and Miura, H., "Approximation Concepts for Efficient Structural Synthesis," NASA CR-2552, March 1976.

61. Lust, R.V. and Schmit, L.A., "Alternative Approximation Concepts for Space Frame Synthesis," NASA CR-172526, March 1985.

62. Desai, C.S. and Abel, J.F., *Introduction to the Finite Element Method*, Van Norstrand Reinhold, New York, 1972.

63. Felippa, Carlos A., "Solution of Linear Equations with Skyline Stored Symmetric Matrix," *Computers and Structures*, Vol. 5, No. 1, 1975, pp. 13-19.

64. Joshi, S.M., "On the Stability of Collocated Controllers in the Presence of Uncertain Nonlinearities and Other Perils," *Proceedings of the Workshop on Identification and Control of Flexible Space Structures*, San Diego, California, July 4-6, 1984, pp. 83-98.

65. Dong, S.B., Wolf, J.A. and Peterson, F.E., "On a Direct-Iterative Eigensolution Technique," *International Journal for Numerical Methods in Engineering*, Vol. 4, 1972, pp. 155-161.

66. Bathe, Klaus-Jurgen, *Finite Element Procedures in Engineering Analysis*, Prentice-Hall, New Jersey, 1982.

67. Prasad, B., "Novel Concepts for Constraint Treatments and Approximations in Efficient Structural Synthesis," *AIAA Journal*, Vol. 22, No. 7, July 1984, pp. 957-966.

68. Starnes, J.H. and Haftka, R.T., "Preliminary Design of Composite Wings for Buckling, Stress and Displacement Constraints,"

Journal of Aircraft, Vol. 16, August 1979, pp. 564-570.

69. Fleury, C. and Braibant, V., "Structural Optimization - A New Dual Method Using Mixed Variables," LTAS Report SA-115, University of Liege, Liege, Belgium, March 1984.

70. Arora, J.S. and Haug, E.J., "Methods of Design Sensitivity in Structural Optimization," *AIAA Journal*, Vol. 17, Sept. 1979, pp. 970-974.

71. Fletcher, R., *Practical Methods of Optimization Volume 2 - Constrained Optimization*, John Wiley and Sons, New York, 1981.

72. Vanderplaats, G.N., *Numerical Optimization Techniques for Engineering Design: With Applications*, McGraw-Hill, New York, 1984.

73. Vanderplaats, G.N. and Moses, F., "Structural Optimization by Methods of Feasible Directions," *Computers and Structures*, Vol. 3, July 1973, pp. 739-755.

74. Vanderplaats, G.N., "CONMIN - A FORTRAN Program for Constrained Function Minimization," NASA TM X-62,282, August 1973.

75. Lasdon, L.S., *Optimization Theory for Large Systems*, Macmillan, New York, 1970, pp. 396-459.

76. Fleury, C., "Structural Weight Optimization by Dual Methods of Convex Programming," *International Journal for Numerical Methods in Engineering*, Vol. 14, No. 12, 1979, pp. 1761-1783.

77. Schmit, L.A. and Fleury, C., "Structural Synthesis by Combining Approximation Concepts and Dual Methods," *AIAA Journal*, Vol. 18, No. 10, 1980, pp. 1252-1260.

78. Horner, G.C. and Walz, J.E., "A Design Technique for Determining Actuator Gains in Spacecraft Vibration Control," *Proceedings of the 26th AIAA/ASME/ASCE/AHS Structures, Structural Dynamics and Materials Conference*, Orlando, Florida, April 15-17, 1985, pp. 143-151.

APPENDIX A

Stiffness Matrices, Mass Matrices and Load Vectors
for Structural Elements

A.1 Prismatic Frame Element

The space frame element, shown in Fig. A1, is a two node, twelve degree of freedom element oriented with the longitudinal axis in the local x coordinate direction and the cross section principal axes in the local y and z coordinate directions. The element is assumed to have linear axial and torsional displacement states given by

$$u(x) = [N_1(x), N_2(x)] \begin{Bmatrix} u_1 \\ u_2 \end{Bmatrix} \tag{A-1}$$

$$\theta_x(x) = [N_1(x), N_2(x)] \begin{Bmatrix} \theta_{x_1} \\ \theta_{x_2} \end{Bmatrix} \tag{A-2}$$

and cubic bending displacement states of the form

$$v(x) = [N_3(x), N_4(x), N_5(x), N_6(x)] \begin{Bmatrix} v_1 \\ \theta_{z_1} \\ v_2 \\ \theta_{z_2} \end{Bmatrix} \tag{A-3}$$

and

$$w(x) = [N_3(x), -N_4(x), N_5(x), -N_6(x)] \begin{Bmatrix} w_1 \\ \theta_{y_1} \\ w_2 \\ \theta_{y_2} \end{Bmatrix}$$

(A-4)

where u, v and w are the displacements in the local x, y and z coordinate directions, θ_x, θ_y and θ_z are the rotations about the x,y and z axes and where the displacement shape functions are given by

$$\begin{aligned} N_1(x) &= 1 - \frac{x}{L} \\ N_2(x) &= \frac{x}{L} \\ N_3(x) &= 1 - 3(\frac{x}{L})^2 + 2(\frac{x}{L})^3 \\ N_4(x) &= L[(\frac{x}{L}) - 2(\frac{x}{L})^2 + (\frac{x}{L})^3] \\ N_5(x) &= 3(\frac{x}{L})^2 - 2(\frac{x}{L})^3 \\ N_6(x) &= L[-(\frac{x}{L})^2 + (\frac{x}{L})^3] \end{aligned} \qquad \text{(A-5)}$$

The assumed displacement states (Eqs. (A-1) - (A-4)) lead to the following strain-displacement relations

Axial strain: $$\frac{\partial u}{\partial x} = [B_1] \begin{Bmatrix} u_1 \\ u_2 \end{Bmatrix}$$

$$\textit{Torsional strain:}\quad \frac{\partial \theta_x}{\partial x} = [B_1] \begin{Bmatrix} \theta_{x_1} \\ \theta_{x_2} \end{Bmatrix} \tag{A-6}$$

$$\textit{Curvature:}\quad \frac{\partial^2 v}{\partial x^2} = [B_2] \begin{Bmatrix} v_1 \\ \theta_{z_1} \\ v_2 \\ \theta_{z_2} \end{Bmatrix}$$

$$\frac{\partial^2 w}{\partial x^2} = [B_3] \begin{Bmatrix} w_1 \\ \theta_{y_1} \\ w_2 \\ \theta_{y_2} \end{Bmatrix}$$

where

$$[B_1] = \left[-\frac{1}{L}, \frac{1}{L} \right]$$

$$[B_2] = \left[-\frac{6}{L^2}\left(1-\frac{2x}{L}\right), -\frac{2}{L}\left(2-\frac{3x}{L}\right), -\frac{6}{L^2}\left(\frac{2x}{L}-1\right), -\frac{2}{L}\left(1-\frac{3x}{L}\right) \right] \tag{A-7}$$

$$[B_3] = \left[-\frac{6}{L^2}\left(1-\frac{2x}{L}\right), \frac{2}{L}\left(2-\frac{3x}{L}\right), -\frac{6}{L^2}\left(\frac{2x}{L}-1\right), \frac{2}{L}\left(1-\frac{3x}{L}\right) \right]$$

The total strain and kinetic energies for the frame element can now be written as

$$\bar{U} = \frac{EA}{2}\int_o^L \{\frac{\partial u}{\partial x}\}^T\{\frac{\partial u}{\partial x}\}dx + \frac{GJ}{2}\int_o^L \{\frac{\partial \theta_x}{\partial x}\}^T\{\frac{\partial \theta_x}{\partial x}\}dx +$$

$$\frac{EI_z}{2}\int_o^L \{\frac{\partial^2 v}{\partial x^2}\}^T\{\frac{\partial^2 v}{\partial x^2}\}dx + \frac{EI_y}{2}\int_o^L \{\frac{\partial^2 w}{\partial x^2}\}^T\{\frac{\partial^2 w}{\partial x^2}\}dx$$

$$= \frac{1}{2}\{q\}^T[K]^e\{q\} \qquad \text{(A-8)}$$

and

$$\bar{T} = \frac{\rho A}{2}\int_o^L \{\frac{\partial u}{\partial t}\}^T\{\frac{\partial u}{\partial t}\}dx + \frac{\rho I_p}{2}\int_o^L \{\frac{\partial \theta_x}{\partial t}\}^T\{\frac{\partial \theta_x}{\partial t}\}dx +$$

$$\frac{\rho A}{2}\int_o^L \{\frac{\partial v}{\partial t}\}^T\{\frac{\partial v}{\partial t}\}dx + \frac{\rho A}{2}\int_o^L \{\frac{\partial w}{\partial t}\}^T\{\frac{\partial w}{\partial t}\}dx$$

$$= \frac{1}{2}\{\dot{q}\}^T[M^e]\{\dot{q}\} \qquad \text{(A-9)}$$

where

ρ	-	mass density
E	-	material modulus of elasticity
G	-	material shear modulus
A	-	cross sectional area
J	-	torsional constant
I_y	-	cross sectional principal moment of inertia about the y axis
I_z	-	cross sectional principal moment of inertia about the z axis
I_p	-	polar moment of inertia

and

$$\{q\}^T = \{u_1\ v_1\ w_1\ \theta_{x_1}\ \theta_{y_1}\ \theta_{z_1}\ u_2\ v_2\ w_2\ \theta_{x_2}\ \theta_{y_2}\ \theta_{z_2}\}$$

Note that the rotational kinetic energy associated with the bending rotations θ_y and θ_z is assumed to be negligible and is therefore not included in the total kinetic energy.

Evaluation of the integrals of Eqs. (A-8) and (A-9) yields the following element stiffness and mass matrices:

$$[K]^e = \frac{E}{L}\begin{bmatrix}
A & 0 & 0 & 0 & 0 & 0 & -A & 0 & 0 & 0 & 0 & 0 \\
 & \frac{12I_z}{L^2} & 0 & 0 & 0 & \frac{6I_z}{L} & 0 & \frac{-12I_z}{L^2} & 0 & 0 & 0 & \frac{6I_z}{L} \\
 & & \frac{12I_y}{L^2} & 0 & \frac{-6I_y}{L} & 0 & 0 & 0 & \frac{-12I_y}{L^2} & 0 & \frac{-6I_y}{L} & 0 \\
 & & & \frac{GJ}{E} & 0 & 0 & 0 & 0 & 0 & \frac{-GJ}{E} & 0 & 0 \\
 & & & & 4I_y & 0 & 0 & 0 & \frac{6I_y}{L} & 0 & 2I_y & 0 \\
 & & & & & 4I_z & 0 & \frac{-6I_z}{L} & 0 & 0 & 0 & 2I_z \\
 & & & & & & A & 0 & 0 & 0 & 0 & 0 \\
 & & \text{Sym.} & & & & & \frac{12I_z}{L^2} & 0 & 0 & 0 & \frac{-6I_z}{L} \\
 & & & & & & & & \frac{12I_y}{L^2} & 0 & \frac{6I_y}{L} & 0 \\
 & & & & & & & & & \frac{GJ}{E} & 0 & 0 \\
 & & & & & & & & & & 4I_y & 0 \\
 & & & & & & & & & & & 4I_z
\end{bmatrix} \qquad \text{(A-10)}$$

$$[M]^e =$$

$$\frac{\rho AL}{420}\begin{bmatrix}
140 & 0 & 0 & 0 & 0 & 0 & 70 & 0 & 0 & 0 & 0 & 0 \\
 & 156 & 0 & 0 & 0 & 22L & 0 & 54 & 0 & 0 & 0 & -13L \\
 & & 156 & 0 & -22L & 0 & 0 & 0 & 54 & 0 & 13L & 0 \\
 & & & \frac{140I_p}{A} & 0 & 0 & 0 & 0 & 0 & \frac{70I_p}{A} & 0 & 0 \\
 & & & & 4L^2 & 0 & 0 & 0 & -13L & 0 & -3L^2 & 0 \\
 & & & & & 4L^2 & 0 & 13L & 0 & 0 & 0 & -3L^2 \\
 & & & & & & 140 & 0 & 0 & 0 & 0 & 0 \\
 & & \text{Sym.} & & & & & 156 & 0 & 0 & 0 & -22L \\
 & & & & & & & & 156 & 0 & 22L & 0 \\
 & & & & & & & & & \frac{140I_p}{A} & 0 & 0 \\
 & & & & & & & & & & 4L^2 & 0 \\
 & & & & & & & & & & & 4L^2
\end{bmatrix}$$

(A-11)

Similarly, the external work expression for the space frame element subject to uniformly distributed loads can be written as

$$W = \int_0^L \{p_x p_y p_z m_x m_y m_z\} \{u(x), v(x), w(x), \theta_x(x), -\frac{dw}{dx}(x), \frac{dv}{dx}(x)\}^T dx \qquad \text{(A-12)}$$

where p_x, p_y and p_z are forces per unit length in the x, y and z directions and m_x, m_y, m_z are moments per unit length about the x, y and z axes. Evaluation of Eq. (A-12) using Eqs. ((A-1) - (A-5)) and assuming p_x, p_y, p_z as well as m_x, m_y, m_z, are constants (uniformly distributed)

leads to the following form for the work equivalent load vector

$$\{P\}^e = \left\{ \frac{p_x L}{2},\ \frac{p_y L}{2} - m_z,\ \frac{p_z L}{2} + m_y,\ \frac{m_x L}{2},\ -\frac{p_z L^2}{12},\ \frac{p_y L^2}{12},\right.$$

$$\left. \frac{p_x L}{2},\ \frac{p_y L}{2} + m_z,\ \frac{p_z L}{2} - m_y,\ \frac{m_x L}{2},\ \frac{p_z L^2}{12},\ -\frac{p_y L^2}{12} \right\} \qquad \text{(A-13)}$$

A.2 Prismatic Truss Element

The space truss element, shown in Fig. A2, is a two node element oriented with the longitudinal axis in the local x direction. The element is assumed to have a linear displacement state of the form

$$u(x) = [1 - \frac{x}{L}, \frac{x}{L}] \begin{Bmatrix} u_1 \\ u_2 \end{Bmatrix} \qquad \text{(A-14)}$$

where u is the displacement in the x direction. This assumed displacement state leads to the following strain-displacement relation

$$\frac{\partial u(x)}{\partial x} = [\frac{-1}{L}, \frac{1}{L}] \begin{Bmatrix} u_1 \\ u_2 \end{Bmatrix} \qquad \text{(A-15)}$$

The strain and kinetic energies for the truss element can now be written as

$$\bar{U} = \frac{EA}{2} \int_o^L \{\frac{\partial u}{\partial x}\}^T \{\frac{\partial u}{\partial x}\} dx$$

$$= \frac{1}{2} \{u_1\ u_2\}[K]^e \{u_1 u_2\}^T \qquad \text{(A-16)}$$

and

$$\bar{T} = \frac{\rho A}{2} \int_o^L \{\frac{\partial u}{\partial t}\}^T \{\frac{\partial u}{\partial t}\} dx$$

$$= \frac{1}{2} \{\dot{u}_1 \; \dot{u}_2\}[K]^e \{\dot{u}_1 \dot{u}_2\}^T$$

which leads to the following expression for the element stiffness matrix in local coordinates

$$[K]^e = \frac{EA}{L} \begin{bmatrix} 1 & -1 \\ -1 & 1 \end{bmatrix} \tag{A-17}$$

$$[M]^e = \frac{\rho AL}{6} \begin{bmatrix} 2 & 1 \\ 1 & 2 \end{bmatrix} \tag{A-18}$$

Similarly, the external work due to a uniformly distributed axial load p_x can be written as

$$W = \int_o^L p_x \, u(x) dx = \{P\}^{e^T} \{u_1 u_2\}^T \tag{A-19}$$

which leads to the following work equivalent load vector

$$\{P\}^e = \frac{p_x L}{2} \{1 \;\; 1\}^T \tag{A-20}$$

Rewriting $[K]^e$, $[M]^e$ and $\{P\}^e$ in terms of the full twelve nodal degrees

of freedom gives

$$[K]^e = \frac{E}{L}\begin{bmatrix} A & 0 & 0 & 0 & 0 & 0 & -A & 0 & 0 & 0 & 0 & 0 \\ & 0 & 0 & 0 & 0 & 0 & 0 & 0 & 0 & 0 & 0 & 0 \\ & & 0 & 0 & 0 & 0 & 0 & 0 & 0 & 0 & 0 & 0 \\ & & & 0 & 0 & 0 & 0 & 0 & 0 & 0 & 0 & 0 \\ & & & & 0 & 0 & 0 & 0 & 0 & 0 & 0 & 0 \\ & & & & & 0 & 0 & 0 & 0 & 0 & 0 & 0 \\ & & & & & & A & 0 & 0 & 0 & 0 & 0 \\ & & & & \text{Sym.} & & & 0 & 0 & 0 & 0 & 0 \\ & & & & & & & & 0 & 0 & 0 & 0 \\ & & & & & & & & & 0 & 0 & 0 \\ & & & & & & & & & & 0 & 0 \\ & & & & & & & & & & & 0 \end{bmatrix} \qquad \text{(A-21)}$$

$$[M]^e = \frac{\rho AL}{6}\begin{bmatrix} 2 & 0 & 0 & 0 & 0 & 0 & 1 & 0 & 0 & 0 & 0 & 0 \\ & 0 & 0 & 0 & 0 & 0 & 0 & 0 & 0 & 0 & 0 & 0 \\ & & 0 & 0 & 0 & 0 & 0 & 0 & 0 & 0 & 0 & 0 \\ & & & 0 & 0 & 0 & 0 & 0 & 0 & 0 & 0 & 0 \\ & & & & 0 & 0 & 0 & 0 & 0 & 0 & 0 & 0 \\ & & & & & 0 & 0 & 0 & 0 & 0 & 0 & 0 \\ & & & & & & 2 & 0 & 0 & 0 & 0 & 0 \\ & & & & \text{Sym.} & & & 0 & 0 & 0 & 0 & 0 \\ & & & & & & & & 0 & 0 & 0 & 0 \\ & & & & & & & & & 0 & 0 & 0 \\ & & & & & & & & & & 0 & 0 \\ & & & & & & & & & & & 0 \end{bmatrix} \tag{A-22}$$

and

$$\{P\}^{e^T} = \frac{p_x L}{2}\{1\,0\,0\,0\,0\,0\,1\,0\,0\,0\,0\,0\} \tag{A-23}$$

APPENDIX B

Position and Velocity Feedback Gain Matrices for Member Controller Element

The member controller element shown in Fig. B1 represents a force actuator connected between two nodes of the structural model. The element is oriented with the longitudinal axis in the local x coordinate direction. It is assumed that the actuator exerts a force proportional to the relative nodal displacements and velocities. For the k-th dynamic load condition, these forces can be written as

$$f_{1_k}(t) = h_{p_k}(u_2 - u_1)_k + h_{v_k}(\dot{u}_2 - \dot{u}_1) \tag{B-1}$$

$$f_{2_k}(t) = -f_{1_k}(t) = h_{p_k}(u_1 - u_2)_k + h_{v_k}(\dot{u}_1 - \dot{u}_2)_k \tag{B-2}$$

where u and $\dot{u}$ are the nodal displacements and velocities in the local x direction and where h_{p_k} and h_{v_k} are the relative position and velocity feedback gains. Equations (B-1) and (B-2) can be combined in matrix form as

$$\begin{Bmatrix} f_1(t) \\ f_2(t) \end{Bmatrix}_k = -h_{p_k} \begin{bmatrix} 1 & -1 \\ -1 & 1 \end{bmatrix} \begin{Bmatrix} u_1 \\ u_2 \end{Bmatrix} - h_{v_k} \begin{bmatrix} 1 & -1 \\ -1 & 1 \end{bmatrix} \begin{Bmatrix} \dot{u}_1 \\ \dot{u}_2 \end{Bmatrix}_k \tag{B-3}$$

or

$$\{F_A\}_k^e = -[H_p]_k^e \{u\}_k^e - [H_v]_k^e \{\dot{u}\}_k^e \tag{B-4}$$

where $\{F_A\}_k^e$ is the member controller force vector and where the element level feedback gain matrices are given by

$$[H_p]_k^e = h_{p_k} \begin{bmatrix} 1 & -1 \\ -1 & 1 \end{bmatrix} \tag{B-5}$$

and

$$[H_v]_k^e = h_{v_k} \begin{bmatrix} 1 & -1 \\ -1 & 1 \end{bmatrix} \tag{B-6}$$

APPENDIX C

Alternative Steady State Response Solution Scheme

Consider the 2n x 2n system of simultaneous linear algebraic equations given by (see Eq. (3-25))

$$\begin{bmatrix} \Omega[C_A] + \gamma[K] & [K_A]-\Omega^2[M] \\ [K_A]-\Omega^2[M] & -\Omega[C_A] - \gamma[K] \end{bmatrix} \begin{Bmatrix} \{c_R\} \\ \{c_I\} \end{Bmatrix} = \begin{Bmatrix} \{0\} \\ \{P\} \end{Bmatrix} \tag{C-1}$$

where the load condition subscripts k have been omitted for convenience. In a more compact notation Eq. (C-1) can be written as

$$\begin{bmatrix} [A] & [B] \\ [B] & -[A] \end{bmatrix} \begin{Bmatrix} \{c_R\} \\ \{c_I\} \end{Bmatrix} = \begin{Bmatrix} \{0\} \\ \{P\} \end{Bmatrix} \tag{C-2}$$

Equation (C-2) is equivalent to the following two equations:

$$[A]\{c_R\} + [B]\{c_I\} = \{0\} \tag{C-3}$$

$$[B]\{c_R\} - [A]\{c_I\} = \{P\} \tag{C-4}$$

As an alternative to solving Eq. (C-1) directly, these two equations can be solved simultaneously.

One possible way of solving Eqs. (C-3) and (C-4) is to first solve Eq. (C-3) for $\{c_I\}$, giving

$$\{c_I\} = -[D]\{c_R\} \tag{C-5}$$

where

$$[D] = [B]^{-1}[A] \tag{C-6}$$

can be obtained by solving

$$[B][D] = [A] \tag{C-7}$$

Substituting Eq. (C-5) into Eq. (C-4) yields

$$([A][D] + [B])\{c_R\} = \{P\} \tag{C-8}$$

Finally, Eq. (C-8) can be solved for $\{c_R\}$ with $\{c_I\}$ being subsequently obtained from (see Eq. (C-3))

$$[B]\{c_I\} = -[A]\{c_R\} \tag{C-9}$$

The approach outlined above is susceptible to numerical difficulties near resonance as the matrix [B] becomes nearly singular. As a means of avoiding this problem Eq. (C-3) can be solved first for $\{c_R\}$, giving

$$\{c_R\} = -[E]\{c_I\} \tag{C-10}$$

where

$$[E] = [A]^{-1}[B] \tag{C-11}$$

can be obtained by solving

$$[A][E] = [B] \tag{C-12}$$

Substituting Eq. (C-10) into Eq. (C-4)

$$([B][E] + [A])\{c_I\} = -\{P\} \tag{C-13}$$

Finally, Eq. (C-13) can be solved for $\{c_I\}$ with $\{c_R\}$ being obtained from (see Eq. (C-3))

$$[A]\{c_R\} = -[B]\{c_I\} \tag{C-14}$$

This later approach will be numerically stable as long as the matrix [A] is non-singular. This can usually be ensured through the use of a small, but reasonable, amount of structural damping.

APPENDIX D

Derivatives of Structural Response Quantities with Respect to Reciprocal Element Properties

D.1 Static Displacement Derivatives

For the linear static structural analysis problem, the displacement derivatives are easily obtained through the implicit differentiation of the governing equilibrium equations with respect to the reciprocals of the element properties. In general, differentiation of Eq. (3-1) with respect to the j-th reciprocal property of the i-th element (x_{ij}) yields

$$\frac{\partial[K]}{\partial x_{ij}} \{u\}_k + [K] \frac{\partial\{u\}_k}{\partial x_{ij}} = \frac{\partial\{P\}_k}{\partial x_{ij}} \; ; \quad k = 1,2,...K_s \tag{D-1}$$

Under the assumption that the external loads are independent of x_{ij} (i.e. $\frac{\partial\{P\}_k}{\partial x_{ij}} = 0$) Eq. (D-1) becomes

$$[K] \frac{\partial\{u\}_k}{\partial x_{ij}} = \bar{V}_{ijk} \quad ; \quad k = 1,2,...K_s \tag{D-2}$$

where the pseudo load vector $\bar{V}_{ijk}$ is given by

$$\bar{V}_{ijk} = - \frac{\partial[K]}{\partial x_{ij}} \{u\}_k \tag{D-3}$$

The system stiffness matrix [K] can be written as

$$[K] = \sum_{i=1}^{I} [\beta]_i^T ([T]_i^T [K]_i^e [T]_i)[\beta]_i \tag{D-4}$$

where $[K]_i^e$ is the element stiffness matrix in local coordinates, $[T]_i$ is the element coordinate transformation matrix, $[\beta]_i$ is the element local

to global degree of freedom transformation matrix and I is the total number of structural elements. Substituting Eq. (D-4) into Eq. (D-3) gives

$$\bar{V}_{ijk} = -[\beta]_i^T [T]_i^T \frac{\partial [K]_i^e}{\partial x_{ij}} [T]_i [\beta]_i \{u\}_k \tag{D-5}$$

Finally, Eq. (D-5) may be rewritten as

$$\bar{V}_{ijk} = \frac{1}{x_{ij}^2} ([\beta]_i^T [T]_i^T [K']_{ij}^e [T]_i [\beta]_i \{u\}_k) \tag{D-6}$$

where it is recognized that

$$[K']_{ij}^e = \frac{\partial [K]_i^e}{\partial (1/x_{ij})} \tag{D-7}$$

is the unit element stiffness matrix formed by assigning the j-th section property a value of unity while the remaining section properties are set to zero.

Using the expression for the pseudo load vector given by Eq. (D-6), Eq. (D-2) can be solved for the unknown displacement derivatives via the same procedure used to solve the equilibrium equations (Eq. (3-1)). Solving Eq. (D-2) directly yields the derivative values for all of the displacement degrees of freedom. For the case where the number of displacement degrees of freedom associated with the retained constraint set is fewer than the number of pseudo load vectors associated with Eq. (D-2) it is computationally more efficient to solve Eq. (D-2) using a partial inverse technique represented by the equation

$$\frac{\partial\{u_R\}_k}{\partial x_{ij}} = [C]\bar{V}_{ijk} \tag{D-8}$$

where $\{u_R\}_k$ represents the displacement degrees of freedom associated with the retained constraint set. The partial inverse matrix [C] is constructed such that its n-th row contains the vector $\{c\}_n^T$ obtained from the solution of the equation

$$[K]\{c\}_n = \{e\}_n \tag{D-9}$$

where $\{e\}_n$ is a unit vector corresponding to the n-th degree of freedom associated with the retained constraint set. It should be noted that the solution of either Eq. (D-2) or Eq. (D-9) requires only the back substitution of the vectors $\bar{V}_{ijk}$ or $\{e\}_n$ if the decomposed stiffness matrix has been saved from the previous structural analysis.

D.2 Static Element Force Derivatives

The static element force derivatives are obtained through the implicit differentiation of the element force-displacement relations. Rewriting Eq. (3-8) in the global coordinate system gives

$$\{F\}_{rk}^g = [K]_r^g \{u\}_{rk} + \{FEF\}_{rk}^g \tag{D-10}$$

where $\{F\}_{rk}^g$, $[K]_r^g$, $\{u\}_{rk}$ and $\{FEF\}_{rk}^g$ are the element force vector, stiffness matrix, vector of nodal displacements and fixed end force vector for the r-th element and k-th load set. Differentiation of Eq. (D-10) with respect to x_{ij} gives

$$\frac{\partial \{F\}^g_{rk}}{\partial x_{ij}} = \begin{cases} \dfrac{\partial [K]^g_r}{\partial x_{ij}} \{u\}_{rk} + [K]^g_r \dfrac{\partial \{u\}_{rk}}{\partial x_{ij}} + \dfrac{\partial \{FEF\}^g_{rk}}{\partial x_{ij}} & ; \quad i = r \\ [K]^g_r \dfrac{\partial \{u\}_{rk}}{\partial x_{ij}} & ; \quad i \neq r \end{cases} \tag{D-11}$$

where the displacement derivatives $\frac{\partial \{u\}_{rk}}{\partial x_{ij}}$ are calculated as described previously. Under the assumption that the external loads are independent of the element properties

$$\frac{\partial \{FEF\}^g_{rk}}{\partial x_{ij}} = 0 \tag{D-12}$$

and Eq. (D-11) becomes

$$\frac{\partial \{F\}^g_{rk}}{\partial x_{ij}} = \begin{cases} \dfrac{\partial [K]^g_r}{\partial x_{ij}} \{u\}_{rk} + [K]^g_r \dfrac{\partial \{u\}_{rk}}{\partial x_{ij}} & ; \quad i = r \\ [K]^g_r \dfrac{\partial \{u\}_{rk}}{\partial x_{ij}} & ; \quad i \neq r \end{cases} \tag{D-13}$$

Rewriting $[K]^g_r$ as

$$[K]^g_r = [T]^T_r [K]^e_r [T]_r \tag{D-14}$$

and substituting into Eq. (D-13) yields

$$\frac{\partial\{F\}^g_{rk}}{\partial x_{ij}} = \begin{cases} [T]_r^T \dfrac{\partial[K]^e_r}{\partial x_{ij}}[T]_r\{u\}_{rk} + [T]_r^T[K]^e_r[T]_r \dfrac{\partial\{u\}_{rk}}{\partial x_{ij}} & ; \quad i = r \\ \\ [T]_r^T[K]^e_r[T]_r \dfrac{\partial\{u\}_{rk}}{\partial x_{ij}} & ; \quad i \neq r \end{cases} \tag{D-15}$$

Introducing the unit element stiffness matrix $[K]^e_{rj}$, Eq. (D-15) becomes

$$\frac{\partial\{F\}^g_{rk}}{\partial x_{ij}} = \begin{cases} -\dfrac{1}{x_{ij}^2}([T]_r^T[K']^e_{rj}[T])_r\{u\}_{rk} + [T]_r^T[K]^e_r[T]_r \dfrac{\partial\{u\}_{rk}}{\partial x_{ij}} & ; \quad i = r \\ \\ [T]_r^T[K]^e_r[T]_r \dfrac{\partial\{u\}_{rk}}{\partial x_{ij}} & ; \quad i \neq r \end{cases} \tag{D-16}$$

Finally, writing the element force derivatives in the local coordinate system gives

$$\frac{\partial\{F\}^e_{rk}}{\partial x_{ij}} = [T]_r \frac{\partial\{F\}^g_{rk}}{\partial x_{ij}} \tag{D-17}$$

or

$$\frac{\partial\{F\}^e_{rk}}{\partial x_{ij}} = \begin{cases} -\dfrac{1}{x_{ij}^2}[K']^e_{rj}[T]_r\{u\}_{rk} + [K]^e_r[T]_r \dfrac{\partial\{u\}_{rk}}{\partial x_{ij}} & ; \quad i = r \\ \\ [K]^e_r[T]_r \dfrac{\partial\{u\}_{rk}}{\partial x_{ij}} & ; \quad i \neq r \end{cases} \tag{D-18}$$

since, by orthogonality of $[T]_r$,

$$[T]_r[T]_r^T = [T]_r[T]_r^{-1} = [I] \tag{D-19}$$

D.3 Dynamic Displacement Derivatives

The derivatives of the steady state dynamic displacements corresponding to the k-th dynamic loading condition

$$\{P(t)\}_k = \{P\}_k e^{i\Omega_k t} \tag{D-20}$$

can be obtained through the implicit differentiation of Eq. (3-27) with respect to x_{ij}, giving

$$\frac{\partial\{u\}_k}{\partial x_{ij}} = \frac{\partial\{u_R\}_k}{\partial x_{ij}} + i\,\frac{\partial\{u_I\}_k}{\partial x_{ij}} \tag{D-21}$$

where, assuming that Ω_k is independent of x_{ij},

$$\frac{\partial\{u_R\}_k}{\partial x_{ij}} = \frac{\partial\{c_R\}_k}{\partial x_{ij}} \cos\Omega_k t - \frac{\partial\{c_I\}_k}{\partial x_{ij}} \sin\Omega_k t \tag{D-22}$$

and

$$\frac{\partial\{u_I\}_k}{\partial x_{ij}} = \frac{\partial\{c_R\}_k}{\partial x_{ij}} \sin\Omega_k t + \frac{\partial\{c_I\}_k}{\partial x_{ij}} \cos\Omega_k t \tag{D-23}$$

Similarly the derivatives of the magnitude of the r-th dynamic displacement are obtained by differentiating Eq. (3-32) with respect to x_{ij}, yielding

$$\frac{\partial|u_{rk}|}{\partial x_{ij}} = (c_{R_{rk}}^2 + c_{I_{rk}}^2)^{-1/2}\left[c_{R_{rk}} \frac{\partial c_{R_{rk}}}{\partial x_{ij}} + c_{I_{rk}} \frac{\partial c_{I_{rk}}}{\partial x_{ij}} \right] \tag{D-24}$$

In both cases, the derivatives of c_R and c_I with respect to x_{ij} are obtained via the implicit differentiation of Eq. (3-25). Writing Eq. (3-25) in the following compact notation,

$$\begin{bmatrix} [A]_k & [B]_k \\ [B]_k & -[A]_k \end{bmatrix} \begin{Bmatrix} \{c_R\}_k \\ \{c_I\}_k \end{Bmatrix} = \begin{Bmatrix} \{0\}_k \\ \{P\}_k \end{Bmatrix} \tag{D-25}$$

and differentiating with respect to x_{ij} yields

$$\begin{bmatrix} \frac{\partial [A]_k}{\partial x_{ij}} & \frac{\partial [B]_k}{\partial x_{ij}} \\ \frac{\partial [B]_k}{\partial x_{ij}} & \frac{-\partial [A]_k}{\partial x_{ij}} \end{bmatrix} \begin{Bmatrix} \{c_R\}_k \\ \{c_I\}_k \end{Bmatrix} + \begin{bmatrix} [A]_k & [B]_k \\ [B]_k & -[A]_k \end{bmatrix} \begin{Bmatrix} \frac{\partial \{c_R\}_k}{\partial x_{ij}} \\ \frac{\partial \{c_I\}_k}{\partial x_{ij}} \end{Bmatrix} =$$

$$\begin{Bmatrix} \{0\}_k \\ \frac{\partial \{P\}_k}{\partial x_{ij}} \end{Bmatrix} \tag{D-26}$$

Under the assumption that the external loading conditions are independent of x_{ij} Eq. (D-26) can be written as

$$\begin{bmatrix} [A]_k & [B]_k \\ [B]_k & -[A]_k \end{bmatrix} \begin{Bmatrix} \frac{\partial \{c_R\}_k}{\partial x_{ij}} \\ \frac{\partial \{c_I\}_k}{\partial x_{ij}} \end{Bmatrix} = \begin{Bmatrix} \overline{V}_{I_{ij}} \\ \overline{V}_{R_{ij}} \end{Bmatrix} \tag{D-27}$$

where the pseudo load vectors $\overline{V}_{I_{ij}}$ and $\overline{V}_{R_{ij}}$ are given by

$$\overline{V}_{I_{ij}} = -\frac{\partial [A]_k}{\partial x_{ij}} \{c_R\}_k - \frac{\partial [B]_k}{\partial x_{ij}} \{c_I\}_k \tag{D-28}$$

and

$$\overline{V}_{R_{ij}} = -\frac{\partial [B]_k}{\partial x_{ij}} \{c_R\}_k + \frac{\partial [A]_k}{\partial x_{ij}} \{c_I\}_k \tag{D-29}$$

Substituting for $[A]_k$ and $[B]_k$ (see Eq. (3-25)), Eqs. (D-28) and (D-29)

become

$$\bar{V}_{I_{ijk}} = -\left[\Omega_k \frac{\partial[C_A]_k}{\partial x_{ij}} + \gamma \frac{\partial[K]}{\partial x_{ij}}\right]\{c_R\}_k - \left[\frac{\partial[K_A]_k}{\partial x_{ij}} - \Omega_k^2 \frac{\partial[M]}{\partial x_{ij}}\right]\{c_I\}_k \quad \text{(D-30)}$$

and

$$\bar{V}_{R_{ijk}} = -\left[\frac{\partial[K_A]_k}{\partial x_{ij}} - \Omega_k^2 \frac{\partial[M]}{\partial x_{ij}}\right]\{c_R\}_k + \left[\Omega_k \frac{\partial[C_A]_k}{\partial x_{ij}} + \gamma \frac{\partial[K]}{\partial x_{ij}}\right]\{c_I\}_k \quad \text{(D-31)}$$

As was the case for the static displacement constraints, the partial derivatives of the global matrices [K], $[K_A]_k$, $[C_A]_k$ and [M] with respect to x_{ij} can be formed via transformation of the element level unit matrices (see Eqs. (D-4) - (D-7)). Once obtained, these quantities can be substituted into Eqs. (D-30) and (D-31), yielding the values for the pseudo load vectors. Having formed the pseudo load vectors, the partial derivatives of $\{c_R\}_k$ and $\{c_I\}_k$ with respect to x_{ij} are obtained by solving Eq. (D-27) either directly or via the partial inverse technique described previously. Finally, the partial derivatives of either the dynamic displacements or their magnitudes with respect to x_{ij} are given by substituting these partial derivatives into either Eq. (D-22), and Eq. (D-23), or Eq. (D-24).

D.4 Member Controller Force Derivatives

The membrane controller force derivatives are given by the implicit differentiation of the actuator force-displacement relations. Rewriting (Eqs. (3-39) - (3-43) in the global coordinate system for the r-th actuator gives

$$\{F_A\}^g_{rk} = \{F_{AR}\}^g_{rk} + i\ \{F_{AI}\}^g_{rk} \tag{D-32}$$

where

$$\{F_{AR}\}^g_{rk} = -\ \{F_2\}^g_{rk}\ \sin\Omega_k t + \{F_1\}^g_{rk}\ \cos\Omega_k t \tag{D-33}$$

$$\{F_{AI}\}^g_{rk} = +\ \{F_1\}^g_{rk}\ \sin\Omega_k t + \{F_2\}^g_{rk}\ \cos\Omega_k t \tag{D-34}$$

and where

$$\{F_1\}^g_{rk} = \Omega_k\ [H_v]^g_{rk}\ \{c_I\}^g_{rk} - [H_p]^g_{rk}\ \{c_R\}^g_{rk} \tag{D-35}$$

$$\{F_2\}^g_{rk} = -\ \Omega_k\ [H_v]^g_{rk}\ \{c_R\}^g_{rk} - [H_p]^g_{rk}\ \{c_I\}^g_{rk} \tag{D-36}$$

Differentiating Eqs. (D-32) - (D-34) with respect to x_{ij} and assuming Ω_k is independent of x_{ij} yields

$$\frac{\partial\{F_A\}^g_{rk}}{\partial x_{ij}} = \frac{\partial\{F_{AR}\}^g_{rk}}{\partial x_{ij}} + i\ \frac{\partial\{F_{AI}\}^g_{rk}}{\partial x_{ij}} \tag{D-37}$$

$$\frac{\partial\{F_{AR}\}^g_{rk}}{\partial x_{ij}} = -\ \frac{\partial\{F_2\}^g_{rk}}{\partial x_{ij}}\ \sin\Omega_k t + \frac{\partial\{F_1\}^g_{rk}}{\partial x_{ij}}\ \cos\Omega_k t \tag{D-38}$$

$$\frac{\partial\{F_{AI}\}^g_{rk}}{\partial x_{ij}} = +\ \frac{\partial\{F_1\}^g_{rk}}{\partial x_{ij}}\ \sin\Omega_k t + \frac{\partial\{F_2\}^g_{rk}}{\partial x_{ij}}\ \cos\Omega_k t \tag{D-39}$$

where

$$\frac{\partial\{F_2\}^g_{rk}}{\partial x_{ij}} = \begin{cases} -[H'_p]^g_{rk}\{c_I\}_{rk} - [H_p]^g_{rk}\{c'_I\}_{rk} - \Omega_k\left([H'_v]^g_{rk}\{c_R\}_{rk} + [H_v]^g_{rk}\{c'_R\}_{rk}\right)\ ;\ i = r \\ -[H_p]^g_{rk}\{c'_I\}_{rk} - \Omega_k[H_v]^g_{rk}\{c'_R\}_{rk}\ ;\ i \neq r \end{cases} \tag{D-40}$$

$$\frac{\partial\{F_1\}^g_{rk}}{\partial x_{ij}} = \begin{cases} -[H'_p]^g_{rk}\{c_R\}_{rk} - [H_p]^g_{rk}\{c'_R\}_{rk} + \Omega_k([H'_v]^g_{rk}\{c_I\}_{rk} + [H_v]^g_{rk}\{c'_I\}_{rk}) \; ; \; i = r \\ -[H_p]^g_{rk}\{c'_R\}_{rk} + \Omega_k[H_v]^g_{rk}\{c'_I\}_{rk} \; ; \; i \neq r \end{cases} \tag{D-41}$$

and where the prime (') denotes differentiation with respect to x_{ij} (i.e. $[H'_p]^g_{rk} = \partial[H_p]^g_{rk}/\partial x_{ij}$). Rewriting $[H_p]^g_{rk}$ and $[H_v]^g_{rk}$ as

$$[H_p]^g_{rk} = [T]^T_r[H_p]^e_{rk}[T]_r \tag{D-42}$$

$$[H_v]^g_{rk} = [T]^T_r[H_v]^e_{rk}[T]_r \tag{D-43}$$

and pre-multiplying both sides of Eqs. (D-33) and (D-34) by $[T]_r$ leads to the following expression for the actuator force derivatives in the local coordinate system:

$$\frac{\partial\{F_A\}^e_{rk}}{\partial x_{ij}} = \frac{\partial\{F_{AR}\}^e_{rk}}{\partial x_{ij}} + i\,\frac{\partial\{F_{AI}\}^e_{rk}}{\partial x_{ij}} \tag{D-44}$$

where

$$\frac{\partial\{F_{AR}\}^e_{rk}}{\partial x_{ij}} = -\frac{\partial\{F_2\}^e_{rk}}{\partial x_{ij}}\sin\Omega_k t + \frac{\partial\{F_1\}^e_{rk}}{\partial x_{ij}}\cos\Omega_k t \tag{D-45}$$

$$\frac{\partial\{F_{AI}\}^e_{rk}}{\partial x_{ij}} = +\frac{\partial\{F_1\}^e_{rk}}{\partial x_{ij}}\sin\Omega_k t + \frac{\partial\{F_2\}^e_{rk}}{\partial x_{ij}}\cos\Omega_k t \tag{D-46}$$

and where

$$\frac{\partial\{F_2\}^e_{rk}}{\partial x_{ij}} = \begin{cases} -[H'_p]^e_{rk}\{c_I\}^e_{rk} - [H_p]^e_{rk}\{c'_I\}^e_{rk} - \Omega_k\,([H'_v]^e_{rk}\{c_R\}^e_{rk} + [H_v]^e_{rk}\{c'_R\}^e_{rk}) \; ; \; i = r \\ -[H_p]^e_{rk}\{c'_I\}^e_{rk} - \Omega_k[H_v]^e_{rk}\{c'_R\}^e_{rk} \; ; \; i \neq r \end{cases} \tag{D-47}$$

$$\frac{\partial\{F_1\}^e_{rk}}{\partial x_{ij}} = \begin{cases} -[H_p']^e_{rk}\{c_R\}^e_{rk} - [H_p]^e_{rk}\{c_R'\}^e_{rk} + \Omega_k\,([H_v']^e_{rk}\{c_I\}^e_{rk} + [H_v]^e_{rk}\{c_I'\}^e_{rk}) \;\; ; \;\; i = r \\ -[H_p]^e_{rk}\{c_R'\}^e_{rk} + \Omega_k[H_v]^e_{rk}\{c_I'\}^e_{rk} \;\; ; \;\; i \neq r \end{cases} \tag{D-48}$$

and

$$\{c_I\}^e_{rk} = [T]_r\{c_I\}_{rk} \tag{D-49}$$

$$\{c_I'\}^e_{rk} = [T]_r\frac{\partial\{c_I\}_{rk}}{\partial x_{ij}} \tag{D-50}$$

$$\{c_R\}^e_{rk} = [T]_r\{c_R\}_{rk} \tag{D-51}$$

$$\{c_R'\}^e_{rk} = [T]_r\frac{\partial\{c_R\}_{rk}}{\partial x_{ij}} \tag{D-52}$$

Finally, the derivatives of the magnitudes of the actuator forces are easily obtained by differentiating Eq. (3-48) with respect to x_{ij}, yielding (for the r-th actuator)

$$\frac{\partial|F^e_{A_{rk}}|}{\partial x_{ij}} = \left[(F^e_{1_{rk}})^2 + (F^e_{2_{rk}})^2\right]^{-1/2}\left[F^e_{1_{rk}}\frac{\partial F^e_{1_{rk}}}{\partial x_{ij}} + F^e_{2_{rk}}\frac{\partial F^e_{2_{rk}}}{\partial x_{ij}}\right] \tag{D-53}$$

where $\frac{\partial F^e_{2_{rk}}}{\partial x_{ij}}$ and $\frac{\partial F^e_{1_{rk}}}{\partial x_{ij}}$ are obtained from Eqs. (D-47) and (D-48), respectively.

D.5 Eigenvalue Derivatives

The derivatives of the structural eigenvalues are obtained by implicitly differentiating Eq. (3-53) with respect to x_{ij}. Rewriting Eq. (3-53) as

$$[[K] - \omega^2\,[M]]\{\phi\} = \{0\} \tag{D-54}$$

and differentiating with respect to x_{ij} gives

$$\frac{\partial[K]}{\partial x_{ij}}\{\phi\} + [K]\frac{\partial\{\phi\}}{\partial x_{ij}} - \frac{\partial\omega^2}{\partial x_{ij}}[M]\{\phi\} - \omega^2\frac{\partial[M]}{\partial x_{ij}}\{\phi\} - \omega^2[M]\frac{\partial\{\phi\}}{\partial x_{ij}} = \{0\} \tag{D-55}$$

Pre-multiplying Eq. (D-55) by $\{\phi\}^T$ and simplifying yields

$$\{\phi\}^T\left[\frac{\partial[K]}{\partial x_{ij}} - \omega^2\frac{\partial[M]}{\partial x_{ij}}\right]\{\phi\} - \frac{\partial\omega^2}{\partial x_{ij}}\{\phi\}^T[M]\{\phi\} +$$

$$\{\phi\}^T\left[[K] - \omega^2[M]\right]\frac{\partial\{\phi\}}{\partial x_{ij}} = \{0\} \tag{D-56}$$

By symmetry of [K] and [M]

$$\{\phi\}^T\left[[K] - \omega^2[M]\right] = \left[[K] - \omega^2[M]\right]\{\phi\} = \{0\} \tag{D-57}$$

Using Eq. (D-57), Eq. (D-56) yields the following expression for the eigenvalue derivative:

$$\frac{\partial\omega^2}{\partial x_{ij}} = \frac{\{\phi\}^T\left[\frac{\partial[K]}{\partial x_{ij}} - \omega^2\frac{\partial[M]}{\partial x_{ij}}\right]\{\phi\}}{\{\phi\}^T[M]\{\phi\}} \tag{D-58}$$

For the case where the eigenvectors are normalized with respect to the mass matrix Eq. (D-58) simplifies to

$$\frac{\partial\omega^2}{\partial x_{ij}} = \{\phi\}^T\left[\frac{\partial[K]}{\partial x_{ij}} - \omega^2\frac{\partial[M]}{\partial x_{ij}}\right]\{\phi\} \tag{D-59}$$

Table 1. Iteration History Data for Problem 1, Case A
Cantilevered Beam, Mass Minimization

Analysis Number	Mass (kg) [Maximum Constraint Violation (%)]		
	Uncontrolled	Controlled 1 actuator	Controlled 2 actuators
0	1937.60 [241.4]	1937.60 [244.1]	1937.60 [99.6]
1	1560.58 [18.9]	1686.56 [13.3]	1788.09 [0.8]
2	1287.93 [0.0]	1300.05 [0.0]	1314.18 [0.0]
3	1024.38 [0.0]	986.48 [0.0]	964.97 [0.0]
4	821.50 [0.0]	766.04 [0.0]	733.67 [0.0]
5	682.32 [0.0]	617.74 [0.0]	582.34 [0.0]
6	588.90 [0.0]	522.04 [0.0]	485.25 [0.0]
7	545.57 [0.0]	477.55 [0.0]	440.14 [0.0]
8	545.57 [0.0]	470.96 [0.0]	434.40 [0.0]
9	545.57 [0.0]	470.65 [0.0]	434.11 [0.0]
10		470.49 [0.0]	434.03 [0.0]

Table 2. Final Designs for Problem 1, Case A
Cantilevered Beam, Mass Minimization

			Final Design (cm, Nt/cm, Nt-sec/cm)		
Element Type	Element Numbers	Design Variables	Uncontrolled	Controlled 1 actuator	Controlled 2 actuators
Frame	1-10	t_b	2.0141	1.6663	1.4975
		t_h	.5000⁻	.5000⁻	.5000⁻
Control	1	h_p		79.3672	79.6817
		h_v		.4216	.3588
	2	h_p			82.6042
		h_v			.4012

- denotes lower bound value

Table 3. Final Design Response Ratios for Problem 1, Case A
Cantilevered Beam, Mass Minimization

Constraint	Response Ratio (R_q)*		
	Uncontrolled	Controlled 1 actuator	Controlled 2 actuators
Tip Displacement	.98958	.99783	.99665
Frequency	.65137	.69271	.72034
Actuator Force (1)		.99829	.99871
Actuator Force (2)			.74927
Total Control Force		.57045	.99884

* R_q = 1.0 indicates that the constraint is critical

Table 4. Iteration History Data for Problem 1, Case B
Cantilevered Beam, Mass Minimization

Analysis Number	Mass (kg) [Maximum Constraint Violation (%)]		
	Uncontrolled	Controlled 1 actuator	Controlled 2 actuators
0	1937.60 [241.4]	1937.60 [244.1]	1937.60 [96.8]
1	1435.58 [5.0]	1445.70 [2.0]	1451.64 [0.0]
2	1060.17 [0.0]	1055.86 [0.0]	1051.61 [0.0]
3	774.72 [0.0]	768.06 [0.0]	762.12 [0.0]
4	571.01 [0.0]	563.48 [0.0]	557.37 [0.0]
5	428.23 [0.0]	420.22 [0.0]	413.16 [0.0]
6	329.83 [0.0]	318.91 [0.0]	311.01 [0.0]
7	293.13 [0.0]	279.29 [0.0]	270.72 [0.0]
8	292.16 [0.0]	276.10 [0.0]	267.58 [0.0]
9	292.16 [0.0]	275.51 [0.0]	266.83 [0.0]
10		274.68 [0.0]	266.09 [0.0]

Table 5. Final Designs for Problem 1, Case B
Cantilevered Beam, Mass Minimization

			Final Design (cm, Nt/cm, Nt-sec/cm)		
Element Type	Element Numbers	Design Variables	Uncontrolled	Controlled 1 actuator	Controlled 2 actuators
Frame	1-2	t_b	1.6100	1.3974	1.2824
	3-4	t_b	1.0570	0.8998	.8156
	5-6	t_b	.5350	.5000⁻	.5000⁻
	7-8	t_b	.5000⁻	.5000⁻	.5000⁻
	9-10	t_b	.5000⁻	.5000⁻	.5000⁻
	1-10	t_h	.5000⁻	.5000⁻	.5000⁻
Control	1	h_p		74.3907	75.2934
		h_v		1.2213	1.0236
	2	h_p			79.4161
		h_v			1.5079

- denotes lower bound value

Table 6. Final Design Response Ratios for Problem 1, Case B
Cantilevered Beam, Mass Minimization

Constraint	Response Ratio (R_q)*		
	Uncontrolled	Controlled 1 actuator	Controlled 2 actuators
Tip Displacement	1.00006	.99793	.99725
Frequency	.11758	.30830	.41180
Actuator Force (1)		1.00023	.98929
Actuator Force (2)			.75857
Total Control Force		.57156	.99877

* R_q = 1.0 indicates that the constraint is critical

Table 7. Iteration History Data for Problem 2, Case A
Cantilevered Beam, Response Minimization

	Tip Displacement (cm) [Maximum Constraint Violation (%)]		
Analysis Number	Uncontrolled	Controlled 1 actuator	Controlled 2 actuators
0	24.14 [241.4]	15.73 [244.1]	12.86 [99.6]
1	10.29 [43.1]	8.19 [54.2]	8.78 [39.4]
2	8.05 [10.7]	7.06 [11.6]	7.45 [2.1]
3	6.51 [0.1]	5.89 [0.1]	5.57 [0.4]
4	5.55 [0.3]	5.06 [0.2]	4.83 [0.2]
5	5.30 [0.0]	4.82 [0.0]	4.60 [0.0]
6	5.30 [0.0]	4.53 [0.0]	4.20 [0.0]
7	5.30 [0.0]	4.35 [0.9]	3.81 [0.7]
8		4.33 [0.1]	3.78 [0.2]
9		4.31 [0.1]	3.76 [0.1]

Table 8. Final Designs for Problem 2, Case A
Cantilevered Beam, Response Minimization

Element Type	Element Numbers	Design Variables	Final Design (cm, Nt/cm, Nt-sec/cm) Uncontrolled	Controlled 1 actuator	Controlled 2 actuators
Frame	1-10	t_b	4.1210	4.1208	4.1207
		t_h	.5000⁻	.5000⁻	.5000
Control	1	h_p		166.7668	195.1923
		h_v		3.3558	3.4610
	2	h_p			190.9900
		h_v			4.6705

- denotes lower bound value

Table 9. Final Design Response Ratios for Problem 2, Case A
Cantilevered Beam, Response Minimization

Constraint	Response Ratio (R_q)*		
	Uncontrolled	Controlled 1 actuator	Controlled 2 actuators
Mass	1.00045	1.00041	1.00039
Frequency	.61204	.61204	.61203
Actuator Force (1)		1.00089	.99954
Actuator Force (2)			.75220
Total Control Force		.57194	1.00100

* R_q = 1.0 indicates that the constraint is critical

Table 10. Iteration History Data for Problem 2, Case B
Cantilevered Beam, Response Minimization

Analysis Number	Tip Displacement (cm) [Maximum Constraint Violation (%)]		
	Uncontrolled	Controlled 1 actuator	Controlled 2 actuators
0	24.14 [241.4]	15.73 [244.1]	12.86 [99.6]
1	15.51 [55.1]	10.84 [40.9]	7.46 [26.2]
2	20.87 [208.7]	11.43 [27.1]	3.23 [0.0]
3	4.20 [0.0]	4.60 [0.0]	2.05 [0.2]
4	2.71 [0.0]	2.81 [0.0]	1.65 [0.0]
5	2.12 [0.0]	2.03 [0.0]	1.48 [0.0]
6	1.93 [0.3]	1.72 [0.7]	1.36 [3.1]
7	1.85 [0.2]	1.55 [0.2]	1.27 [6.6]
8	1.81 [0.2]	1.45 [0.3]	1.27 [0.8]
9	1.79 [0.0]	1.43 [0.7]	1.26 [0.6]
10	1.79 [0.0]	1.43 [0.7]	1.26 [0.9]
11	1.79 [0.0]	1.43 [0.2]	1.25 [0.2]

Table 11. Final Designs for Problem 2, Case B
Cantilevered Beam, Response Minimization

Element Type	Element Numbers	Design Variables	Final Design (cm, Nt/cm, Nt-sec/cm) Uncontrolled	Controlled 1 actuator	Controlled 2 actuators
Frame	1-2	t_b	8.2810	8.2805	8.2701
	3-4	t_b	6.2360	6.2388	6.2426
	5-6	t_b	3.8119	3.8149	3.8490
	7-8	t_b	1.7654	1.7634	1.7670
	9-10	t_b	.5000⁻	.5000⁻	.5000⁻
	1-10	t_h	.5000⁻	.5000⁻	.5000⁻
Control	1	h_p		554.9204	635.5459
		h_v		3.3034	3.0415
	2	h_p			739.5169
		h_v			4.1872

- denotes lower bound value

Table 12. Final Design Response Ratios for Problem 2, Case B
Cantilevered Beam, Response Minimization

Constraint	Response Ratio $(R_q)^*$		
	Uncontrolled	Controlled 1 actuator	Controlled 2 actuators
Mass	1.00000	1.00014	1.00148
Frequency	-2.46838	-2.46920	-2.46126
Actuator Force (1)		1.00191	1.00245
Actuator Force (2)			.75143
Total Control Force		.57252	1.00222

* R_q = 1.0 indicates that the constraint is critical

Table 13. Iteration History Data for Problem 3, Case A
Cantilevered Beam, Control Force Minimization

	Control Force (Nt) [Maximum Constraint Violaton (%)]		
Analysis Number	Actuator No. 1	Actuator No. 2	Combined
0	1621.8 [261.3]	1326.9 [294.9]	2429.4 [259.5]
1	1790.3 [200.9]	1374.7 [217.7]	2816.0 [198.2]
2	2339.4 [70.7]	1945.1 [79.8]	3535.1 [47.8]
3	3178.6 [23.6]	2829.9 [50.6]	4168.7 [0.0]
4	3591.7 [0.0]	3731.6 [39.6]	3991.8 [0.0]
5	3379.6 [0.0]	4696.5 [17.4]	3844.3 [0.0]
6	3194.7 [0.0]	4174.6 [24.6]	3719.9 [0.0]
7	3055.5 [0.0]	4106.4 [12.1]	3518.1 [0.0]
8	3000.0 [0.0]	4213.1 [5.3]	3323.9 [0.0]
9	2879.6 [0.0]	3990.6 [0.1]	3191.5 [0.0]
10	2854.3 [0.0]	3955.0 [0.1]	3114.7 [0.0]
11	2835.7 [0.0]	3916.7 [0.1]	3000.6 [0.0]
12			2946.6 [0.0]
13			2920.3 [0.0]
14			2887.8 [0.0]
15			2871.1 [0.0]

Table 14. Final Designs for Problem 3, Case A
Cantilevered Beam, Control Force Minimization

			Final Design (cm, Nt/cm, Nt-sec/cm)		
Element Type	Element Numbers	Design Variables	Actuator #1	Actuator #2	Combined
Frame	1-10	t_b	1.3391	1.3413	1.3400
		t_h	.5000⁻	.5000⁻	.5000⁻
Control	1	h_p	559.8847		548.3611
		h_v	4.6400		3.5447
	2	h_p		1080.5325	30.8545
		h_v		10.6129	0.6400

- denotes lower bound value

Table 15. Final Design Response Ratios for Problem 3, Case A
Cantilevered Beam, Control Force Minimization

	Response Ratio $(R_q)^*$		
Constraint	Actuator #1	Actuator #2	Combined
Mass	.99957	1.00075	1.00009
Tip Displacement	.99407	.99170	.99060
Frequency	.75210	.75161	.75188
Actuator Force (1)	.70894		.68747
Actuator Force (2)		.97918	.03187

* $R_q = 1.0$ indicates that the constraint is critical

Table 16. Iteration History Data for Problem 3, Case B
Cantilevered Beam, Control Force Minimization

	Control Force (Nt) [Maximum Constraint Violaton (%)]		
Analysis Number	Actuator No. 1	Actuator No. 2	Combined
0	1191.2 [225.0]	1378.0 [228.1]	1847.8 [202.7]
1	1269.4 [42.4]	1434.3 [47.1]	1841.1 [33.6]
2	1617.8 [8.2]	1805.5 [14.2]	1625.6 [5.4]
3	1343.8 [0.0]	1543.5 [0.0]	1318.3 [0.0]
4	1127.9 [0.0]	1409.1 [0.0]	1167.0 [0.0]
5	964.6 [0.0]	1341.9 [0.0]	1074.7 [0.0]
6	902.2 [0.0]	1251.4 [0.0]	997.4 [0.0]
7	842.9 [0.0]	1231.9 [0.0]	950.9 [0.0]
8	822.0 [0.1]	1218.4 [0.1]	897.1 [0.0]
9	812.2 [0.1]	1214.8 [0.1]	879.2 [0.1]
10	811.4 [0.1]	1214.8 [0.1]	871.1 [0.0]
11	810.5 [0.1]		867.4 [0.1]
12			866.6 [0.1]

Table 17. Final Designs for Problem 3, Case B
Cantilevered Beam, Control Force Minimization

Element Type	Element Numbers	Design Variables	Final Design (cm, Nt/cm, Nt-sec/cm) Actuator #1	Actuator #2	Combined
Frame	1-2	t_b	2.7099	2.7013	2.6999
	3-4	t_b	1.9018	1.8976	1.9151
	5-6	t_b	1.0813	1.1018	1.0857
	7-8	t_b	.5000⁻	.5000⁻	.5000⁻
	9-10	t_b	.5000⁻	.5000⁻	.5000⁻
	1-10	t_h	.5000⁻	.5000⁻	.5000⁻
Control	1	h_p	196.9884		172.6867
		h_v	1.9062		1.5341
	2	h_p		452.6438	52.3790
		h_v		4.1980	1.2029

- denotes lower bound value

Table 18. Final Design Response Ratios for Problem 3, Case B
Cantilevered Beam, Control Force Minimization

	Response Ratio $(R_q)^*$		
Constraint	Actuator #1	Actuator #2	Combined
Mass	.99932	1.00015	1.00016
Tip Displacement	1.00092	1.00100	1.00091
Frequency	-.81666	-.81196	-.81387
Actuator Force (1)	.20264		.17686
Actuator Force (2)		.30370	.04000

* $R_q = 1.0$ indicates that the constraint is critical

Table 19. Iteration History Data for Problem 4
Cantilevered Beam, Multiple Loading Conditions

Analysis Number	Mass (kg) [Maximum Constraint Violation (%)]		
	Uncontrolled	Controlled 1 actuator	Controlled 2 actuators
0	1937.60 [241.4]	1937.60 [244.1]	1937.60 [199.6]
1	1435.58 [5.0]	1445.70 [2.0]	1450.12 [0.0]
2	1060.25 [0.0]	1056.75 [0.0]	1050.51 [0.0]
3	774.67 [0.0]	764.82 [0.0]	762.41 [0.0]
4	586.29 [0.0]	559.22 [0.0]	559.19 [0.0]
5	525.75 [0.0]	482.77 [1.2]	434.07 [0.0]
6	502.78 [0.0]	446.32 [0.0]	363.08 [0.0]
7	491.28 [0.0]	425.22 [0.7]	318.91 [0.3]
8	484.39 [0.0]	409.00 [0.0]	297.34 [0.0]
9	478.81 [0.0]	399.44 [0.3]	288.51 [0.0]
10	476.29 [0.0]	397.69 [0.1]	288.40 [0.3]
11	475.00 [0.0]	397.20 [0.0]	283.72 [0.0]
12	473.58 [0.0]	397.03 [0.0]	281.41 [0.0]
13	473.18 [0.1]	396.90 [0.0]	281.20 [0.0]
14	473.18 [0.1]		281.20 [0.0]

Table 20. Final Designs for Problem 4
Cantilevered Beam, Multiple Loading Conditions

			Final Design (cm, Nt/cm, Nt-sec/cm)		
Element Type	Element Numbers	Design Variables	Uncontrolled	Controlled 1 actuator	Controlled 2 actuators
Frame	1-2	t_b	2.1628	1.9997	1.0930
	3-4	t_b	1.6528	1.2940	.9583
	5-6	t_b	1.3692	.9611	.7579
	1-6	t_h	.5000⁻	.5000⁻	.5000⁻
	7-8	t_b	1.0222	.7462	.6138
		t_h	.6024	.5308	.5000⁻
	9-10	t_b	1.3199	1.0629	.5251
		t_h	1.3012	1.0493	.5000⁻
Control	1	h_p		20.7929	68.3930
		h_v		3.1488	1.6856
	2	h_p			96.0628
		h_v			2.4295

- denotes lower bound value

Table 21. Final Design Response Ratios for Problem 4
Cantilevered Beam, Multiple Loading Conditions

Constraint	Loading Condition	Response Ratio (R_q)* Uncontrolled	Controlled 1 actuator	Controlled 2 actuators
Tip Displacement	1	1.00076	1.00010	.99867
	2	.98334	.99097	.99887
Tip Rotation	3	.60900	.73928	1.00003
Frequency (u.b.)		.94251	.98495	.99572
Actuator Force (1)	1		.99901	.99739
	2		.25756	.85395
Actuator Force (2)	1			.99934
	2			.88125

* R_q = 1.0 indicates that the constraint is critical

Table 22. Iteration History Data for Problem 5
Cantilevered Beam, Lumped Mass Design Elements

Analysis Number	Mass (kg) [Maximum Constraint Violation (%)]		
	Uncontrolled	Controlled 1 actuator	Controlled 2 actuators
0	1947.60 [335.8]	1947.60 [279.5]	1947.60 [219.1]
1	1445.78 [22.3]	1470.50 [16.0]	1477.12 [0.0]
2	1445.41 [3.3]	1091.00 [0.0]	1082.43 [0.0]
3	1070.74 [0.0]	784.28 [0.0]	776.74 [0.0]
4	786.11 [0.0]	579.72 [0.0]	573.58 [0.0]
5	592.42 [0.0]	462.35 [0.0]	447.21 [0.0]
6	523.86 [0.0]	421.49 [0.0]	378.56 [0.0]
7	500.25 [0.0]	402.11 [0.0]	337.62 [0.0]
8	488.48 [0.0]	391.04 [0.2]	317.22 [0.0]
9	479.45 [0.0]	388.08 [0.1]	301.70 [0.9]
10	474.24 [0.0]	387.80 [0.1]	290.24 [0.0]
11	472.14 [0.0]	387.80 [0.1]	285.13 [0.0]
12	471.40 [0.0]		284.81 [0.2]
13	470.87 [0.0]		283.76 [0.1]
14	470.32 [0.0]		283.55 [0.1]
15	469.74 [0.0]		283.37 [0.1]
16	469.41 [0.0]		
17	468.90 [0.1]		
18	468.90 [0.1]		
19	468.90 [0.1]		

Table 23. Final Designs for Problem 5
Cantilevered Beam, Lumped Mass Design Elements

			Final Design (cm, Nt/cm, Nt-sec/cm)		
Element Type	Element Numbers	Design Variables	Uncontrolled	Controlled 1 actuator	Controlled 2 actuators
Frame	1-2	t_b	2.1284	1.9958	1.1297
	3-4	t_b	1.7070	1.3627	.9633
	5-6	t_b	1.3557	.8371	.7831
	7-8	t_h	1.0189	.6469	.5395
	1-8	t_h	.5000⁻	.5000⁻	.5000⁻
		t_b	1.1861	.9707	.5000⁻
	9-10	t_h	1.2065	.9586	.5000⁻
Control	1	h_p		20.2639	68.7099
		h_v		3.1582	1.7001
	2	h_p			93.0644
		h_v			2.6498
Mass	1	m	4.3082	3.2333	1.7656
	2	m	5.0644	3.4966	1.8026

- denotes lower bound value

Table 24. Final Design Response Ratios for Problem 5
Cantilevered Beam, Lumped Mass Design Elements

Constraint	Loading Condition	Response Ratio (R_q)* Uncontrolled	Controlled 1 actuator	Controlled 2 actuators
Tip Displacement	1	1.00070	1.00073	.99240
	2	.99900	.99907	.96440
Tip Rotation	3	.61209	.77017	1.00081
Frequency (u.b)		.94385	.99922	.99872
Actuator Force (1)	1		1.00070	.99677
	2		.25306	.99242
Actuator Force (2)	1			.82830
	2			.82127

* R_q = 1.0 indicates that the constraint is critical

Table 25. Iteration History Data for Problem 6
Cantilevered Beam, Independent Actuator Gains

Analysis Number	Mass (kg) [Maximum Constraint Violation (%)] Controlled 1 actuator	Controlled 2 actuators
0	1937.60 [244.1]	1937.60 [99.6]
1	1445.70 [2.0]	1450.12 [0.0]
2	1056.75 [0.0]	1050.51 [0.0]
3	764.82 [0.0]	762.41 [0.0]
4	559.22 [0.0]	559.19 [0.0]
5	435.14 [0.0]	434.07 [0.0]
6	372.52 [0.0]	362.88 [0.0]
7	343.94 [0.0]	318.18 [0.5]
8	334.23 [0.0]	296.23 [0.0]
9	333.89 [0.0]	286.76 [0.0]
10	333.78 [0.1]	281.17 [0.0]
11	333.77 [0.1]	281.11 [0.0]
12		280.89 [0.1]

Table 26. Final Designs for Problem 6
Cantilevered Beam, Independent Actuator Gains

Element Type	Element Numbers	Design Variables	Final Design (cm, Nt/cm, Nt-sec/cm) Controlled 1 actuator	Controlled 2 actuators
Frame	1-2	t_b	1.4020	1.0626
	3-4	t_b	1.1673	.9112
	5-6	t_b	.9463	.8546
	7-8	t_b	.6508	.6126
	1-8	t_h	.5000⁻	.5000⁻
	9-10	t_b	.7572	.5000⁻
		t_h	.7473	.5000⁻
Control	1	h_{p_1}	77.3350	76.3698
		h_{v_1}	.7720	.9318
		h_{p_2}	20.0000*	20.0000*
		h_{v_2}	5.0000*	5.0000*
	2	h_{p_1}		106.1478
		h_{v_1}		1.5067
		h_{p_2}		20.0000*
		h_{v_2}		5.0000*

- indicates lower bound value
* indicates initial design value

Table 27. Final Design Response Ratios for Problem 6
Cantilevered Beam, Independent Actuator Gains

Constraint	Loading Condition	Response Ratio (R_q)* Controlled 1 actuator	Controlled 2 actuators
Tip Displacement	1	1.00063	1.00075
	2	.75560	.54411
Tip Rotation	3	.84822	.99961
Frequency (u.b)		.99178	.98059
Actuator Force (1)	1	.99582	.99712
	2	.18890	.13603
Actuator Force (2)	1		.99926
	2		.09930

* R_q = 1.0 indicates that the constraint is critical

Table 28. Iteration History Data for Problem 7
Planar Truss, Control Force Minimization

Analysis Number	Control Force (lbf) [Maximum Constraint Violation (%)]		
	Case I	Case II	Case III
0	264.91 [16.6]	264.91 [46.1]	264.91 [32.81]
1	289.48 [0.0]	295.97 [8.1]	329.07 [8.9*]
2	273.87 [0.0]	251.30 [0.0]	241.06 [10.2*]
3	261.23 [0.0]	196.44 [0.0]	170.59 [0.0]
4	236.34 [0.0]	159.51 [0.0]	131.08 [0.0]
5	212.26 [0.0]	134.16 [0.0]	109.39 [0.0]
6	181.52 [0.0]	116.94 [0.0]	89.71 [0.0]
7	171.31 [0.0]	94.11 [0.0]	70.27 [0.0]
8	162.92 [0.0]	83.93 [0.0]	56.79 [0.0]
9	158.91 [0.0]	77.63 [0.0]	44.94 [0.0]
10	157.82 [0.0]	70.91 [0.0]	40.22 [0.0]
11	156.55 [0.0]	64.77 [0.0]	39.99 [0.0]
12	156.53 [0.0]	62.63 [0.4]	39.75 [0.0]
13	156.51 [0.0]	60.97 [0.2]	39.51 [0.0]
14		60.24 [0.1]	39.27 [0.0]
15		60.24 [0.1]	

* indicates that the constraint was not included in the approximate problem

Table 29. Final Designs for Problem 7
Planar Truss, Control Force Minimization

Element Type	Element Numbers	Design Variables	Final Design (in^2, lbf/in, lbf-sec/in) Case I	Case II	Case III
Truss	1	A	.1000	.0418	.0384
	2	A	.1000	.2612	.0358
	3	A	.1000	.0418	.0380
	4	A	.1000	.1458	.1512
	5	A	.1000	.0884	.0304
	6	A	.1000	.1464	.1525
	7	A	.1000	.0474	.0430
	8	A	.1000	.0474	.0435
	9	A	.1000	.1318	.1918
	10	A	.1000	.1307	.1908
Control	1	h_p	137.6488	58.2634	30.8160
		h_v	.8188	.4716	.8784
	2	h_p	170.0123	57.3637	31.1041
		h_v	.9489	.4677	.8793
	3	h_p	3.2195	3.6974	5.0606
		h_v	.1276	.1818	.8134
	4	h_p	3.2190	3.6981	5.0605
		h_v	.1276	.1819	.8139

Table 30. Iteration History Data for Problem 8
Antenna, Response Minimization

Analysis Number	Displacement (cm) [Maximum Constraint Violation (%)] Uncontrolled	Controlled
0	.2914 [224.4]	.3461 [232.9]
1	.3773 [27.6]	.3204 [32.5]
2	.4055 [2.3]	.2515 [4.3]
3	.3741 [0.0]	.2297 [0.0]
4	.3382 [0.0]	.2172 [0.0]
5	.3000 [0.0]	.2027 [0.0]
6	.2667 [0.0]	.1933 [0.0]
7	.2501 [0.0]	.1863 [0.0]
8	.2501 [0.0]	.1765 [0.0]
9	.2501 [0.0]	.1649 [0.0]
10		.1552 [0.0]
11		.1478 [0.0]
12		.1478 [0.0]
13		.1478 [0.0]

Table 31. Final Structural Designs for Problem 8
Antenna, Response Minimization

Element Type	Element Numbers	Design Variables	Final Design (cm) Uncontrolled	Controlled
		b	25.0000+	25.0000+
	1	h	18.5854	14.8938
		t	.7156	1.0000+
		b	23.7507	25.0000+
	2	h	21.5130	16.1376
		t	.5686	.6678
		b	25.0000+	25.0000+
Frame	3,4	h	25.0000+	25.0000+
		t	.7222	1.0000+
		b	23.5134	20.7033
	5,6	h	19 3385	15.1999
		t	.5687	.3616
		b	22.6945	21.5850
	7-8	h	24.1004	25.0000+
		t	.5419	1.0000+

+ indicates an upper bound value.

Table 32. Final Design Actuator Forces for Problem 8
Antenna, Response Minimization

	Actuator Forces (Nt)	
Actuator Location (Node Number)	Load Condition #1	Load Condition #2
2	9.4292	9.6983
4	9.9723	9.6279
5	6.0490	9.2117
7	4.7160	9.5934

Table 33. Iteration History Data for Problem 9
Grillage

	Objective Function (lb) [Maximum Constraint Violation (%)]	
Analysis Number	Control Force	Weight
0	9.00 [2.2]	94.20 [249.4]
1	18.53 [0.0]	89.82 [0.0]
2	11.73 [0.0]	85.43 [0.0]
3	7.29 [0.0]	77.42 [6.1]
4	6.70 [0.0]	67.94 [0.0]
5	5.94 [0.0]	61.76 [0.0]
6	5.32 [0.0]	59.00 [0.0]
7	4.66 [0.0]	58.02 [0.2]
8	4.50 [0.0]	58.04 [0.0]
9	3.68 [0.0]	57.55 [0.0]
10	3.65 [0.0]	57.07 [0.4]
11	3.61 [0.0]	56.85 [0.0]
12		56.72 [0.0]
13		56.14 [0.4]
14		55.57 [0.1]
15		55.49 [0.0]

Table 34. Actuator Forces for Problem 9 Grillage

Actuator Location (Grid Number)	Actuator Forces (lb)		
	Initial	Control Force Minimization	Weight Minimization
1,11	.6396	.0277	.1339
3,9	1.0144	.1116	.0872
5,7	1.0571	.4320	.0397
23,33	.3260	.0321	.1297
25,31	.5777	.0242	.0618
27,28	.5754	.0207	.0730
45,55	.9735	.4037	.3301
47,53	1.0011	.0635	.0900
49,51	.8194	.0455	.0754
67,77	.9138	.5201	.5506
69,75	.7511	.0712	.0877
71,73	.6155	.0529	.0759

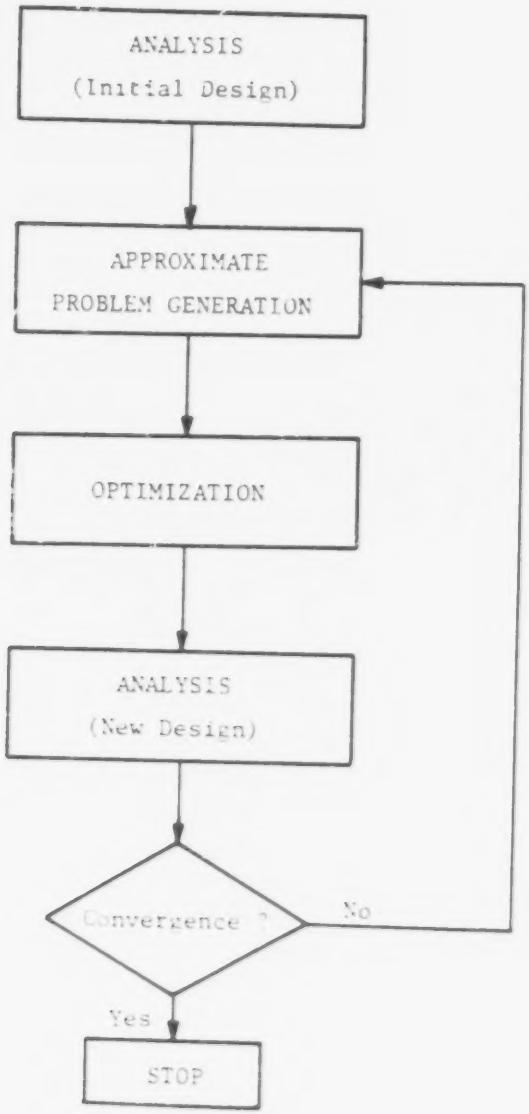

Fig. 1 Design Methodology Flow Diagram

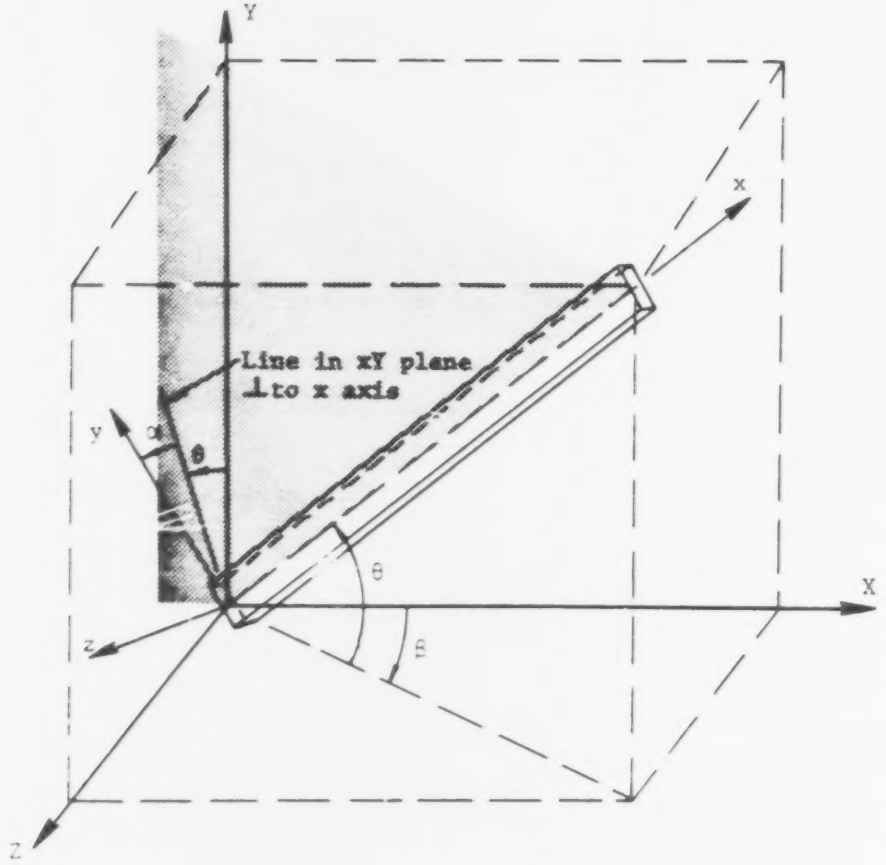

Fig. 2 Structural Element Orientation

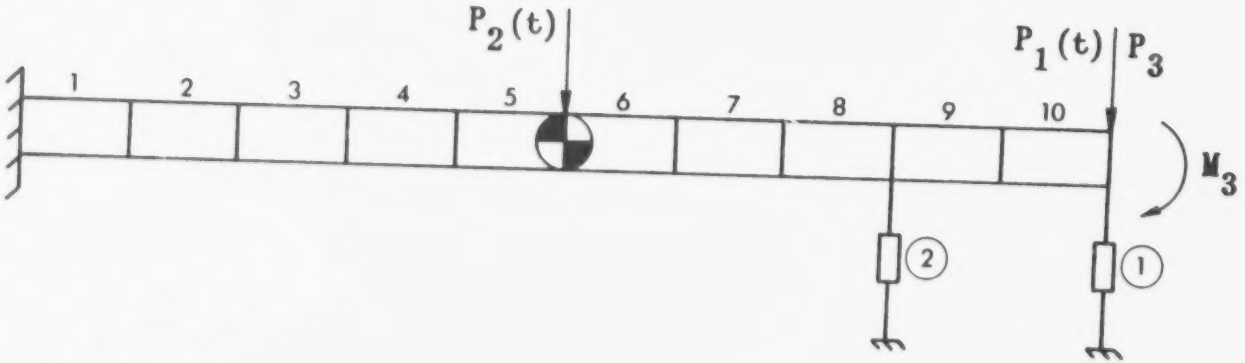

$E = 7.10 \times 10^{6}$ Nt/cm^2

$\rho = 2.768 \times 10^{-3}$ kg/cm^3

$\nu = .3$

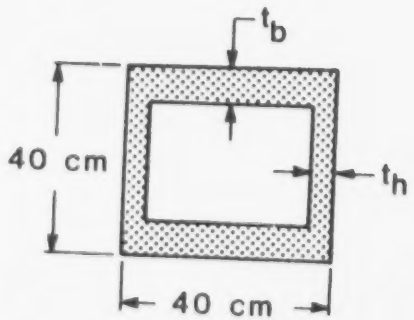

Fig. 3 Cantilevered Beam, Problems 1-6

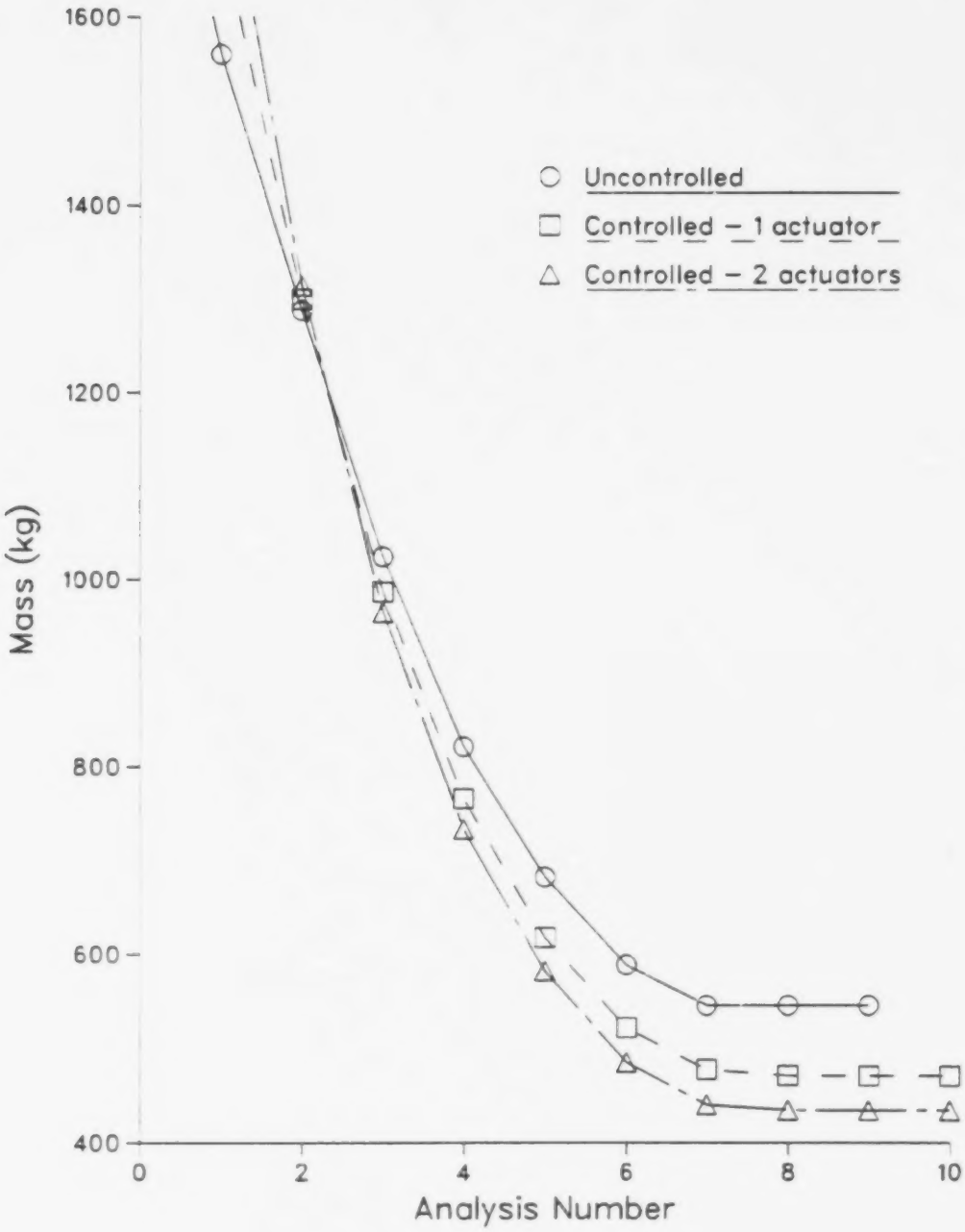

Fig. 4 Iteration Histories for Problem 1, Case A
Cantilevered Beam, Mass Minimization

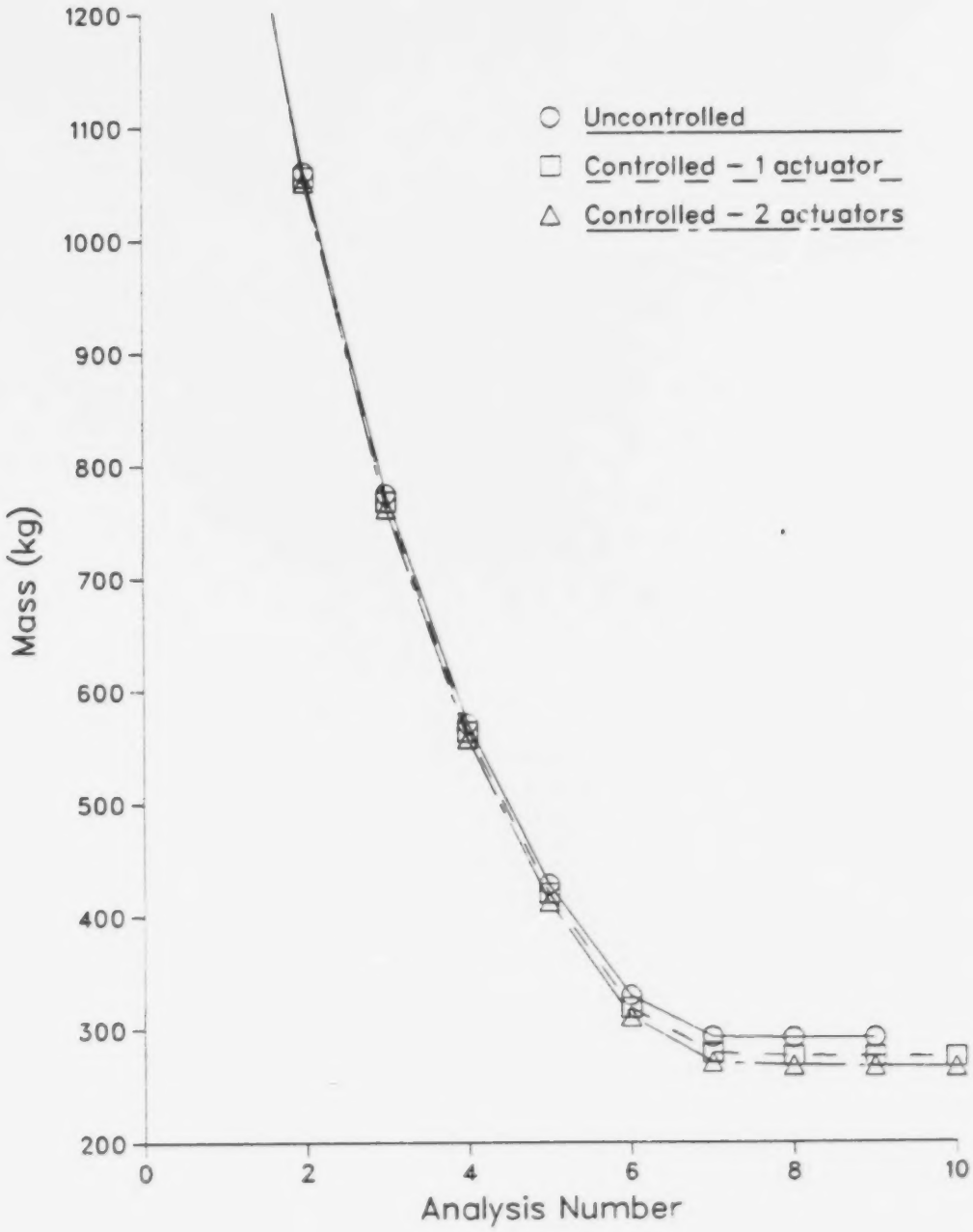

Fig. 5 Iteration Histories for Problem 1, Case B
Cantilevered Beam, Mass Minimization

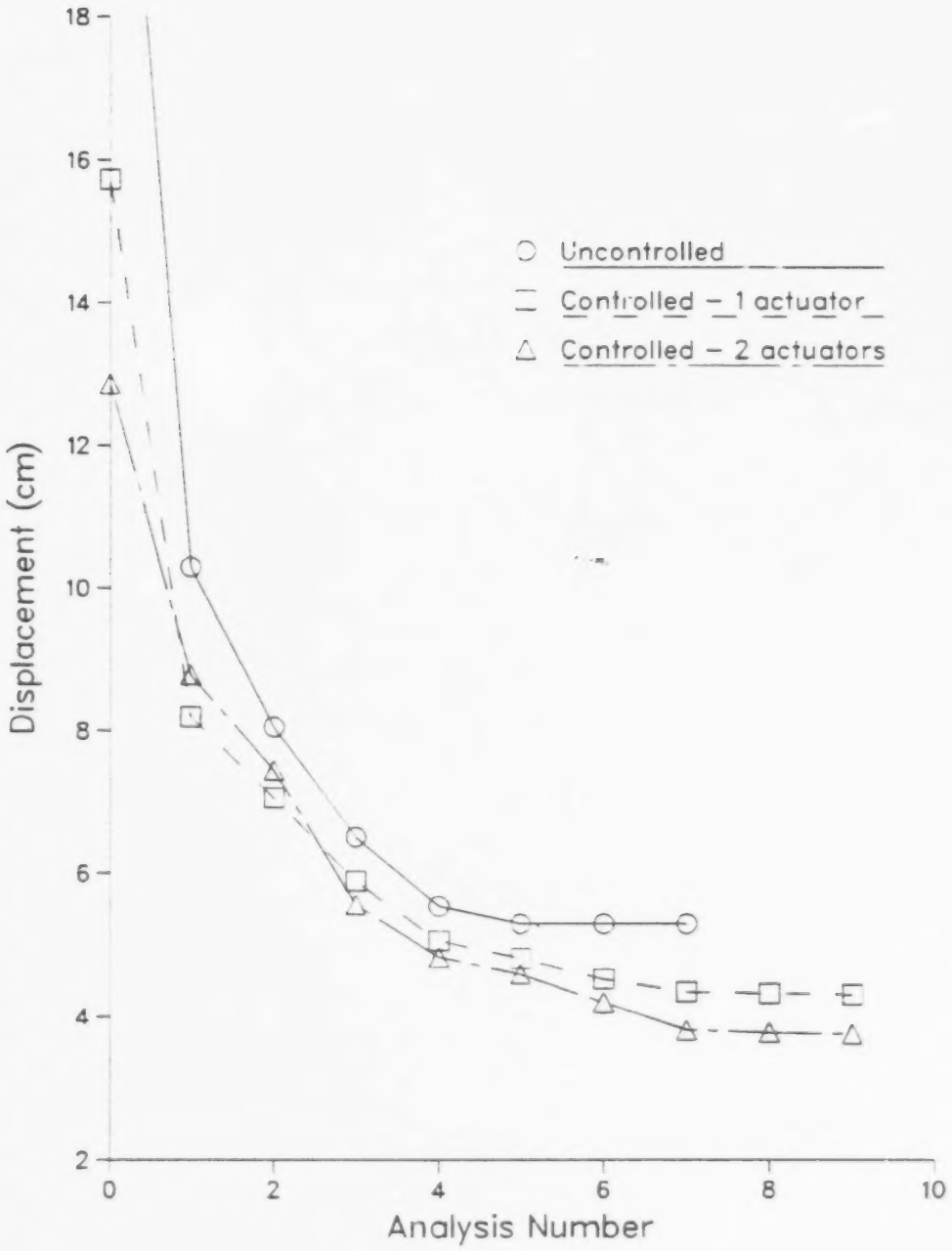

Fig. 6 Iteration Histories for Problem 2, Case A
Cantilevered Beam, Response Minimization

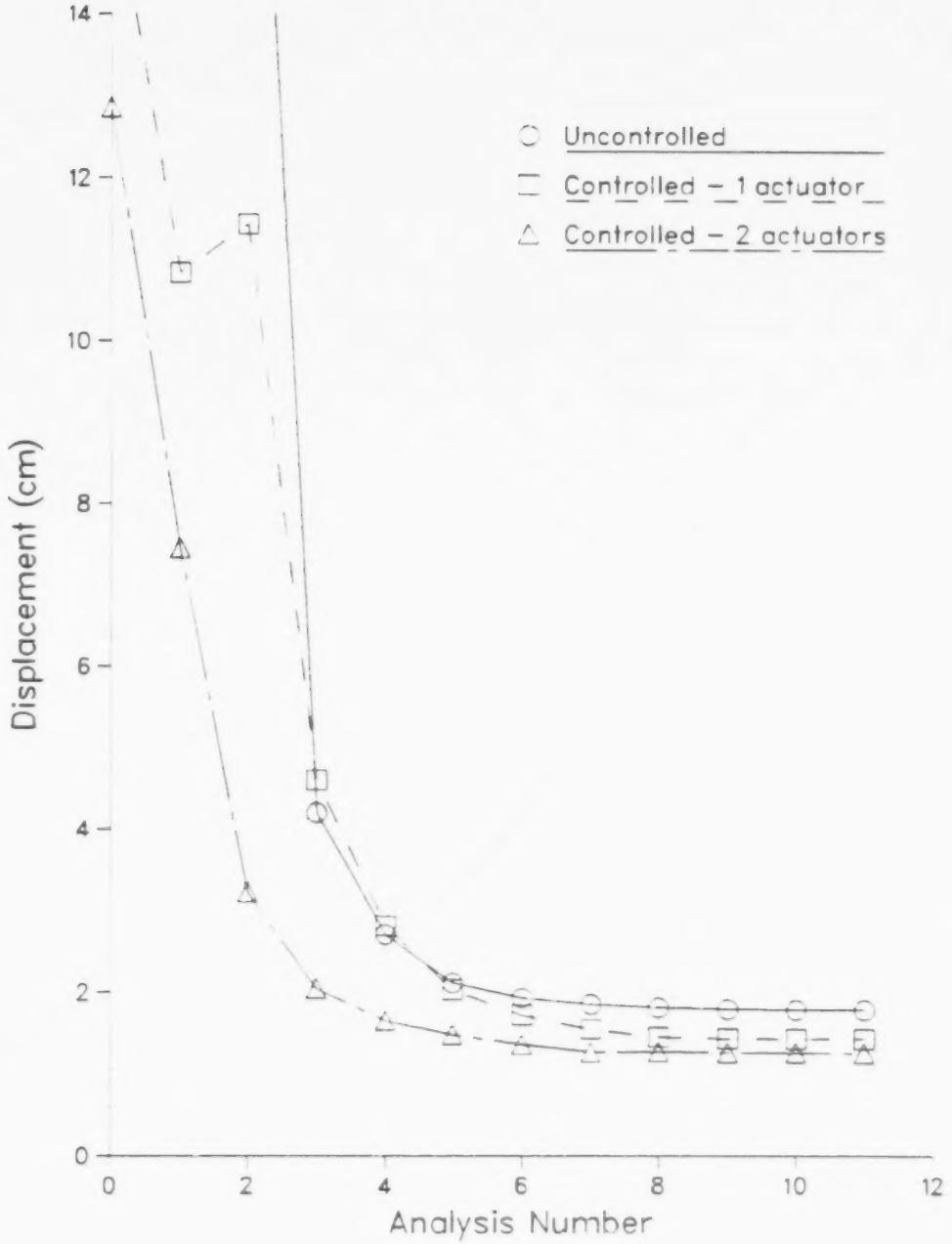

Fig. 7 Iteration Histories for Problem 2, Case B
Cantilevered Beam, Response Minimization

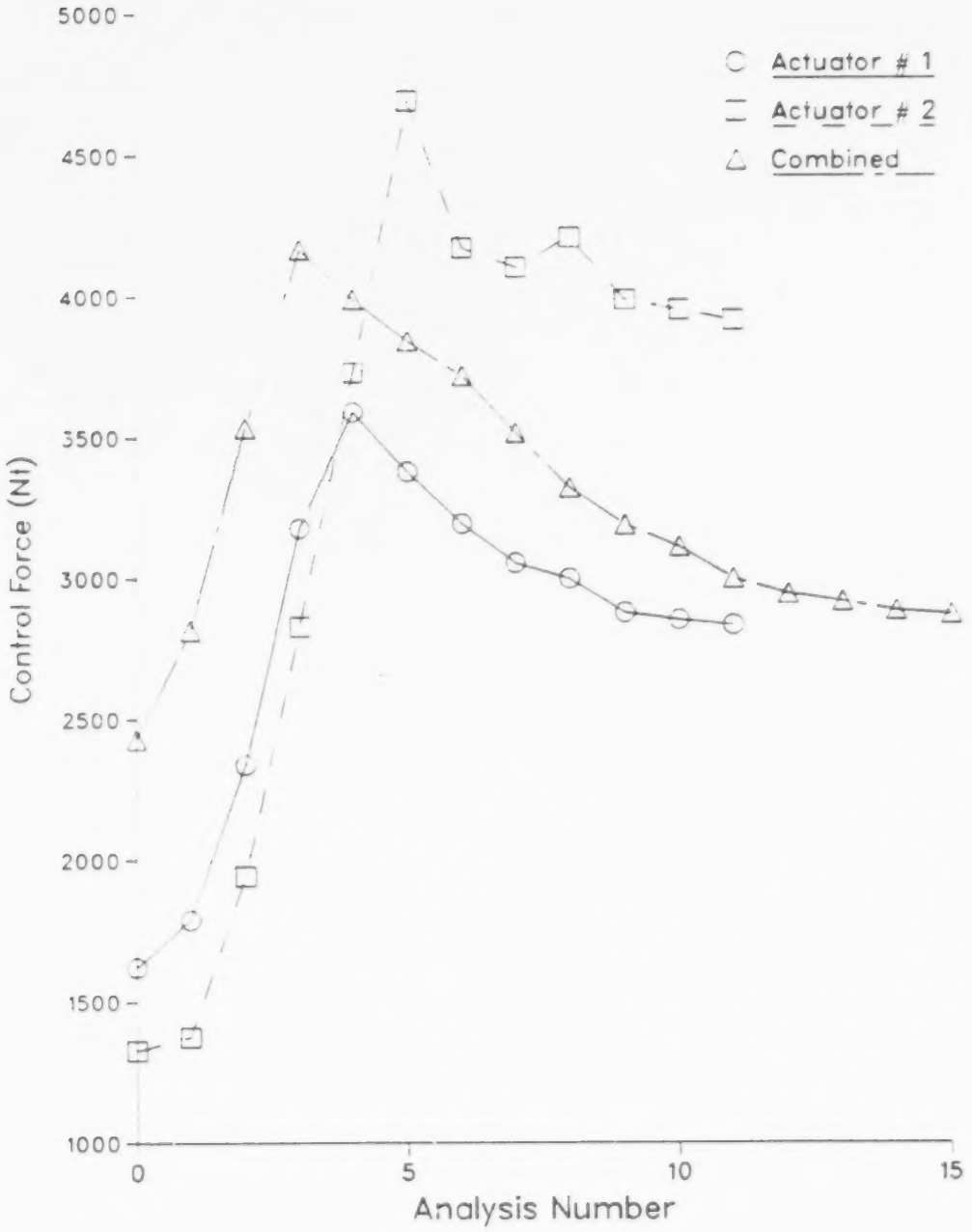

Fig. 8 Iteration Histories for Problem 3, Case A
Cantilevered Beam Control Force Minimization

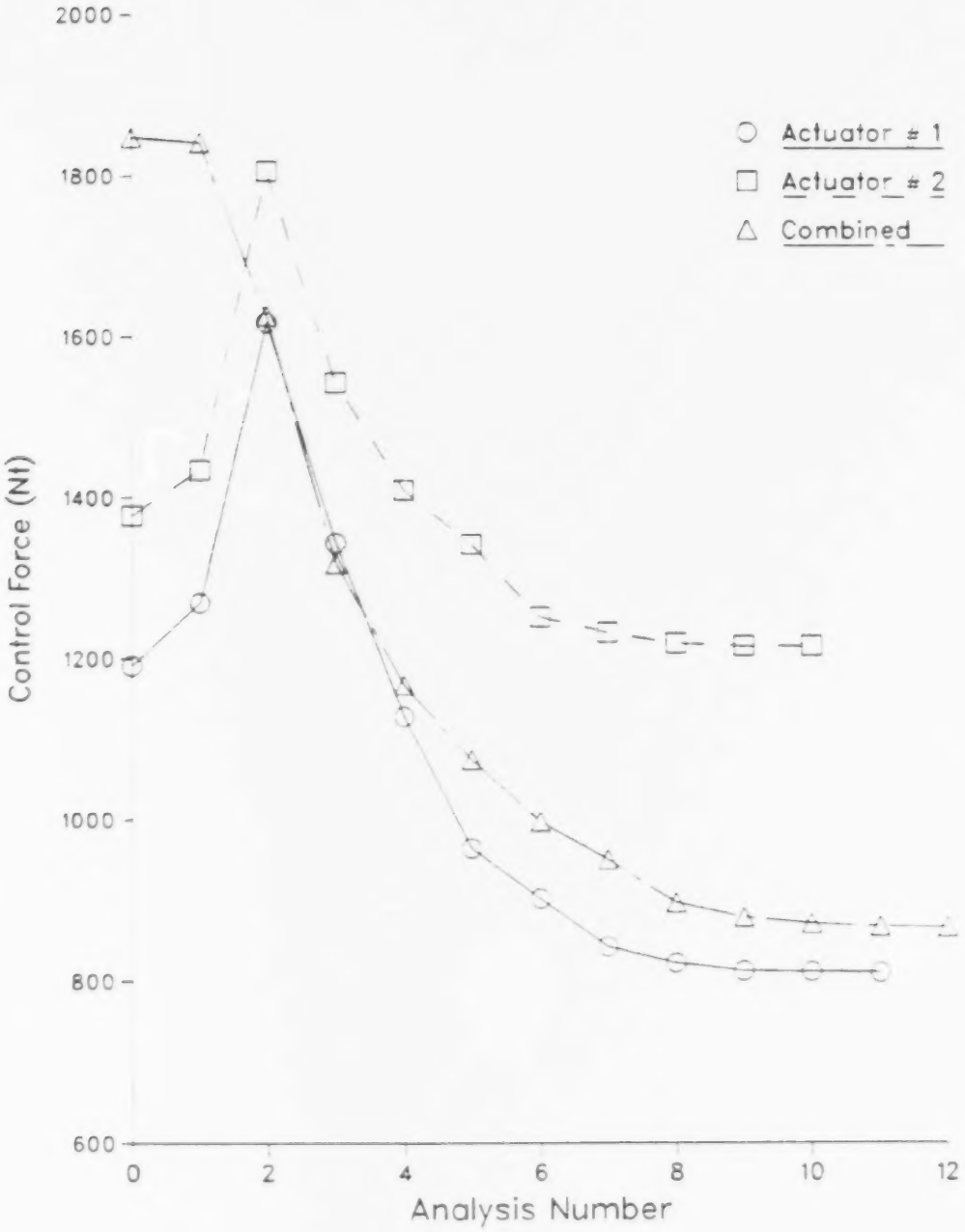

Fig. 9 Iteration Histories for Problem 3, Case B
Cantilevered Beam, Control Force Minimization

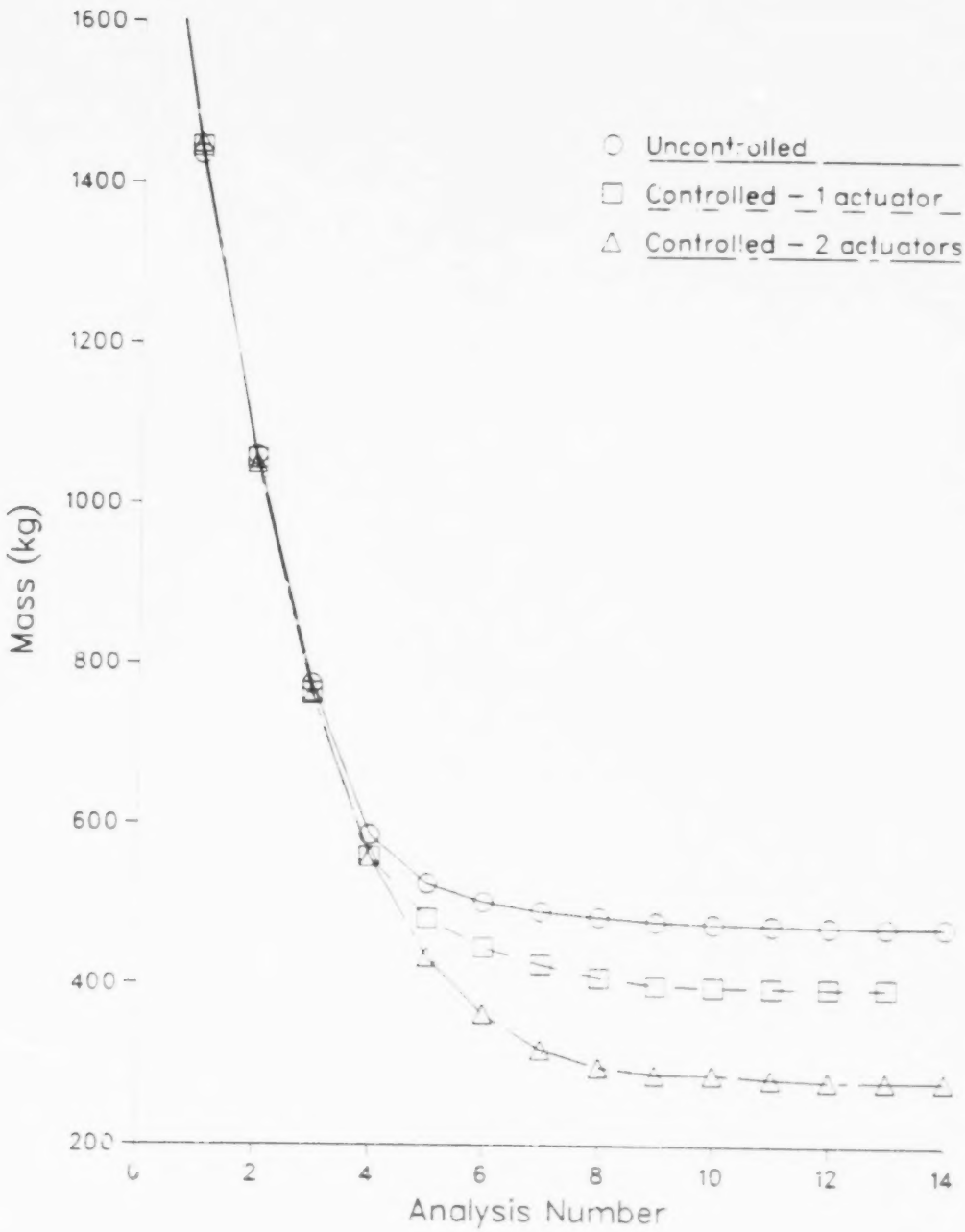

Fig. 10 Iteration Histories for Problem 4
Cantilevered Beam, Multiple Loading Conditions

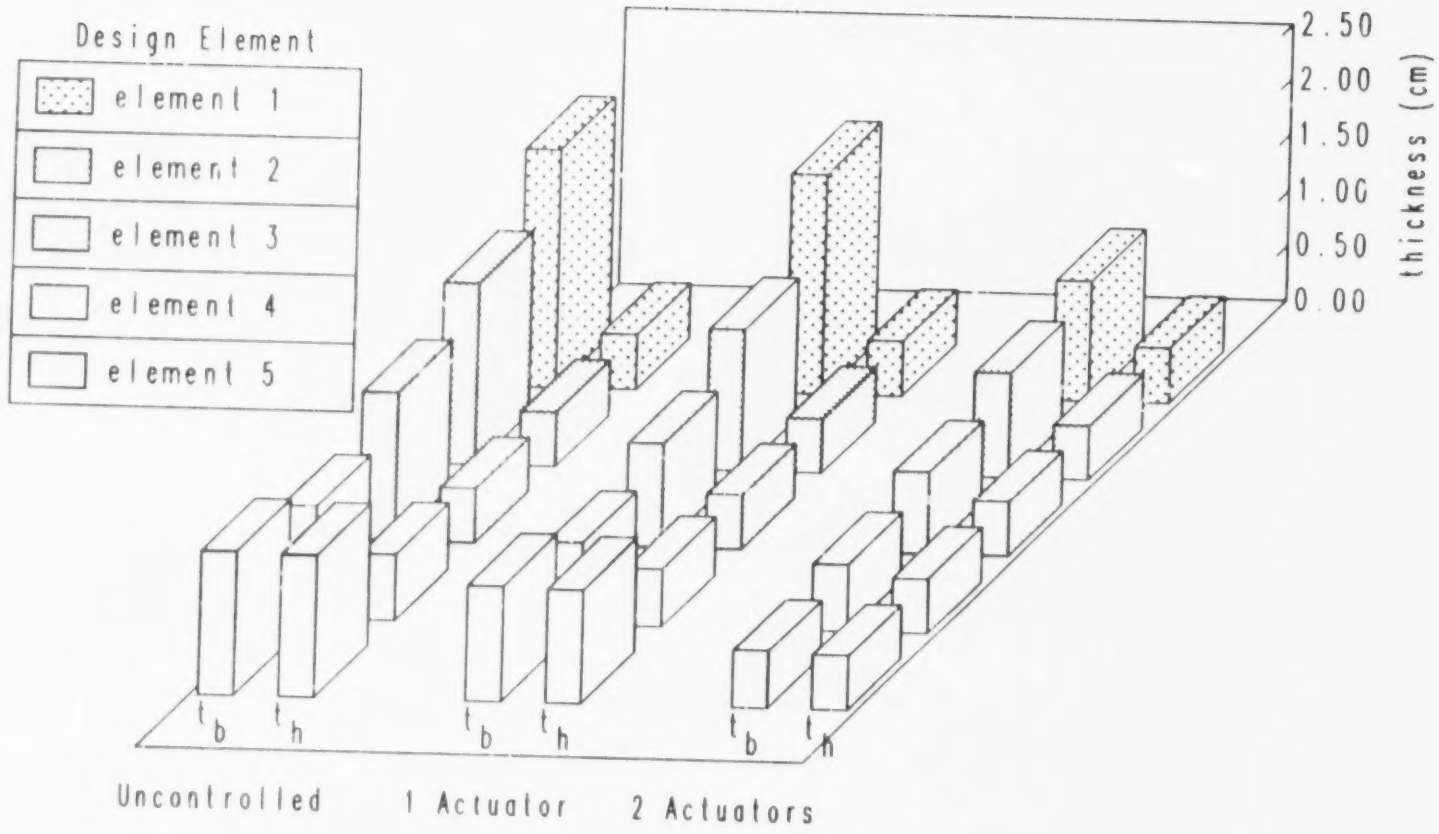

Fig. 11 Final Design Thickness Distributions for Problem 4
Cantilevered Beam, Multiple Loading Conditions

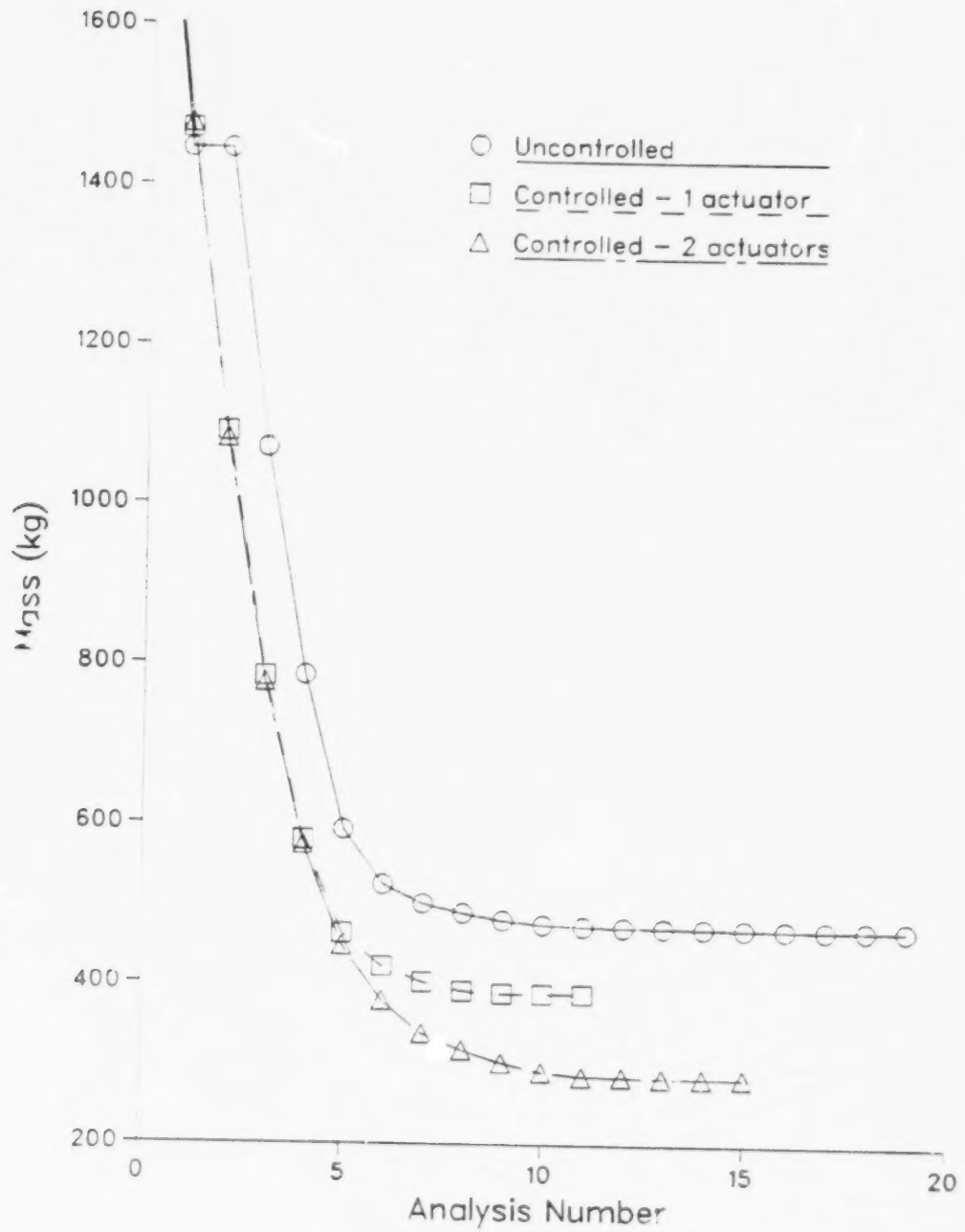

Fig. 12 Iteration Histories for Problem 5
Cantilevered Beam, Lumped Mass Design Elements

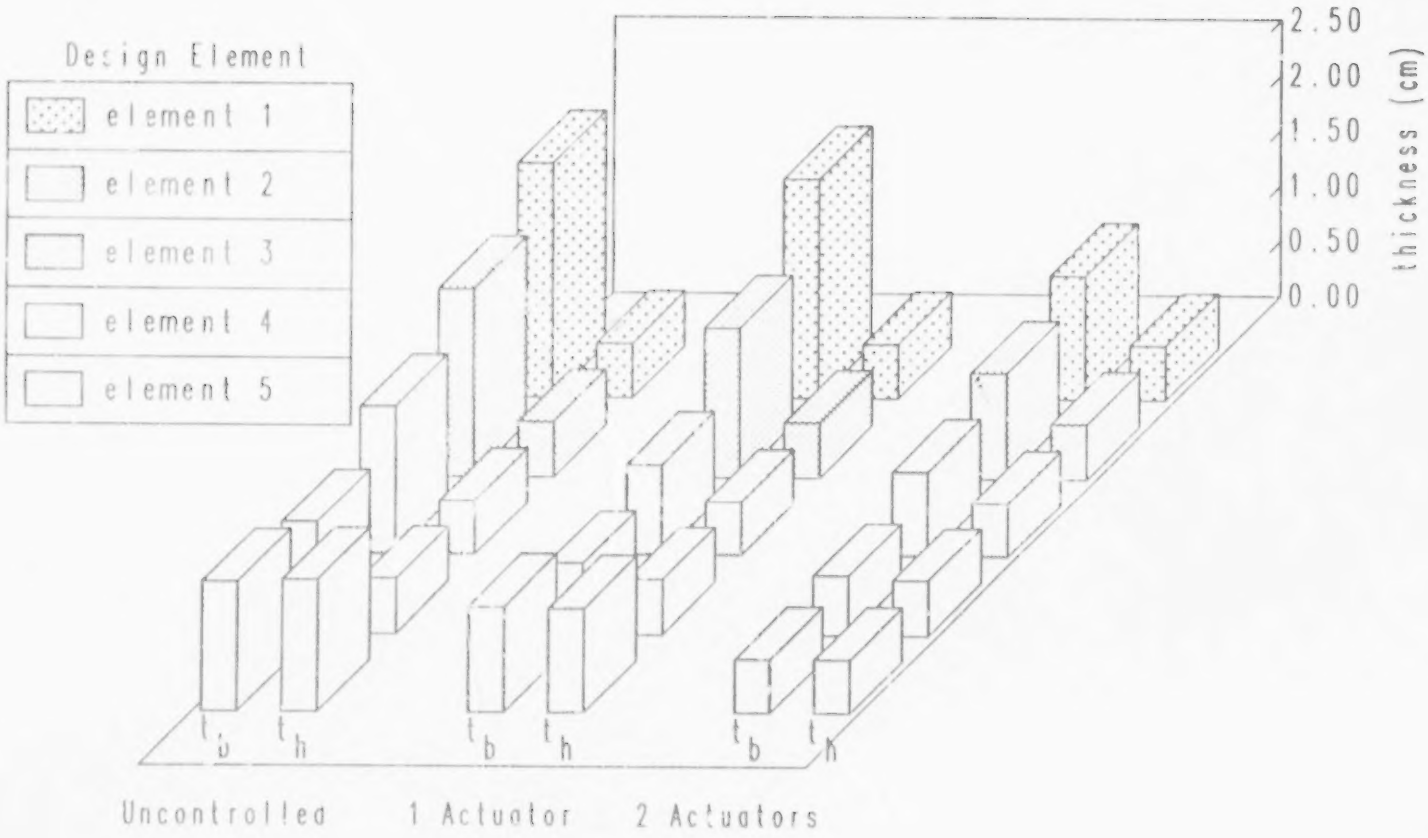

Fig. 13 Final Design Thickness Distributions for Problem 5
Cantilevered Beam, Lumped Mass Design Elements

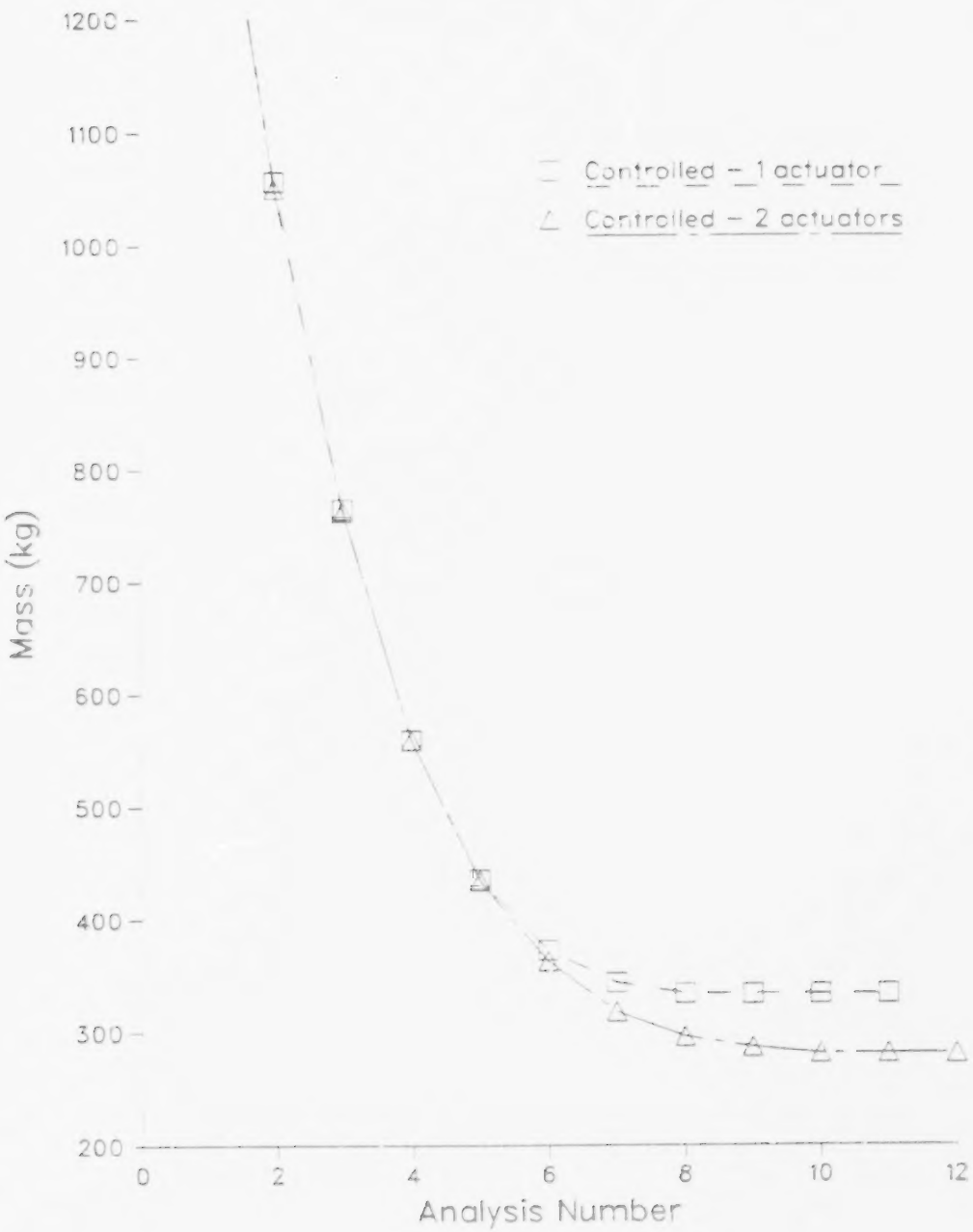

Fig. 14 Iteration Histories for Problem 6
Cantilevered Beam, Independent Actuator Gains

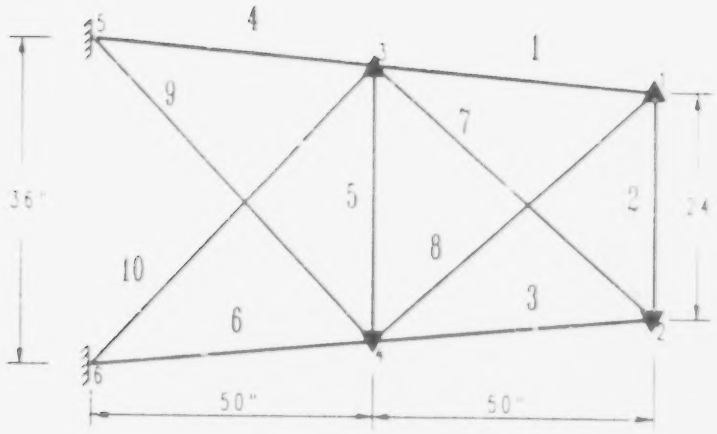

Actuator Locations

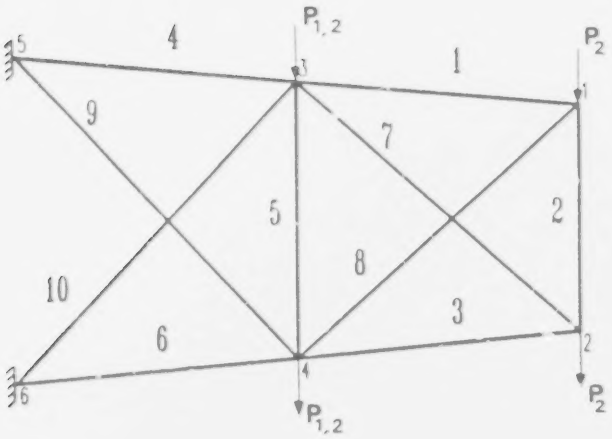

Loading Conditions

Fig. 15 Planar Truss, Problem 7

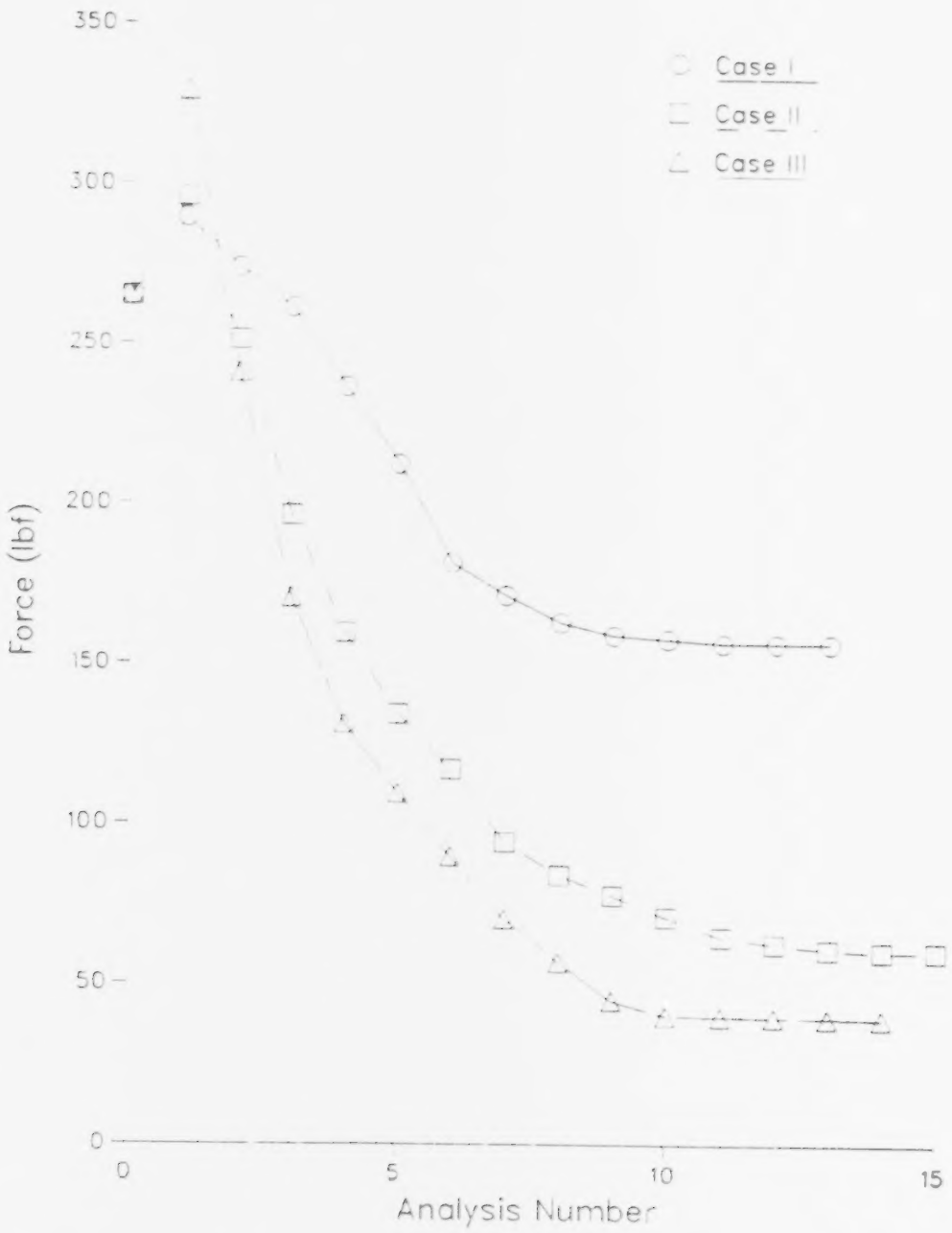

Fig. 16 Iteration Histories for Problem 7
Planar Truss, Control Force Minimization

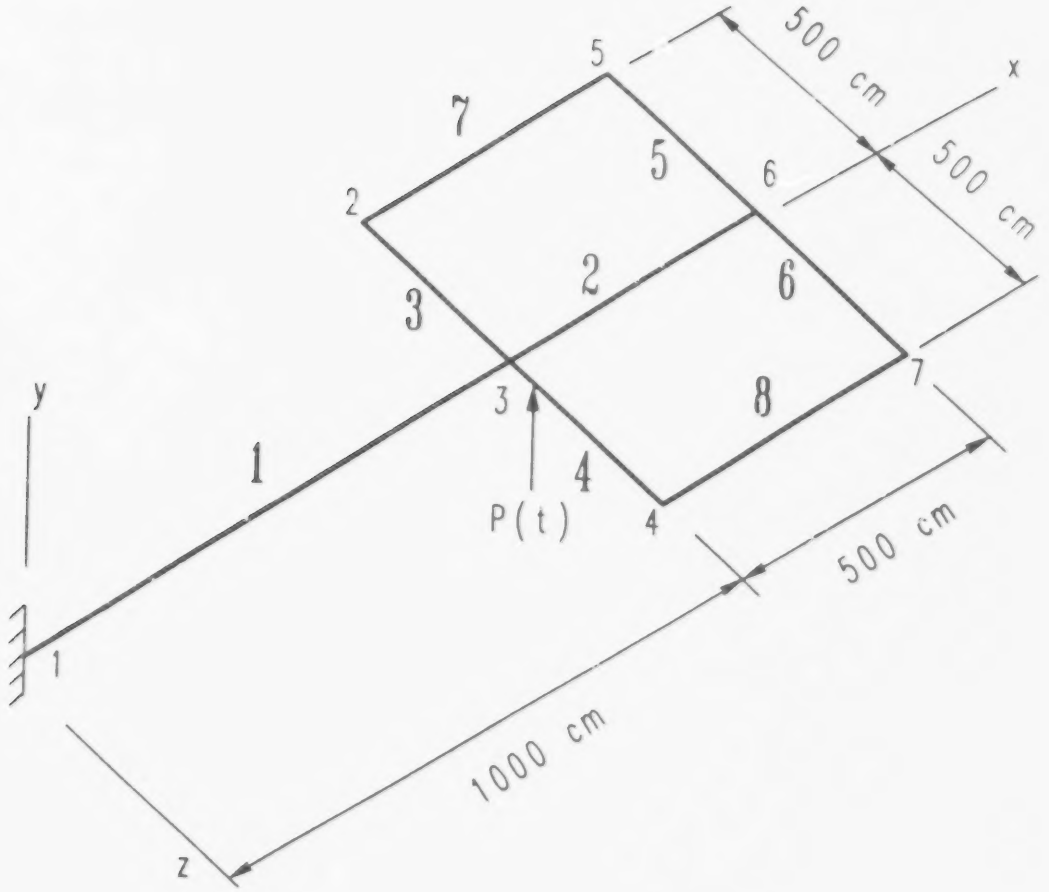

Fig. 17 Antenna, Problem 8

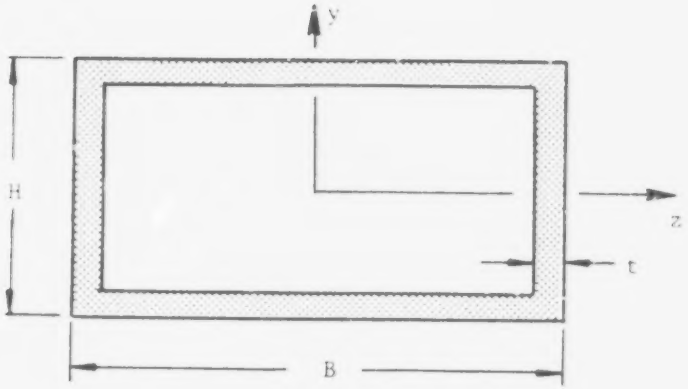

Cross Sectional Dimensions

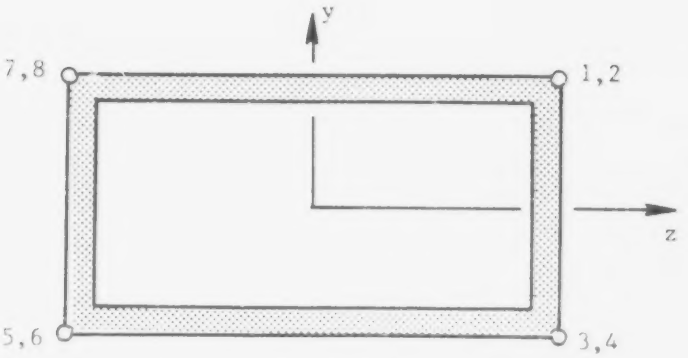

Stress Constraint Evaluation Points

Fig. 18 Beam Cross Section

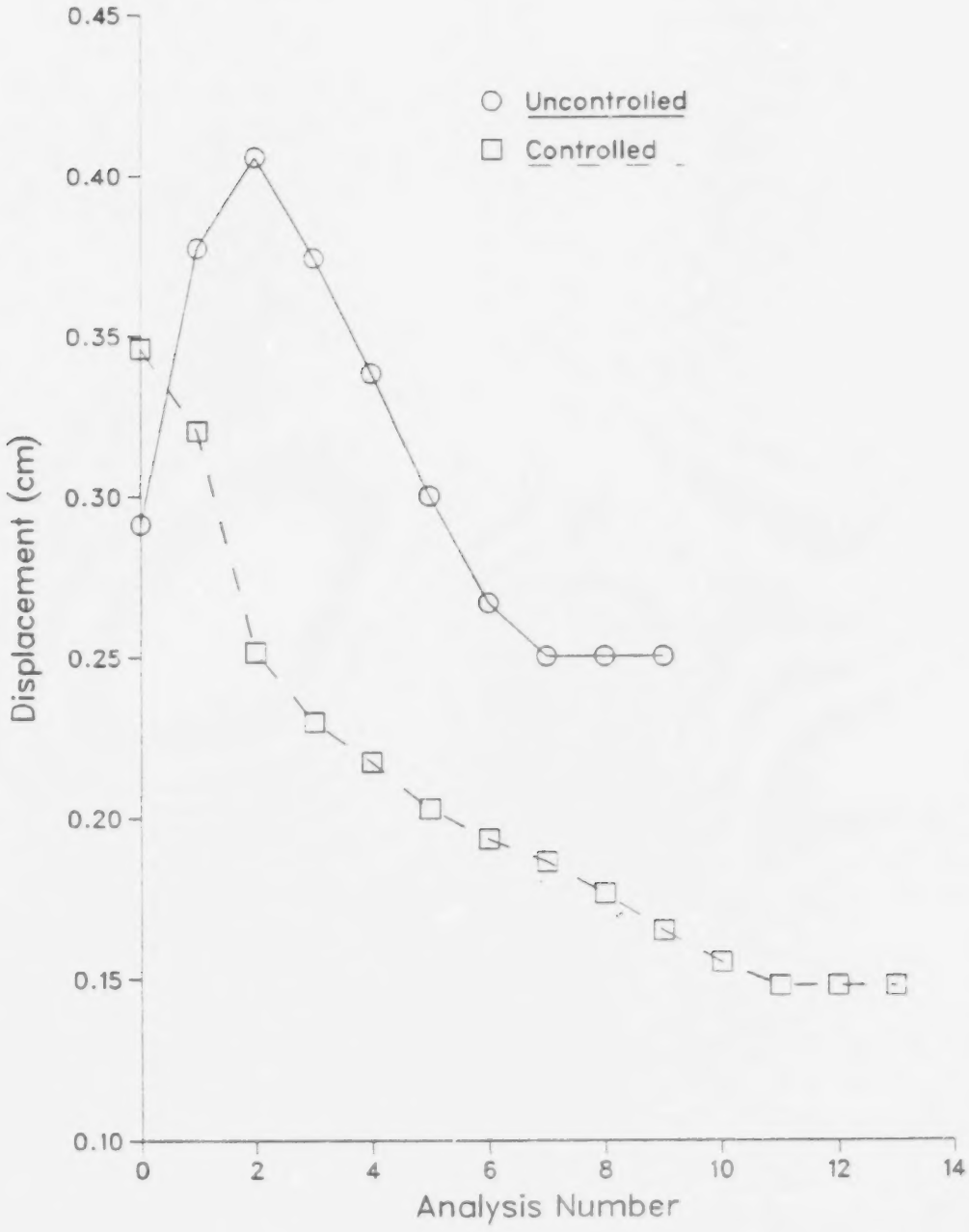

Fig. 19 Iteration Histories for Problem 8
Antenna, Response Minimization

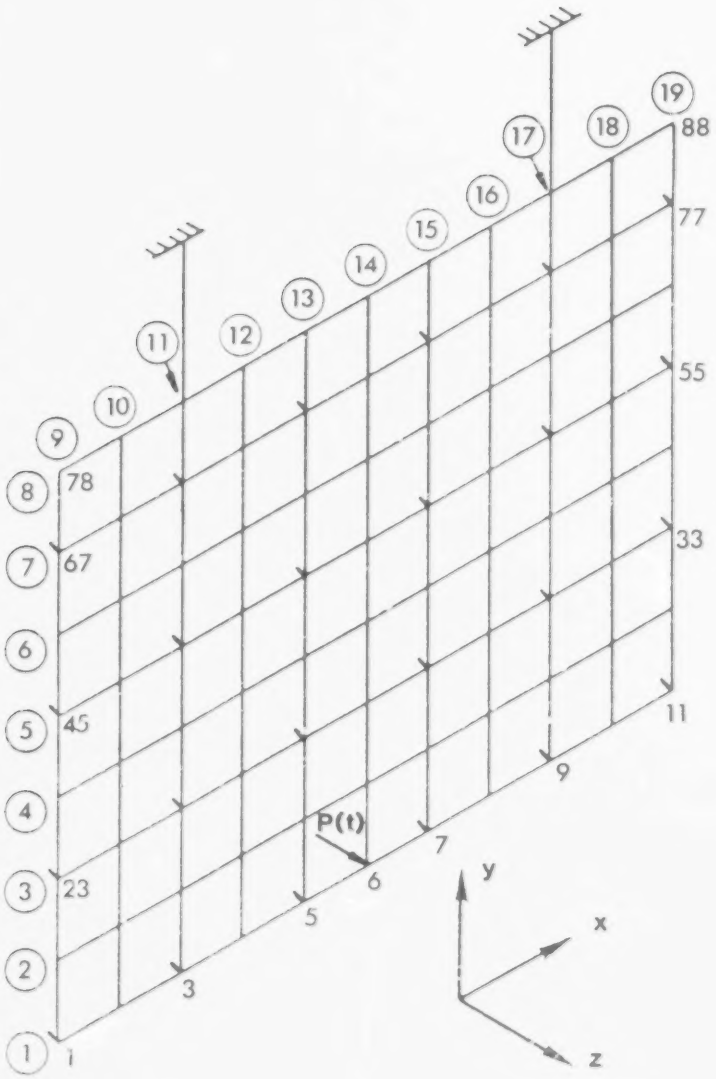

Fig. 20 Grillage, Problem 9

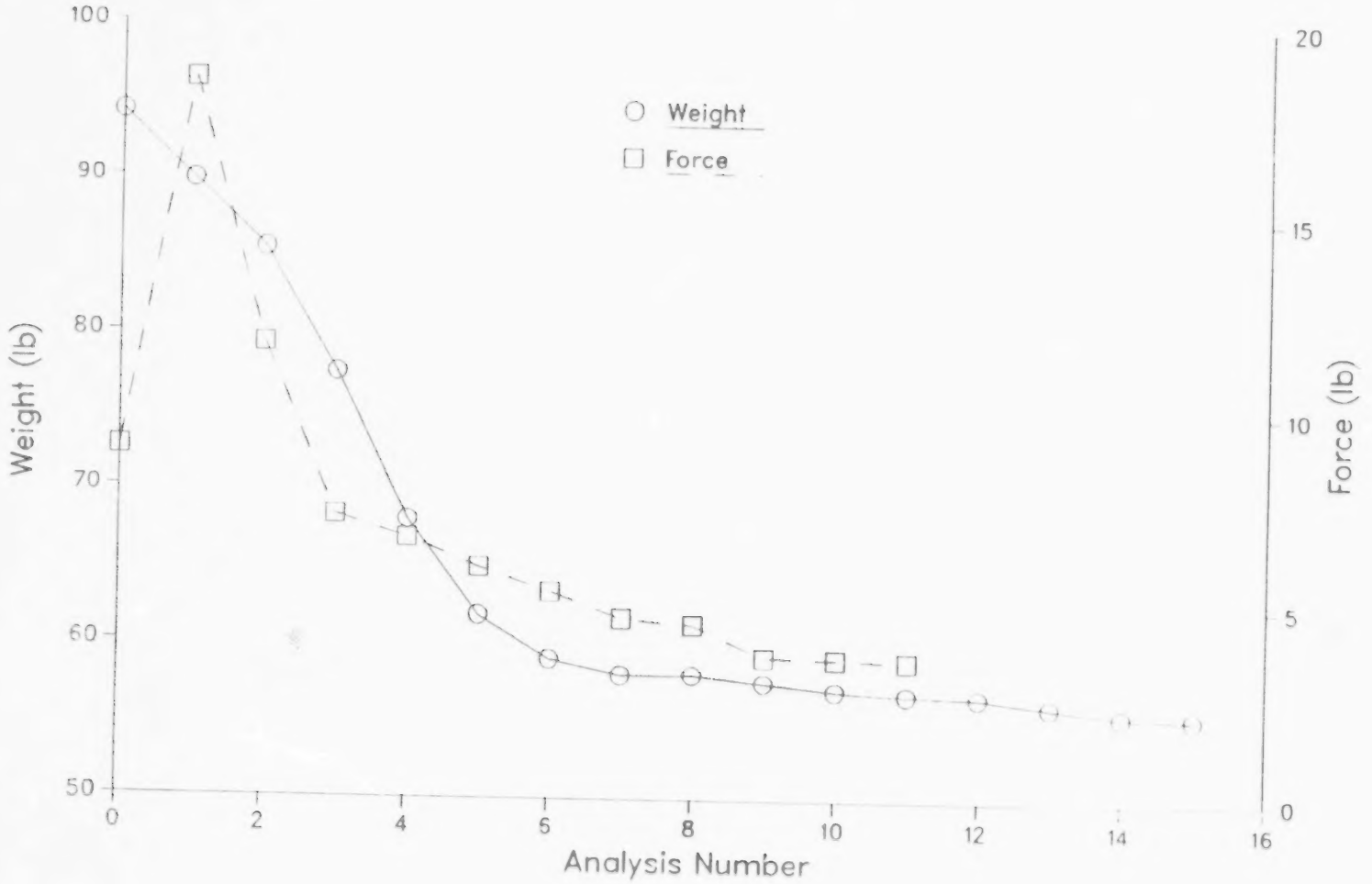

Fig. 21 Iteration Histories for Problem 9, Grillage

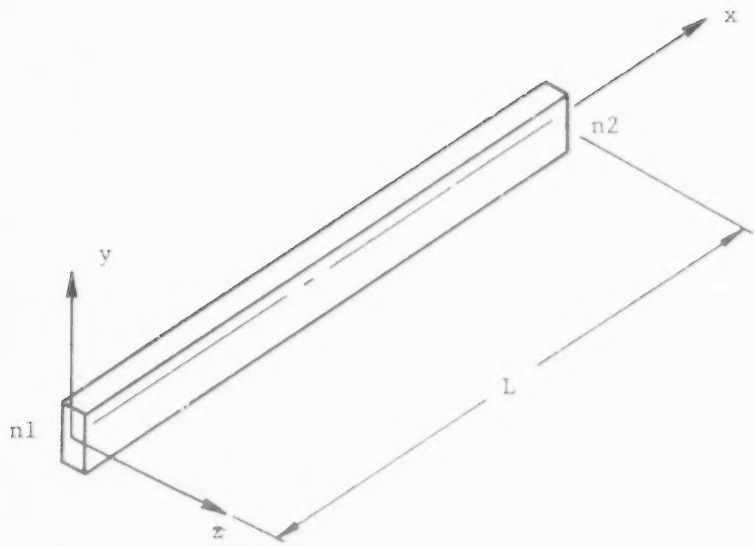

Fig. A1 Space Frame Element

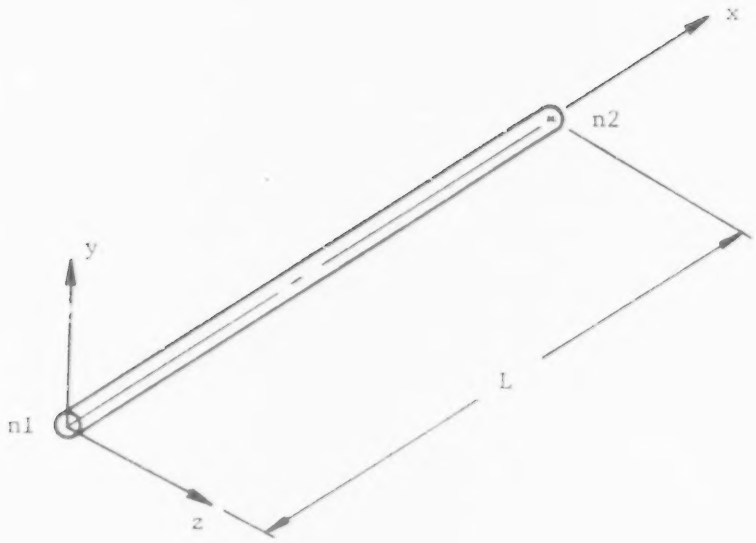

Fig. A2 Space Truss Element

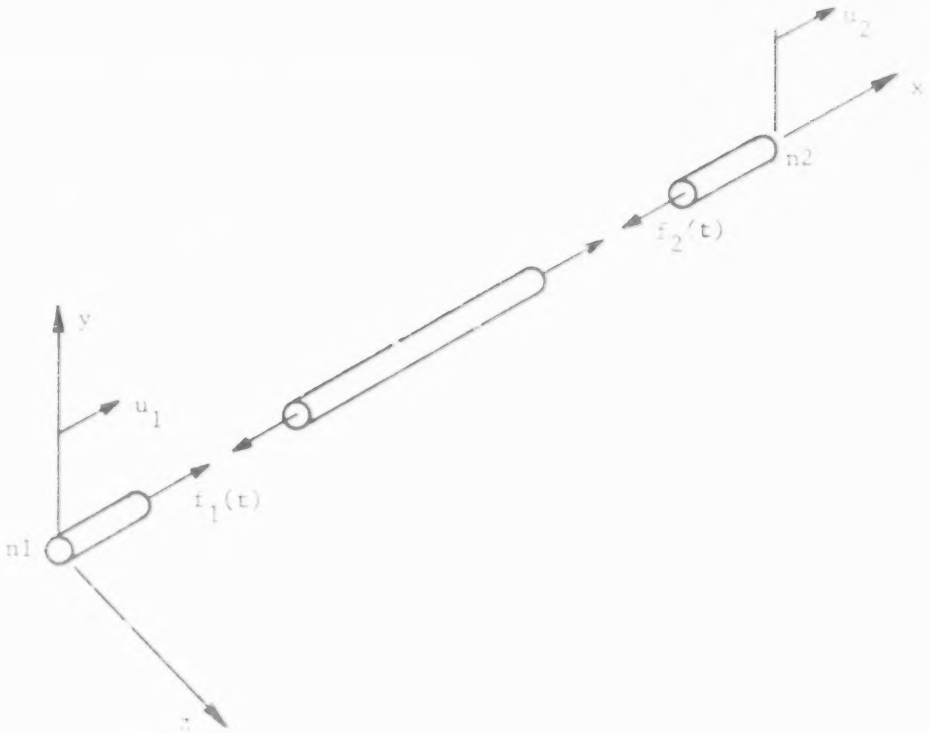

Fig. A3 Axial Control Element

NASA

Report Documentation Page

1. Report No.	2. Government Accession No.	3. Recipient's Catalog No.
NASA CR-4132		

4. Title and Subtitle
Control Augmented Structural Synthesis

5. Report Date
April 1988

6. Performing Organization Code

7. Author(s)
Robert V. Lust and Lucien A. Schmit

8. Performing Organization Report No.

10. Work Unit No.
505-63-11-01

9. Performing Organization Name and Address
University of California, Los Angeles
Department of Engineering and Applied Science
Los Angeles, CA 90024-1593

11. Contract or Grant No.
NSG-1490

13. Type of Report and Period Covered
Contractor Report

12. Sponsoring Agency Name and Address
National Aeronautics and Space Administration
Langley Research Center
Hampton, VA 23665-5225

14. Sponsoring Agency Code

15. Supplementary Notes
Langley Technical Monitor: Jaroslaw Sobieski

16. Abstract
A methodology for control augmented structural synthesis is proposed for a class of structures which can be modeled as an assemblage of frame and/or truss elements. It is assumed that both the plant (structure) and the active control system dynamics can be adequately represented with a linear model. The structural sizing variables, active control system feedback gains and non-structural lumped masses are treated simultaneously as independent design variables. Design constraints are imposed on static and dynamic displacements, static stresses, actuator forces and natural frequencies to ensure acceptable system behavior. Multiple static and dynamic loading conditions are considered. Side constraints imposed on the design variables protect against the generation of unrealizable designs. While the proposed approach is fundamentally more general, here the methodology is developed and demonstrated for the case where (1) the dynamic loading is harmonic and thus the steady state reponse is of primary interest, (2) direct output feedback is used for the control system model; and (3) the actuators and sensors are collocated.

17. Key Words (Suggested by Author(s))
Design
Structures
Optimization
Sensitivity
Active Control

18. Distribution Statement
Unclassified - Unlimited

Subject Category 05

19. Security Classif. (of this report)	20. Security Classif. (of this page)	21. No. of pages	22. Price
Unclassified	Unclassified	192	A09

NASA FORM 1626 OCT 86

For sale by the National Technical Information Service, Springfield, Virginia 22161-2171